Chapter 2
PDAE Modeling and Discretization

Giuseppe Alì, Massimiliano Culpo, Roland Pulch, Vittorio Romano, and Sebastian Schöps

Abstract We consider mathematical modeling in nanoelectronics, which causes coupled systems of differential algebraic equations and partial differential equations. Both modeling and discretization are investigated for the inclusion of advanced semiconductor behavior, heat conduction and electromagnetic effects within electric networks.

2.1 Introduction on Modeling and PDAEs

In this chapter, we introduce the mathematical modeling for the simulation of circuits and devices in nanoelectronics. To include the significant effects, a refined modeling using partial differential algebraic equations (PDAEs) is necessary.

G. Alì (✉)
Department of Mathematics, University of Calabria, 87036 Arcavacata di Rende (CS), Italy
e-mail: giuseppe.ali@unical.it,

M. Culpo
Università di Bologna, Bologna, Italy
e-mail: m.culpo@cineca.it

R. Pulch
Institut für Mathematik und Informatik, Ernst Moritz Arndt Universität Greifswald, Walther-Rathenau-Straße 47, D-17487 Greifswald, Germany
e-mail: pulchr@uni-greifswald.de

V. Romano
Dipartimento di Matematica e informatica, Università di Catania, Viale A. Doria no, 95125 Catania, Italy
e-mail: romano@dmi.unict.it

S. Schöps
Graduate School of Excellence Computational Engineering, TU Darmstadt, Dolivostraße 15, 64293 Darmstadt, Germany
e-mail: schoeps@gsc.tu-darmstadt.de

M. Günther (ed.), *Coupled Multiscale Simulation and Optimization in Nanoelectronics*, Mathematics in Industry 21,
DOI 10.1007/978-3-662-46672-8_2

2.1.1 Mathematical Modeling in Nanoelectronics

The mathematical modeling of electronic circuits is typically based on some network approach. Thereby, we analyse the transient behavior of node voltages and branch currents. The basic elements of the circuit exhibit corresponding relations between voltages and currents, which represent differential equations or algebraic equations. The topology of the circuit is considered via Kirchhoff's current law and Kirchhoff's voltage law, which are algebraic equations. It follows a system of differential algebraic equations (DAEs).

For example, mathematical modeling using the modified nodal analysis (MNA), see [26], yields systems of the form

$$\begin{aligned} A_C \frac{\mathrm{d}\mathbf{q}}{\mathrm{d}t} + A_R \mathbf{r}(A_R^T \mathbf{e}) + A_L \mathbf{i}_L + A_V \mathbf{i}_V + A_I \mathbf{i}_I &= 0, \\ \frac{\mathrm{d}\boldsymbol{\phi}}{\mathrm{d}t} - A_L^T \mathbf{e} &= 0, \\ A_V^T \mathbf{e} - \mathbf{v}_V &= 0, \\ \mathbf{q} - \mathbf{q}_C(A_C^T \mathbf{e}) &= 0, \\ \boldsymbol{\phi} - \boldsymbol{\phi}_L(\mathbf{i}_L) &= 0, \end{aligned} \tag{2.1}$$

where $\mathbf{e}, \mathbf{i}_L, \mathbf{i}_V$ are the unknown node voltages and branch currents through inductors and voltage sources. The unknowns $\mathbf{q}, \boldsymbol{\phi}$ represent charges and fluxes, respectively. The functions $\mathbf{r}, \mathbf{q}_C, \boldsymbol{\phi}_L$ are predetermined. Independent current sources $\mathbf{i}_I$ and voltage sources $\mathbf{v}_V$ may appear. The incidence matrices A_C, A_L, A_R, A_V, A_I follow from the topology of the electronic circuit.

For a transient analysis of the system (2.1), consistent initial values have to be specified. The differential index of the DAE system (2.1) follows from the topology only. An appropriate mathematical modeling implies an index of one or two. Hence we can use common numerical methods for initial value problems of DAEs.

This modeling approach applies with the assumption of ideally joint lumped elements in the electronic circuit. No spatial coordinates appear, since the information on the topology is given by the incidences of the elements. For quite a long time, the mathematical modeling via time-dependent systems of DAEs has been sufficiently accurate to reproduce the transient behavior of the underlying physical circuit, i.e., the modeling error was sufficiently small. However, miniaturization causes parasitic effects in nanoelectronics, which cannot be neglected any more. Corresponding phenomena are, for example:

- *Quantum effects*: The down-scaling of transistors decreases also the size of the channel. The channel length comes close to the atomic scale. Hence quantum effects appear and have to be considered in the mathematical models.
- *Heating*: The faster clock rate in chips causes a higher power loss in the electronic network. The down-scaling implies that more heat is produced within

a unit area. Since cooling cannot ensure a homogeneous temperature any more, the heat distribution and the heat conduction has to be considered. In particular, thermal effects of transistors appear due to the semiconductor's dependence on temperature.

- *Electromagnetic effects*: The distance between transmission lines on a chip becomes tiny due to the miniaturization. The current through some transmission line can induce a significant current in a neighboring component. Thus the interference of transmission lines has to be taken into account.

These parasitic phenomena represent spatial effects. Thus corresponding mathematical models apply partial differential equations (PDEs) in time as well as space. Firstly, PDE models are required, which reproduce phenomena like quantum and thermal effects with a high accuracy. Secondly, the parasitic effects are considered in the electronic network, i.e., the PDEs are coupled to the circuit's DAEs. It follows a system of partial differential algebraic equations (PDAEs).

On the one hand, the basic network approaches for modeling electronic circuits yield time-dependent systems of DAEs, which can be written in the general form

$$\mathbf{F} : \mathbb{R}^k \times \mathbb{R}^k \times I \to \mathbb{R}^k, \quad \mathbf{F}\left(\frac{\mathrm{d}\mathbf{y}}{\mathrm{d}t}, \mathbf{y}, t\right) = 0, \tag{2.2}$$

where $\mathbf{y} : I \to \mathbb{R}^k$ denotes the unknown solution in a time interval $I := [t_0, t_1]$. The MNA equations (2.1) represent an often used model of the type (2.2). A consistent initial value $\mathbf{y}(t_0) = \mathbf{y}_0$ has to be given. On the other hand, a parasitic phenomenon is included via PDEs. We arrange the general formulation

$$\mathscr{L} : D \times I \times V \to \mathbb{R}^m, \quad \mathscr{L}(\mathbf{x}, t, \mathbf{u}) = 0 \tag{2.3}$$

with a differential operator $\mathscr{L}$. Thereby, $D \subset \mathbb{R}^d$ for $d \in \{1, 2, 3\}$ represents the underlying spatial domain. The solution $\mathbf{u} : D \times I \to \mathbb{R}^m$ belongs to some function space V. Initial and boundary conditions have to be specified appropriately.

Coupling the DAEs (2.2) and the PDEs (2.3) yields systems of PDAEs in time as well as space. The coupling is feasible via

- (Artificial) coupling variables,
- Source terms,
- Boundary conditions (BCs).

More sophisticated couplings also appear. The involved PDEs may be of mixed type (elliptic, hyperbolic, parabolic). For example, the drift-diffusion equations for semiconductors, the telegrapher's equation for transmission lines or the heat equation for resistors are used in practice. The types of PDAEs, which result from the modeling in nanoelectronics, are discussed in the following subsection.

2.1.2 Classification of PDAE Models

As introduced above, we consider mathematical models of PDAEs, i.e., coupled systems of DAEs (2.2) and PDEs (2.3). The notion PDAE is also applied in the context of singular PDEs. For example, we discuss the linear PDE

$$A\frac{\partial \mathbf{u}}{\partial t} + B\frac{\partial \mathbf{u}}{\partial x} = \mathbf{s}(x, t, \mathbf{u}) \tag{2.4}$$

with matrices $A, B \in \mathbb{R}^{k\times k}$. If A and/or B are singular, then a singular PDE appears. PDAEs in the sense of singular PDEs are investigated in [44], for example. For electronic circuits with amplitude modulated signals or frequency modulated signals, the introduction of different time variables transforms the circuit's DAEs (2.1) into singular PDEs, see [51].

If the matrix B is regular and the matrix A singular and $B^{-1}A$ diagonalizable, then the system of PDEs (2.4) can be transformed into the equivalent system

$$\begin{aligned}\frac{\partial \tilde{\mathbf{u}}_1}{\partial t} + \tilde{B}_1\frac{\partial \tilde{\mathbf{u}}_1}{\partial x} &= \tilde{\mathbf{s}}_1(x, t, \tilde{\mathbf{u}}_1, \tilde{\mathbf{u}}_2),\\ \frac{\mathrm{d}\tilde{\mathbf{u}}_2}{\mathrm{d}x} &= \tilde{\mathbf{s}}_2(x, t, \tilde{\mathbf{u}}_1, \tilde{\mathbf{u}}_2).\end{aligned}$$

The result can be seen as a coupled systems of PDEs and ODEs, i.e., a PODE. The source term causes the coupling within the right-hand sides. Likewise, a coupled system of PDEs and DAEs appears for other cases of the matrices A, B. Thus some singular PDEs correspond to systems of PDAEs.

In the following, we consider PDAEs in the sense of coupled systems of DAEs and PDEs only. We present a rough classification of PDAE models in nanoelectronics according to [12]. Two approaches for PDAE modeling exist: refined modeling and multiphysical extensions.

2.1.2.1 Refined Modeling

Complex elements of the circuit with a spatial distribution like semiconductors and transmission lines can be modeled via substitute circuits consisting of lumped basic elements. These companion models include artificial parameters, which have to be chosen appropriately to approximate the behavior of the element. Alternatively, PDE models exist, which describe these elements directly. We consider one or several components of the electronic circuit by its PDE model and couple the PDE to the system of DAEs modeling the surrounding network.

The resulting PDAE system is more difficult to analyze and more costly to solve numerically than a DAE system based on companion models. Nevertheless, the refined modeling allows to describe certain elements of the circuits with a higher

accuracy, i.e., the modeling error becomes relatively low. Hence we can focus on critical components of an electronic circuit. Moreover, the refined modeling yields results, which can be used for the construction and the validation of better companion models. Sophisticated PDE models for semiconductor behavior have been developed for this purpose, see [7–9, 48, 49, 53–58], for example. The aim is to reproduce the electric input-output behavior of the semiconductor with a high accuracy in the presence of quantum and thermal effects.

The coupling of the DAE network and the PDE systems is performed via voltages and currents. The node potentials of the connecting network yield boundary conditions of Dirichlet type for the Ohmic contacts of the PDE model. At other boundaries without electric contacts, homogeneous boundary conditions of von-Neumann type may appear. Vice versa, the output of the PDE model represents an electric current, which enters the surrounding network. It follows a source term for the DAE system. The refined modeling yields PDAE systems of the form

$$\begin{aligned} A\tfrac{\partial}{\partial t}\mathbf{u} + \mathscr{L}_D\mathbf{u} - \mathbf{s}(\mathbf{u},t) &= \mathbf{p}(\mathbf{y}) && \text{(PDE in } I\times D\text{)} \\ \mathbf{u}|_{\Gamma_1} &= \mathbf{g}(\mathbf{y}) && \text{(Dirichlet BC)} \\ \tfrac{\partial}{\partial \mathbf{n}}\mathbf{u}\big|_{\Gamma_2} &= \mathbf{h}(\mathbf{y}) && \text{(Neumann BC)} \\ \mathbf{F}\left(\tfrac{\mathrm{d}}{\mathrm{d}t}\mathbf{y},\mathbf{y},t\right) &= \mathbf{r}(\mathbf{u}) && \text{(DAE in } I\text{)} \end{aligned} \tag{2.5}$$

with a matrix A and a spatial differential operator $\mathscr{L}_D$ with domain D. The coupling can be realized via the source terms $\mathbf{p}, \mathbf{r}$ or the boundary conditions $\mathbf{g}, \mathbf{h}$, where the boundary is decomposed into $\partial D = \Gamma_1 \cup \Gamma_2$.

We categorize the refined modeling into the following cases:

- *Semiconductors*: Several transistors or diodes of the electronic circuit are modeled via drift-diffusion equations or quantum mechanical equations, which are coupled to the electric network. Existence and uniqueness of solutions for models including stationary or non-stationary drift-diffusion equations is analyzed in [4, 5]. The drift-diffusion equations represent PDEs of mixed type. Hydrodynamical models for semiconductors, which represent hyperbolic PDEs, are considered in [6].
- *Transmission lines*: Telegrapher's equation describes the physical effects in transmission lines, i.e., a PDE model of hyperbolic type. The coupling of these PDEs and the network's DAEs exhibits the form (2.5). For further details, see [36, 37].

2.1.2.2 Multiphysical Extensions

Refined modeling can be seen as a partitioning of the electronic circuit, where we describe some parts by PDEs and model the remaining larger part via the traditional DAE formulation. Moreover, the involved systems of PDEs always

describe the electric or electromagnetic behavior of some components of the circuits. In contrast, multiphysical modeling introduces an additional distributed effect within the complete circuit. We consider the circuit as two or more layers, where one layer corresponds to the common network description and the other layers model another physical effect given by PDEs.

Multiphysical modeling includes the following phenomena, for example:

- *Thermal aspects*: The faster clock rate implies a significant heat production in particular parts of the electronic circuit. Thus cooling cannot achieve a homogeneous and moderate temperature. Since the electric behavior of the components depends on the temperature (for example, strongly for resistors), the heat distribution and conduction has to be considered in the numerical simulation.

  In addition to the electric network, a thermal network can be arranged, which describes the heat flow within the circuit, see [29]. The thermal network consists of zero-dimensional elements as in the electric network. Moreover, a refined modeling of the thermal network is feasible, where some elements are replaced by a PDE model based on the heat equation in one, two or three space dimensions. The heat equation, i.e., Fourier's law, represents a parabolic PDE. Further details can be found in [11]. Modeling, analysis and discretization corresponding to two dimensional heat equations is considered in [3, 20, 21, 25].

  A special case is given by the usage of the heat equation with a spatial domain including the complete electronic circuit. Consequently, we obtain two layers in parallel: the electric network described by DAEs and the thermal aspects modeled via a PDE.
- *Electromagnetics*: On the one hand, Maxwell's equations imply the network approaches, which produce the DAE formulations (2.2), via according simplifications. The aim is to achieve an efficient numerical simulation. On the other hand, the electronic circuit can be described completely by the full Maxwell's equations, i.e., a PDE system. However, this approach would cause a huge computational effort.

  Alternatively, just some parts or components of the circuit can be modeled by Maxwell's equations or its variants like the magnetoquasistatic formulation. The systems of PDEs are coupled to the network's DAEs again. Hence the same effects are described in different ways, i.e., distinct mathematical models. This approach is similar to a refined modeling. Nevertheless, the model represents a multiphysical extension, since the magnetic fluxes are considered in addition to the purely electric behavior of the circuit. An application based on magnetoquasistatic equations is presented in [59].

We note that refined modeling and multiphysical extensions can also be combined. In a multiphysical framework, we can arrange a refined modeling of some components (semiconductors, transmission lines) within the layer of the common electric network. However, such a complex structure is not considered in the following, i.e., we apply either refined modeling or multiphysical extensions.

In this chapter, we present some examples of mathematical models, which yield systems of PDAEs. The chapter is organized as follows. In Sect. 2.2.1, a refined modeling for semiconductor devices is performed, where diodes are described by systems of PDEs including two space dimensions. The resulting system of PDAEs is discussed. In Sect. 2.2.2, a multiphysical modeling is performed by considering thermal behavior at the system level. The electric network is coupled to the heat equation. In Sect. 2.2.3, multiphysical modeling of the electric circuits is considered based on Maxwell's equations. The approach applies a magnetoquasistatic formulation. In Sect. 2.2.4, a description of thermal and quantum effects for semiconductor devices is presented to obtain according mathematical models. Thereby, the focus is on the PDE level, which can be used as a module in further refined models.

2.2 Modeling, Analysis and Discretization of Coupled Problems

We present four applications of coupled problems in nanoelectronics to illustrate the essential strategies.

2.2.1 Refined Modeling of Networks with Devices

We investigate electric networks including semiconductor devices. Some devices are described by more sophisticated mathematical models based on partial differential equations now, whereas the surrounding electric network is still represented by traditional models using differential algebraic equations.

2.2.1.1 Modeling of Electric Networks

An RCL electric network is a directed graph with n_v vertices (or nodes), and n_a arcs (or branches) which contain resistors, capacitors and inductors, and independent voltage and current sources, $\mathbf{v}_V(t) \in \mathbb{R}^{n_V}$ and $\mathbf{i}_I(t) \in \mathbb{R}^{n_I}$. The branches are usually labelled according to the components they contain: R for resistors, C for capacitors, L for inductors, V for voltage sources, I for current sources.

The topology of the network can be described by an incidence matrix $A = (a_{ij}) \in \mathbb{R}^{n_v \times n_a}$, defined by:

$$a_{ij} = \begin{cases} -1 \text{ if the branch } j \text{ leaves the node } i, \\ 1 \text{ if the branch } j \text{ enters the node } i, \\ 0 \text{ otherwise.} \end{cases} \tag{2.6}$$

To keep track of different branches, they are collected according to their labels (R, C, L, I, V), and write

$$A = (A_R, A_C, A_L, A_I, A_V) \in \mathbb{R}^{n_v \times (n_R + n_C + n_L + n_I + n_V)} \equiv \mathbb{R}^{n_v \times n_a}.$$

The electric behavior of the network is described by a set of time-dependent variables associated to its nodes and branches. An applied potential is associated to each node ($\mathbf{u} \in \mathbb{R}^{n_v}$), a voltage drop and a current is associated to each branch ($\mathbf{v}, \mathbf{i} \in \mathbb{R}^{n_a}$). To keep track of the different labels, we write

$$\mathbf{v} = \begin{pmatrix} \mathbf{v}_R \\ \mathbf{v}_C \\ \mathbf{v}_L \\ \mathbf{v}_I \\ \mathbf{v}_V \end{pmatrix}, \quad \mathbf{i} = \begin{pmatrix} \mathbf{i}_R \\ \mathbf{i}_C \\ \mathbf{i}_L \\ \mathbf{i}_I \\ \mathbf{i}_V \end{pmatrix}.$$

The direction of each branch coincides with the positive direction of the voltage drop and the current through the branch. The voltage drops and the applied potentials are related by the voltage relation:

$$\mathbf{v} = A^\top \mathbf{u}. \tag{2.7}$$

The currents satisfy Kirchhoff's current law:

$$A\mathbf{i} = 0, \tag{2.8}$$

which ensures charge conservation. To the above relations we need to add constitutive relations for the RCL components:

$$\mathbf{i}_R = \mathbf{r}(\mathbf{v}_R), \quad \mathbf{i}_C = \frac{d\mathbf{q}}{dt}, \quad \mathbf{v}_L = \frac{d\boldsymbol{\phi}}{dt}, \tag{2.9}$$

with

$$\mathbf{q} = \mathbf{q}_C(\mathbf{v}_C), \quad \boldsymbol{\phi} = \boldsymbol{\phi}_L(\mathbf{i}_L). \tag{2.10}$$

Here, $\mathbf{q}_C$ collects the charges inside the capacitors, and $\boldsymbol{\phi}_L$ is a flux term for the inductors. Finally, for the branches with sources we assume to know the time-dependent functions $\mathbf{i}_I(t)$, $\mathbf{v}_V(t)$.

Following the formalism of Modified Nodal Analysis (MNA) [40, 50], we use the relations (2.9) in Kirchhoff's current law (2.8), together with the voltage relation (2.7) and the relations (2.10), to obtain the DAE equation (2.1), for the unknowns $\mathbf{q}$, $\boldsymbol{\phi}$, $\mathbf{u}$, $\mathbf{i}_L$, $\mathbf{i}_V$. Sometimes it is convenient to reduce the number of

variables, eliminating $\mathbf{q}$ and $\boldsymbol{\phi}$. This leads to the following alternative form of the MNA equations, for the unknowns $\mathbf{u}$, $\mathbf{i}_L$, $\mathbf{i}_V$:

$$\begin{aligned} A_C \frac{\mathrm{d}\mathbf{q}_C(A_C^T\mathbf{u})}{\mathrm{d}t} + A_R\mathbf{r}(A_R^T\mathbf{u}) + A_L\mathbf{i}_L + A_V\mathbf{i}_V + A_I\mathbf{i}_I &= 0, \\ \frac{\mathrm{d}\boldsymbol{\phi}_L(\mathbf{i}_L)}{\mathrm{d}t} - A_L^T\mathbf{u} &= 0, \\ A_V^T\mathbf{u} - \mathbf{v}_V &= 0. \end{aligned} \tag{2.11}$$

The above equations apply also to electric circuits with semiconductor devices, provided that the devices are described by concentrated (companion) models, i.e., by means of equivalent RCL circuits. In this framework, a semiconductor device is represented by a subnetwork of the overall electric network. In following subsection we will show how to replace these subnetworks with distributed models for semiconductor devices.

2.2.1.2 Distributed Models for Devices

In this subsection, we consider an electric network with n_D semiconductor devices. We assume that the i-th device has $1 + K_i$ contacts. More precisely, we model the i-th device by a d-dimensional domain Ω^i, $i = 1, \ldots, n_D$, with $d = 1, 2$, or 3, and we assume that the boundary $\partial\Omega^i$ is made of a Dirichlet part Γ_D^i, union of $1 + K_i$ disjoint parts, which represent Ohmic contacts, and of a Neumann part Γ_N^i, which represents insulating boundaries (for $d > 1$),

$$\Gamma_D^i = \bigcup_{j=0}^{K_i} \Gamma_{D,j}^i, \quad \Gamma_N^i = \partial\Omega^i \setminus \Gamma_D^i, \quad i = 1, \ldots, n_D.$$

In total, the devices contain n_{vD} Ohmic contacts, with

$$n_{vD} := n_D + \sum_{j=1}^{n_D} K_j.$$

Each contact must be connected to a node of the electric network. To relate the contacts of the devices to the nodes of the network, we need to introduce a contact-to-node selection matrix, $\mathbf{S}_D = (s_{D,ij}) \in \mathbb{R}^{n_v \times n_{vD}}$, defined by:

$$s_{D,ij} = \begin{cases} 1, \text{ if the contact } j \text{ is connected to the node } i, \\ 0, \text{ otherwise.} \end{cases} \tag{2.12}$$

This definition differs with the definition of branch-to-node incidence matrix, previously given. In fact, the branch-to-node incidence matrix relates each branch

to two nodes, and the values 1 and -1 give information on the orientation of the branch, while the contact-to-node selection matrix relate each contact to one node.

The behavior of the i-th device is described by an electric potential $\phi^i(\mathbf{x}, t)$, and by a vector variable $\mathbf{U}^i(\mathbf{x}, t)$, which collects the other macroscopic variables for the device, such as carrier density, flux density, energy, etc. Several models can be used, with different mathematical characters, but sharing some common features.

1. The first common feature is that the electric potential ϕ^i is generated by the built-in charge, $\rho^i_{\rm bi}(\mathbf{x})$, due to the dopants embedded in the semiconductor, and by the charge density $\rho^i(\mathbf{U}^i)$, due to the carriers, so that it satisfies the Poisson equation:

$$-\nabla\cdot(\epsilon^i\nabla\phi^i) = \rho^i_{\rm bi} + \rho^i(\mathbf{U}^i), \tag{2.13}$$

where $\epsilon^i(\mathbf{x})$ is the dielectric constant. This equation is supplemented with the following boundary conditions:

$$\begin{cases} \phi^i = \phi^i_{\rm bi}(\rho^i_{\rm bi}) + u^i_{D,j}, & \text{on } \Gamma^i_{D,j},\ j = 0, 1, \ldots, K_i, \\ \boldsymbol{\nu}^i\cdot\nabla\phi^i = 0, & \text{on } \Gamma^i_N, \end{cases} \tag{2.14}$$

where $\phi^i_{\rm bi}(\rho^i_{\rm bi})$ is the built-in potential, $u^i_{D,j}$, $j = 0, 1, \ldots, K_i$, are the applied potentials at the Ohmic contacts of the i-th device, and the symbol $\boldsymbol{\nu}^i$ denotes the external unit normal to $\partial\Omega^i$. For later use, we comprise the applied voltages in the vectors:

$$\mathbf{u}^i_D = \begin{pmatrix} u^i_{D,0} \\ \vdots \\ u^i_{D,K_i} \end{pmatrix} \in \mathbb{R}^{1+K_i}, \quad \mathbf{u}_D = \begin{pmatrix} \mathbf{u}^1_D \\ \vdots \\ \mathbf{u}^{n_D}_D \end{pmatrix} \in \mathbb{R}^{n_{vD}}.$$

2. The second common feature, is that the device variable $\mathbf{U}^i$ satisfies a system of partial differential equations, which is coupled to the electric potential only through the electric field $\mathbf{E}^i = -\nabla\phi^i$. Symbolically, we can write

$$\mathscr{F}^i\left(\mathbf{U}^i, \tfrac{\partial}{\partial t}\mathbf{U}^i, \nabla\mathbf{U}^i, \ldots; \mathbf{E}^i\right) = 0. \tag{2.15}$$

In the following sections we will see explicitly several of these partial differential models.

3. The last common feature is that (2.15) is consistent with the conservation of the charge density:

$$\frac{\partial\rho^i(\mathbf{U}^i)}{\partial t} + \nabla\cdot\mathbf{J}^i(\mathbf{U}^i) = 0. \tag{2.16}$$

Here, $\mathbf{J}^i(\mathbf{U}^i)$ is the electric current, which can be a component of the variable $\mathbf{U}^i$, or can be evaluated as a functional of the said variable. The electric current $\mathbf{J}^i$

depends also on the applied potentials $u^i_{D,j}$, $j = 0, 1, \ldots, K_i$, due to the coupling of (2.15) with the Poisson's equation (2.13), through the electric field $\mathbf{E}^i$.

As a consequence of (2.13) and (2.16), we have

$$\nabla \cdot \left(\epsilon^i \frac{\partial}{\partial t} \mathbf{E}^i + \mathbf{J}^i(\mathbf{U}^i) \right) = 0 \tag{2.17}$$

The term $\epsilon \frac{\partial}{\partial t} \mathbf{E}^i$ is the displacement current, and represents the current induced by time-variations of the electric field. Then, the total current in the i-th device is given by

$$\mathbf{j}^i := \epsilon^i \frac{\partial}{\partial t} \mathbf{E}^i + \mathbf{J}^i(\mathbf{U}^i). \tag{2.18}$$

The current $j^i_{D,j}$ through the j-th contact of the i-th device, is defined by:

$$j^i_{D,j} = -\int_{\Gamma^i_{D,j}} \mathbf{j}^i \cdot \boldsymbol{\nu}^i \, d\sigma(\mathbf{x}). \tag{2.19}$$

We introduce the vectors

$$\mathbf{j}^i_D = \begin{pmatrix} j^i_{D,0} \\ \vdots \\ j^i_{D,K_i} \end{pmatrix} \in \mathbb{R}^{1+K_i}, \quad \mathbf{j}_D = \begin{pmatrix} \mathbf{j}^1_D \\ \vdots \\ \mathbf{j}^{n_D}_D \end{pmatrix} \in \mathbb{R}^{n_{vD}}.$$

Recalling the definition of the selection matrix, the MNA equations need to be modified in the following way:

$$\begin{aligned} A_C \frac{\mathrm{d}\mathbf{q}}{\mathrm{d}t} + A_R \mathbf{r}(A_R^T \mathbf{u}) + A_L \mathbf{i}_L + A_V \mathbf{i}_V + A_I \mathbf{i}_I + \boldsymbol{\lambda} &= 0, \\ \frac{\mathrm{d}\boldsymbol{\phi}}{\mathrm{d}t} - A_L^T \mathbf{u} &= 0, \\ A_V^T \mathbf{u} - \mathbf{v}_V &= 0. \\ \mathbf{q} - \mathbf{q}_C(A_C^T \mathbf{u}) &= 0, \\ \boldsymbol{\phi} - \boldsymbol{\phi}_L(\mathbf{i}_L) &= 0, \end{aligned} \tag{2.20}$$

where the auxiliary variable $\boldsymbol{\lambda} \in \mathbb{R}^{n_v}$ is given by the device-to-network coupling relation:

$$\boldsymbol{\lambda} = \mathbf{S}_D \mathbf{j}_D. \tag{2.21}$$

To close the system, we also need the network-to-device coupling relation:

$$\mathbf{u}_D = \mathbf{S}_D^\top \mathbf{u}. \tag{2.22}$$

Remark 2.1 The components of the vector $\mathbf{j}_D$ are not independent. In fact, by using (2.17), after integrating by parts over Ω^i, we find

$$\sum_{j=0}^{K_i} j_{D,j}^i = 0, \quad i = 1, \dots, n_D. \tag{2.23}$$

This means that we can express $\mathbf{j}_D^i$ and, consequently, $\mathbf{j}_D$ in terms of the vectors

$$\mathbf{i}_D^i = \begin{pmatrix} j_{D,1}^i \\ \vdots \\ j_{D,K_i}^i \end{pmatrix} \in \mathbb{R}^{K_i}, \quad \mathbf{i}_D = \begin{pmatrix} \mathbf{i}_D^1 \\ \vdots \\ \mathbf{i}_D^{n_D} \end{pmatrix} \in \mathbb{R}^{n_{aD}}, \tag{2.24}$$

with $n_{aD} = \sum_{i=1}^{n_D} K_i$, by means of the relations:

$$\mathbf{j}_D^i = \mathbf{A}_D^{*i}\, \mathbf{i}_D^i, \qquad \mathbf{j}_D = \mathbf{A}_D^*\, \mathbf{i}_D, \tag{2.25}$$

where

$$\mathbf{A}_D^{*i} = \begin{pmatrix} -1 & \cdots & -1 \\ 1 & \cdots & 0 \\ \vdots & \ddots & \vdots \\ 0 & \cdots & 1 \end{pmatrix} \in \mathbb{R}^{(1+K_i)\times K_i}, \tag{2.26}$$

$$\mathbf{A}_D^* = \mathrm{diag}(\mathbf{A}_D^{*1}, \dots, \mathbf{A}_D^{*n_D}) \in \mathbb{R}^{n_{vD}\times n_{aD}}. \tag{2.27}$$

Remark 2.2 The components of the vector $\mathbf{j}_D^i$ depend only on the voltage drops

$$\mathbf{v}_D^i = \mathbf{A}_D^{*i\top} \mathbf{u}_D^i, \quad i = 1, \dots, n_D. \tag{2.28}$$

Thus, the components of the overall vector $\mathbf{j}_D$ depend only on the voltage drops

$$\mathbf{v}_D = \mathbf{A}_D^{*\top} \mathbf{u}_D. \tag{2.29}$$

In fact, recalling (2.15), the variables $\mathbf{U}^i$ are coupled to the Poisson equation only through the electric field $\mathbf{E}^i$, and so are the components of the electric current $\mathbf{J}^i(\mathbf{U}^i)$, and the components of $\mathbf{j}^i$, which appear in (2.19). Since the electric field is not affected by a time-dependent translation of the electric potential,

$\phi_D^i \to \phi_D^i + u_{D,0}^i(t)$, we have a dependence of $\mathbf{j}^i$ on the voltage drops $v_{D,j}^i := u_{D,j}^i - u_{D,0}^i$, $j = 1, \ldots, K_i$, which in compact form can be written as in (2.28).

As a consequence of the previous remarks, the coupling conditions (2.21) and (2.22) can be replaced by the conditions

$$\boldsymbol{\lambda} = \mathbf{A}_D \mathbf{i}_D, \tag{2.30}$$

$$\mathbf{v}_D = \mathbf{A}_D^\top \mathbf{u}, \tag{2.31}$$

where we have introduced the device incidence matrix

$$\mathbf{A}_D := \mathbf{S}_D \mathbf{A}_D^*. \tag{2.32}$$

We call this matrix "incidence matrix" because, for devices with two Ohmic contacts, it reduces to the usual incidence matrix for branches with two-terminal devices.

2.2.1.3 Displacement Current and Device Capacitance Matrix

The displacement currents, present in the definition of $\mathbf{i}_D$, will cause an additional capacitance effect. To see this, we introduce the auxiliary functions φ_j^i, defined by:

$$\begin{cases} -\nabla \cdot (\epsilon^i \nabla \varphi_j^i) = 0, & \text{in } \Omega^i \\ \varphi_j^i = \delta_{jk}, & \text{on } \Gamma_{D,k}^i,\ k = 0, 1, \ldots, K_i, \\ \boldsymbol{\nu}^i \cdot \nabla \varphi_j^i = 0, & \text{on } \Gamma_N^i, \end{cases} \tag{2.33}$$

where δ_{jk} is the Kronecker delta. The auxiliary functions φ_j^i, $j = 0, 1, \ldots, K_i$, are not independent, since

$$\varphi_0^i = 1 - \sum_{j=1}^{K_i} \varphi_j^i. \tag{2.34}$$

Using these functions, we can find an alternative expression for the current $j_{D,j}^i$ through the j-th contact of the i-th device:

$$j_{D,j}^i \equiv -\int_{\partial\Omega^i} \varphi_j^i \mathbf{j}^i \cdot \boldsymbol{\nu}^i \, d\sigma = -\int_{\Omega^i} \nabla \varphi_j^i \cdot \mathbf{j}^i \, d\mathbf{x}, \tag{2.35}$$

where we have used the identity (2.17). Recalling the definition (2.18), the current $\mathbf{j}^i$ is the sum of the displacement current and the current due to the carriers. For the

displacement current part, we find

$$
\begin{aligned}
-\int_{\Omega^i} \nabla\varphi_j^i \cdot \epsilon^i \frac{\partial}{\partial t}\mathbf{E}^i \, d\mathbf{x} &= \frac{\mathrm{d}}{\mathrm{d}t}\int_{\Omega^i} \nabla\cdot(\epsilon^i \nabla\varphi_j^i \phi^i)\, d\mathbf{x} \\
&= \frac{\mathrm{d}}{\mathrm{d}t}\sum_{k=0}^{K_i}\int_{\Gamma_{D,k}^i} \boldsymbol{\nu}\cdot(\epsilon^i\nabla\varphi_j^i(\phi_{\mathrm{bi}}^i + u_{D,k}^i)\varphi_k^i)\, d\sigma \\
&= \sum_{k=0}^{K_i}\int_{\Gamma_{D,k}^i} \boldsymbol{\nu}\cdot(\epsilon^i\nabla\varphi_j^i\varphi_k^i)\, d\sigma \frac{\mathrm{d}u_{D,k}^i}{\mathrm{d}t},
\end{aligned}
$$

which, using the divergence theorem and identity (2.34), leads to

$$
-\int_{\Omega^i} \nabla\varphi_j^i \cdot \epsilon^i \frac{\partial}{\partial t}\mathbf{E}^i \, d\mathbf{x} = \sum_{k=1}^{K_i}\int_{\Omega^i} \epsilon^i \nabla\varphi_j^i\cdot\nabla\varphi_k^i \, d\mathbf{x}\frac{\mathrm{d}v_{D,k}^i}{\mathrm{d}t}, \tag{2.36}
$$

with $v_{D,k}^i = u_{D,k}^i - u_{D,0}^i$. Combining this identity with (2.35), we find

$$
j_{D,j}^i = \sum_{k=1}^{K_i} C_{D,jk}^i \frac{\mathrm{d}v_{D,k}^i}{\mathrm{d}t} - \int_{\Omega^i}\nabla\varphi_j^i\cdot\mathbf{J}^i\, d\mathbf{x}, \tag{2.37}
$$

with

$$
C_{D,jk}^i = \int_{\Omega^i}\epsilon^i\nabla\varphi_j^i\cdot\nabla\varphi_k^i\, d\mathbf{x}. \tag{2.38}
$$

In concise form, we can write:

$$
\mathbf{i}_D = \mathbf{C}_D\frac{\mathrm{d}\mathbf{v}_D}{\mathrm{d}t} + \mathscr{I}_D(\mathbf{J}), \tag{2.39}
$$

with $\mathbf{C}_D = \mathrm{diag}(\mathbf{C}_D^1,\ldots,\mathbf{C}_D^{n_D})$, $\mathbf{C}_D^i = (C_{D,jk}^i) \in \mathbb{R}^{K_i\times K_i}$, and

$$
\mathscr{I}_D(\mathbf{J}) = \begin{pmatrix} \mathscr{I}_D^1(\mathbf{J}^1) \\ \vdots \\ \mathscr{I}_D^{n_D}(\mathbf{J}^{n_D}) \end{pmatrix}, \quad \mathscr{I}_D^i(\mathbf{J}^i) = \begin{pmatrix} \mathscr{I}_1^i(\mathbf{J}^i) \\ \vdots \\ \mathscr{I}_{K_i}^i(\mathbf{J}^i) \end{pmatrix}, \quad \mathscr{I}_j^i(\mathbf{J}^i) = -\int_{\Omega^i}\nabla\varphi_j^i\cdot\mathbf{J}^i\, d\mathbf{x}
$$

for $j = 1,\ldots,K_i$. Using the expression (2.39), the device-to-network coupling relation (2.30) becomes

$$
\boldsymbol{\lambda} = \mathbf{A}_D\,\mathbf{i}_D = \mathbf{A}_D\mathbf{C}_D\frac{\mathrm{d}\mathbf{v}_D}{\mathrm{d}t} + \mathbf{A}_D\mathscr{I}_D(\mathbf{J}). \tag{2.40}
$$

The matrix $\mathbf{C}_D$ is symmetric and positive definite, and can be interpreted as a capacitance matrix [2]. Thus we can write the previous relation as

$$\boldsymbol{\lambda} = \mathbf{A}_D \frac{\mathrm{d}\mathbf{q}_D}{\mathrm{d}t} + \mathbf{A}_D \mathscr{I}_D(\mathbf{J}), \tag{2.41}$$

$$\mathbf{q}_D = \mathbf{C}_D \mathbf{v}_D. \tag{2.42}$$

These relations represent an alternative formulation of the device-to-network coupling relation (2.30), to be used together with the network-to-device coupling relation (2.31).

2.2.1.4 The Drift-Diffusion Model

In what follows we exemplify the coupled equations for an electric network with semiconductor devices, by using a specific distributed model for the devices. For simplicity, we consider an RLC network which contains a single device ($n_D = 1$), with K terminals.

The basic distributed model for semiconductor devices is the drift-diffusion model. In this model, the electric behavior is described in terms of two charge carriers: electrons, with negative elementary charge $q_n = -q$, and holes, with positive elementary charge $q_p = q$. We denote by n, p, respectively, the electron and hole number density. The carrier number densities are coupled with the electric potential ϕ through Poisson's equation

$$-\nabla \cdot (\epsilon \nabla \phi) = \rho_{\mathrm{bi}} + \rho(n, p) \equiv q N_{\mathrm{bi}} - q n + q p, \tag{2.43}$$

with the doping profile N_{bi}, and satisfy the balance laws

$$\frac{\partial n}{\partial t} + \nabla \cdot \mathbf{j}_n = -R, \quad \frac{\partial p}{\partial t} + \nabla \cdot \mathbf{j}_p = -R, \tag{2.44}$$

where $\mathbf{j}_n$, $\mathbf{j}_p$ are the electron and hole density flux, respectively, given by the following constitutive relations:

$$\mathbf{j}_n = -D_n \nabla n + \mu_n n \nabla \phi, \quad \mathbf{j}_p = -D_p \nabla p - \mu_p p \nabla \phi. \tag{2.45}$$

In the previous equations, $R = R(n, p)$ is the recombination-generation term, which is assumed to have the following structure:

$$R(n, p) = F(n, p) \cdot \Big(\frac{np}{n_{\mathrm{i}}^2} - 1 \Big), \tag{2.46}$$

for some rational function $F(n, p)$, with intrinsic concentration n_{i}. In the constitutive relations, D_n, D_p are the electron and hole diffusivity, respectively, and μ_n,

μ_p are the electron and hole mobility, respectively. Diffusivities and mobilities are functions of $(n, p, \mathbf{E}, \mathbf{x})$. Generally, they satisfy the Einstein's relations

$$D_n = V_{\text{th}}\mu_n, \quad D_p = V_{\text{th}}\mu_p,$$

with thermal potential V_{th}.

The drift-diffusion equations (2.43)–(2.45) are considered for $(\mathbf{x}, t) \in \Omega \times I \subset \mathbb{R}^d \times \mathbb{R}$, $I = [t_0, t_e]$, with the following initial-boundary conditions:

- Boundary conditions for the Poisson equation:

$$\begin{cases} \phi = \phi_{\text{bi}} + u_{D,j}(t), & \text{on } \Gamma_{D,j},\ j = 0, 1, \ldots, K, \\ \boldsymbol{\nu} \cdot \nabla\phi = 0, & \text{on } \Gamma_N, \end{cases} \tag{2.47}$$

  where ϕ_{bi} is the built-in potential, given by

$$\phi_{\text{bi}} = V_{\text{th}} \ln\left(\frac{N_{\text{bi}}}{2n_{\text{i}}} + \sqrt{\left(\frac{N_{\text{bi}}}{2n_{\text{i}}}\right)^2 + 1}\right),$$

  $u^i_{D,j}$, $j = 0, 1, \ldots, K$, are the applied potentials at the Ohmic contacts of the device, and $\boldsymbol{\nu}$ is the external unit normal to $\partial\Omega$. Notice that here the time $t \in I$ appears as a parameter, through the boundary data $u_{D,j}(t)$.
- Initial-boundary conditions for the continuity equations:

$$\begin{cases} n = n_{\text{bi}}, \quad p = p_{\text{bi}}, & \text{on } \Gamma_D \times I, \\ \boldsymbol{\nu} \cdot \nabla n = 0, \quad \boldsymbol{\nu} \cdot \nabla p = 0, & \text{on } \Gamma_N \times I, \\ n = n_0, \quad p = p_0, & \text{on } \Omega \times \{t_0\}, \end{cases} \tag{2.48}$$

  where the Dirichlet data n_{bi}, p_{bi} are given by

$$n_{\text{bi}} = \frac{N_{\text{bi}}}{2} + \sqrt{\left(\frac{N_{\text{bi}}}{2}\right)^2 + n_{\text{i}}^2}, \quad p_{\text{bi}} = -\frac{N_{\text{bi}}}{2} + \sqrt{\left(\frac{N_{\text{bi}}}{2}\right)^2 + n_{\text{i}}^2},$$

  and the initial data n_0, p_0 are arbitrary functions. It is interesting to notice the identities $\phi_{\text{bi}} = V_{\text{th}} \ln(n_{\text{bi}}/n_{\text{i}})$, and $n_{\text{bi}} p_{\text{bi}} = n_{\text{i}}^2$.

  The total electric current due to the carriers is:

$$\mathbf{J} = -q\mathbf{j}_n + q\mathbf{j}_p. \tag{2.49}$$

It is possible to show that $\mathbf{J}$ satisfies (2.16), with $\rho = -qn + qp$. Then we can apply the formalism described in the previous subsections.

For convenience of the reader, we write below the full coupled system.

(i) **Network equations**:

$$\begin{aligned} A_C \frac{\mathrm{d}\mathbf{q}}{\mathrm{d}t} + A_R \mathbf{r}(A_R^T \mathbf{u}) + A_L \mathbf{i}_L + A_V \mathbf{i}_V + A_I \mathbf{i}_I + \boldsymbol{\lambda} &= 0, \\ \frac{\mathrm{d}\boldsymbol{\phi}}{\mathrm{d}t} - A_L^T \mathbf{u} &= 0, \\ A_V^T \mathbf{u} - \mathbf{v}_V &= 0. \\ \mathbf{q} - \mathbf{q}_C(A_C^T \mathbf{u}) &= 0, \\ \boldsymbol{\phi} - \boldsymbol{\phi}_L(\mathbf{i}_L) &= 0, \end{aligned} \tag{2.50}$$

with initial data for the differential part,

$$\mathbf{P}_C \mathbf{q}(t_0) = \mathbf{P}_C \mathbf{q}_0, \quad \boldsymbol{\phi}(t_0) = \boldsymbol{\phi}_0, \tag{2.51}$$

where $\mathbf{P}_C$ is projector which picks the component of a vector outside the null-space of the incidence matrix A_C [24]. We also need to assume index-1 conditions, that is, the algebraic equations can be solved uniquely for the remaining variables in terms of the differential variables $\mathbf{P}_C \mathbf{q}$, $\boldsymbol{\phi}$.

(ii) **Poisson equation**:

$$-\nabla \cdot (\epsilon \nabla \phi) = q N_{\mathrm{bi}} - qn + qp, \tag{2.52}$$

with boundary data:

$$\begin{cases} \phi = \phi_{\mathrm{bi}} + u_{D,j}(t), & \text{on } \Gamma_{D,j}, \ j = 0, 1, \ldots, K, \\ \boldsymbol{\nu} \cdot \nabla \phi = 0, & \text{on } \Gamma_N. \end{cases} \tag{2.53}$$

(iii) **Device equations**:

$$\begin{aligned} \frac{\partial n}{\partial t} + \nabla \cdot \mathbf{j}_n &= -R, \\ \frac{\partial p}{\partial t} + \nabla \cdot \mathbf{j}_p &= -R, \\ \mathbf{j}_n &= -D_n \nabla n + \mu_n n \nabla \phi, \\ \mathbf{j}_p &= -D_p \nabla p - \mu_p p \nabla \phi, \end{aligned} \tag{2.54}$$

with initial-boundary data:

$$\begin{cases} n = n_{\mathrm{bi}}, \quad p = p_{\mathrm{bi}}, & \text{on } \Gamma_D \times I, \\ \boldsymbol{\nu} \cdot \nabla n = 0, \quad \boldsymbol{\nu} \cdot \nabla p = 0, & \text{on } \Gamma_N \times I, \\ n = n_0, \quad p = p_0, & \text{on } \Omega \times \{t_0\}. \end{cases} \tag{2.55}$$

(iv) **Network-to-device coupling:**

$$\mathbf{v}_D = \mathbf{A}_D^{*\top} \mathbf{u}_D, \qquad \mathbf{u}_D = \mathbf{S}_D^{\top} \mathbf{u}, \tag{2.56}$$

where

$$\mathbf{A}_D^* = \begin{pmatrix} -1 & \cdots & -1 \\ 1 & \cdots & 0 \\ \vdots & \ddots & \vdots \\ 0 & \cdots & 1 \end{pmatrix}, \quad \mathbf{u}_D = \begin{pmatrix} u_{D,0} \\ u_{D,1} \\ \vdots \\ u_{D,K} \end{pmatrix}.$$

(v) **Device-to-network coupling:**

$$\boldsymbol{\lambda} = \mathbf{A}_D \mathbf{i}_D, \tag{2.57}$$

with $\mathbf{A}_D = \mathbf{S}_D \mathbf{A}_D^*$, and

$$\mathbf{i}_D = \begin{pmatrix} j_{D,1} \\ \vdots \\ j_{D,K} \end{pmatrix}, \qquad j_{D,i} = -\int_{\Gamma_{D,i}} \mathbf{j} \cdot \boldsymbol{\nu} \, d\sigma, \quad i = 1, \ldots, K, \tag{2.58}$$

where

$$\mathbf{j} := \epsilon \frac{\partial}{\partial t} \mathbf{E} - q \mathbf{j}_n + q \mathbf{j}_p.$$

As we have seen, the device-to-network coupling relation can be replaced by the equivalent relation:

(v)′ **Device-to-network coupling (alternative formulation):**

$$\begin{aligned} \boldsymbol{\lambda} &= \mathbf{A}_D \frac{\mathrm{d}\mathbf{q}_D}{\mathrm{d}t} + \mathbf{A}_D \mathscr{I}_D(\mathbf{J}), \\ \mathbf{q}_D &= \mathbf{C}_D \mathbf{v}_D, \end{aligned} \tag{2.59}$$

with $\mathbf{J} = -q\mathbf{j}_n + q\mathbf{j}_p$, and $\mathbf{C}_D = (C_{D,ij}) \in \mathbb{R}^{K\times K}$,

$$C_{D,ij} = \int_\Omega \epsilon \nabla\varphi_i \cdot \nabla\varphi_j \, d\mathbf{x}, \quad i, j = 1, \ldots, K, \tag{2.60}$$

where φ_j are defined by (2.33), and

$$\mathscr{I}_D(\mathbf{J}) = \begin{pmatrix} \mathscr{I}_1(\mathbf{J}) \\ \vdots \\ \mathscr{I}_K(\mathbf{J}) \end{pmatrix}, \quad \mathscr{I}_j(\mathbf{J}) = -\int_\Omega \nabla\varphi_j \cdot \mathbf{J} \, d\mathbf{x}.$$

2.2.1.5 Space Discretization of the Distributed Model: The Gummel Map

In this section we discuss the space discretization of the drift-diffusion model, for later use in the following chapter. We need to address two different topics: (1) space discretization of the PDE model, and (2) derivation of discrete device-to-network coupling relations.

Whatever method we use, the space discretization amounts to replacing the space-dependent unknowns, depending on a continuous variable $\mathbf{x} \in \Omega \subset \mathbb{R}^d$, with corresponding index-dependent unknowns, that is, vector unknowns, depending on an index $i \in \mathscr{I} \subset \mathbb{N}$. At the same time, the space-differential operators appearing in the equations are mapped to finite-dimensional operators on $\mathbb{R}^{|\mathscr{I}|}$, with values on the same space. This mapping procedure is achieved, for finite difference methods or Box Integration methods by discretizing the operator itself, while for finite element methods by "discretizing" the functional space on which the original operator acts, that is, by constructing appropriate finite-dimensional functional spaces with dimension $|\mathscr{I}|$.

Since the starting model is generally nonlinear, the discretization is performed after linearizing the system by iteration. The linearization procedure is better discussed at a continuos level. For simplicity, in this discussion we do not write explicitly the initial-boundary conditions. Let us consider the drift-diffusion equations, written in the form:

$$\begin{aligned} \nabla \cdot \mathbf{D} &= qN_{\text{bi}} - qn + qp, \\ \frac{\partial n}{\partial t} + \nabla \cdot \mathbf{j}_n &= -R, \\ \frac{\partial p}{\partial t} + \nabla \cdot \mathbf{j}_p &= -R, \\ \mathbf{D} &= -\epsilon\nabla\phi, \\ \mathbf{j}_n &= -D_n\nabla n + \mu_n n\nabla\phi, \\ \mathbf{j}_p &= -D_p\nabla p - \mu_p p\nabla\phi, \end{aligned} \tag{2.61}$$

where $\mathbf{D}$ is the electric displacement field. In this formulation, we have singled out the fluxes, and after replacing their expressions in the remaining equations, we get a parabolic-elliptic system of partial differential equations. Nonlinearities are present only in the recombination-generation term R, and in the constitutive equations for the carrier density fluxes $\mathbf{j}_n, \mathbf{j}_p$.

The nonlinearities in the constitutive equations are the more delicate to treat because, roughly speaking, the solution of the drift-diffusion equations tends rapidly to the equilibrium solution, in which there is an exponential relationship between the carrier densities and the electric potential. Thus, in a small region, such as a discretization cell, there might be small variations of the electric field and the carrier density fluxes but big variations of the carrier densities. For this reason, it is not convenient to linearize the system in the form written below, and the natural variables n, p are usually transformed into a different set of variables. The Slotboom variables ρ_n, ρ_p are the most common choice. They are defined by the relations:

$$n = n_{\mathrm{i}} \rho_n \exp\left(\frac{\phi}{V_{\mathrm{th}}}\right), \quad p = n_{\mathrm{i}} \rho_p \exp\left(-\frac{\phi}{V_{\mathrm{th}}}\right), \tag{2.62}$$

where n_{i} is the intrinsic concentration and V_{th} is the thermal potential. In equilibrium, the difference

$$np - n_{\mathrm{i}}^2 = n_{\mathrm{i}}^2(\rho_n \rho_p - 1)$$

is identically zero, so we can conclude that equilibrium is characterized by the product of the Slotboom variables to be equal to 1.

In these new variables, system (2.61) becomes

$$\begin{aligned}
\nabla \cdot \mathbf{D} &= q N_{\mathrm{bi}} - q n_{\mathrm{i}} \rho_n e^{\phi/V_{\mathrm{th}}} + q n_{\mathrm{i}} \rho_p e^{-\phi/V_{\mathrm{th}}}, \\
\frac{\partial}{\partial t}\left(n_{\mathrm{i}} \rho_n e^{\phi/V_{\mathrm{th}}}\right) + \nabla \cdot \mathbf{j}_n &= -R, \\
\frac{\partial}{\partial t}\left(n_{\mathrm{i}} \rho_p e^{-\phi/V_{\mathrm{th}}}\right) + \nabla \cdot \mathbf{j}_p &= -R, \\
\mathbf{D} &= -\epsilon \nabla \phi, \\
\mathbf{j}_n &= -D_n n_{\mathrm{i}} e^{\phi/V_{\mathrm{th}}} \nabla \rho_n, \\
\mathbf{j}_p &= -D_p n_{\mathrm{i}} e^{-\phi/V_{\mathrm{th}}} \nabla \rho_p.
\end{aligned} \tag{2.63}$$

This system is usually solved in three steps, by using an iteration procedure called Gummel map, $(\phi^{k-1}, \rho_n^{k-1}, \rho_p^{k-1}) \mapsto (\phi^k, \rho_n^k, \rho_p^k)$, starting from an initial guess $(\phi^0, \rho_n^0, \rho_p^0)$.

First step We solve the Poisson equation for ϕ^k:

$$\begin{aligned} \nabla \cdot \mathbf{D}^k &= qN_{\rm bi} - qn_{\rm i}\rho_n^{k-1}e^{\phi^k/V_{\rm th}} + qn_{\rm i}\rho_p^{k-1}e^{-\phi^k/V_{\rm th}}, \\ \mathbf{D}^k &= -\epsilon\nabla\phi^k. \end{aligned} \tag{2.64}$$

This is a nonlinear problem, so it can be solved by using a modified Raphson-Newton method, which involves another iteration procedure. Starting from an initial guess $\phi^{[0]}$ which satisfies the boundary conditions, given an approximate solution $\phi^{[i-1]}$, we compute the solution $\phi^{[i]}$, given by

$$\begin{aligned} \phi^{[i]} &= \phi^{[i-1]} + \delta\phi^{[i]}, \\ -\nabla\cdot(\epsilon\nabla\delta\phi^{[i]}) &= -\frac{qn_{\rm i}}{V_{\rm th}}\left(\rho_n^{k-1}e^{\phi^{[i-1]}/V_{\rm th}} + \rho_p^{k-1}e^{-\phi^{[i-1]}/V_{\rm th}}\right)\delta\phi^{[i]} \\ &\quad +\nabla\cdot(\epsilon\nabla\phi^{[i-1]}) + qN_{\rm bi} - qn_{\rm i}\rho_n^{k-1}e^{\phi^{[i-1]}/V_{\rm th}} + qn_{\rm i}\rho_p^{k-1}e^{-\phi^{[i-1]}/V_{\rm th}}. \end{aligned}$$

This equation for $\delta\phi^{[i]}$ is linear and can be discretized and solved by using any appropriate numerical method.

Second step We solve the continuity equation for ρ_n^k:

$$\begin{aligned} \frac{\partial}{\partial t}\left(n_{\rm i}\rho_n^k e^{\phi^k/V_{\rm th}}\right) + \nabla\cdot\mathbf{j}_n^k &= -R_n^k, \\ \mathbf{j}_n^k &= -D_n^k n_{\rm i} e^{\phi^k/V_{\rm th}}\nabla\rho_n^k. \end{aligned} \tag{2.65}$$

Here, the recombination-generation term R_n^k is the usual term R evaluated at ρ_n^{k-1}, ρ_p^{k-1} in such a way to be a linear relaxation term for ρ_n^k. Recalling the general expression (2.46) for $R(n,p)$, it is sufficient to take

$$R_n^k = F(n_{\rm i}\rho_n^{k-1}e^{\phi^{k-1}/V_{\rm th}}, n_{\rm i}\rho_p^{k-1}e^{-\phi^{k-1}/V_{\rm th}})n_{\rm i}^2(\rho_n^k\rho_p^{k-1} - 1).$$

As for the diffusivity D_n^k, it is usually dependent on the electric field $\mathbf{E} = -\nabla\phi$, so it should be evaluated at $\phi = \phi^k$. The resulting equation is linear parabolic for the unknown ρ_n^k, and can be discretized and solved by using any appropriate numerical method.

For the discretization of the constitutive relation for $\mathbf{j}_n^k$, exponential interpolation is the most common choice. The basic example is the Scharfetter-Gummel discretization, which provides a formula for the carrier density flux

$$j_{n,ij}^k := \mathbf{j}_n^k\cdot\mathbf{n}_{ij} \equiv D_n^k n_{\rm i} e^{\phi^k/V_{\rm th}}\frac{{\rm d}\rho_n^k}{{\rm d}s},$$

along the line connecting two adjacent grid points $\mathbf{x}_i, \mathbf{x}_j$. In this definition, the vector $\mathbf{n}_{ij} := \frac{\mathbf{x}_j - \mathbf{x}_i}{|\mathbf{x}_j - \mathbf{x}_i|}$ is the unit vector along the segment $[\mathbf{x}_i, \mathbf{x}_j]$, and the parameter s is the

line element on the same segment, so that $s_j - s_i = |\mathbf{x}_j - \mathbf{x}_i|$. Assuming that the density flux $j^k_{n,ij}$ and the electric field

$$E^k_{ij} := \mathbf{E}^k \cdot \mathbf{n}_{ij} \equiv -\frac{\mathrm{d}\phi^k}{\mathrm{d}s},$$

are approximately constant along the connecting line, we have

$$\begin{aligned}
&\frac{\mathrm{d}}{\mathrm{d}s}\left(D^k_n n_\mathrm{i} e^{\phi^k/V_\mathrm{th}} \frac{\mathrm{d}\rho^k_n}{\mathrm{d}s}\right) = 0, \quad s \in [s_i, s_j],\\
&\rho^k_n(s_i) = \rho^k_{n,i} := \rho^k_n(\mathbf{x}_i), \quad \rho^k_n(s_j) = \rho^k_{n,j} := \rho^k_n(\mathbf{x}_j),
\end{aligned}$$

with

$$\begin{aligned}
&\frac{\mathrm{d}^2\phi^k}{\mathrm{d}s^2} = 0, \quad s \in [s_i, s_j],\\
&\phi^k(s_i) = \phi^k_i := \phi^k(\mathbf{x}_i), \quad \phi^k(s_j) = \phi^k_j := \phi^k(\mathbf{x}_j).
\end{aligned}$$

The result for the electric potential is

$$\frac{\phi^k(s) - \phi^k(s_i)}{s - s_i} = \frac{\phi^k(s_j) - \phi^k(s_i)}{s_j - s_i} \equiv -E^k_{ij},$$

and thus, assuming that the diffusivity depends only on the electric field, we find

$$j^k_{n,ij} = D^k_{n,ij} n_\mathrm{i} e^{\phi^k_i/V_\mathrm{th}} B\left(\frac{\phi^k_i - \phi^k_j}{V_\mathrm{th}}\right) \frac{\rho^k_{n,j} - \rho^k_{n,i}}{|\mathbf{x}_j - \mathbf{x}_i|}, \tag{2.66}$$

where $D^k_{n,ij} = D_n(E^k_{ij})$, and B is the Bernoulli function,

$$B(z) = \begin{cases} \frac{z}{e^z - 1}, & \text{if } z \neq 0,\\ 1, & \text{if } z = 0. \end{cases}$$

Third step We solve the continuity equation for ρ^k_p:

$$\begin{aligned}
\frac{\partial}{\partial t}\left(n_\mathrm{i}\rho^k_p e^{-\phi^k/V_\mathrm{th}}\right) + \nabla\cdot\mathbf{j}^k_p &= -R^k_p,\\
\mathbf{j}^k_p &= -D^k_p n_\mathrm{i} e^{-\phi^k/V_\mathrm{th}} \nabla\rho^k_p,
\end{aligned} \tag{2.67}$$

with

$$R^k_p = F(n_\mathrm{i}\rho^{k-1}_n e^{\phi^{k-1}/V_\mathrm{th}}, n_\mathrm{i}\rho^{k-1}_p e^{-\phi^{k-1}/V_\mathrm{th}}) n^2_\mathrm{i}(\rho^k_n\rho^k_p - 1).$$

As before, the diffusivity D_p^k is evaluated at $\phi = \phi^k$. This equation is linear parabolic for the unknown ρ_p^k, and can be discretized and solved by using any appropriate numerical method. A Scharfetter-Gummel discretization for the hole density flux $\mathbf{j}_p^k$ can be derived using a similar argument as before. The result is

$$j_{p,ij}^k = D_{p,ij}^k n_{\mathrm{i}} e^{-\phi_i^k / V_{\mathrm{th}}} B\left(\frac{\phi_j^k - \phi_i^k}{V_{\mathrm{th}}}\right) \frac{\rho_{n,i}^k - \rho_{n,j}^k}{|\mathbf{x}_j - \mathbf{x}_i|}, \tag{2.68}$$

with obvious notation.

The Gummel map generally converges after few iterations. Instead of separating the original nonlinear problem in three subproblems, it is also possible to apply a Newton-like method to the full system. In either case, we end up with a sequence of linear problems that can be thought as a method for solving a nonlinear differential algebraic system. As we have seen in the description of the Gummel map, it is not simple to obtain an explicit representation of this differential algebraic system, nor is it relevant to know it. In fact, what really matters is the convergence and stability of the method.

For later use in the next chapter, it is nevertheless useful to have at least an explicit example. For this reason we derive a space-discretized system by using the Box Integration method [27, 60]. The discretized coupling conditions will be discussed diffusely for this example, since the general treatment follows along the same line.

2.2.1.6 Space Discretization of the Distributed Model: The Box Integration Method

The Box Integration method consists of two sets of equations – a set of exact equations for the fluxes on the boundaries of the Voronoi cells of a numerical grid, and a set of approximate equations for the fluxes in terms of the value of the unknown function on the grid points. In addition, we need discrete equations for supplementing the boundary conditions. To exemplify the Box Integration method, first we give a rough sketch of its application for the Poisson equation, and then we just show the result of the method for the continuity equations.

Some notation, first. We consider a tessellation $\mathscr{T}_h$ of the domain Ω, which might be a Delaunnay triangulation, a rectangular grid, or a hybrid grid, with vertices (grid points) $\mathscr{X}_h = \{\mathbf{x}_1, \ldots, \mathbf{x}_N\}$ and edges $\mathscr{E}_h = \{e_1, \ldots, e_M\}$. We also consider the set of the internal grid points, $\mathscr{X}_h' = \{\mathbf{x}_1, \ldots, \mathbf{x}_{N'}\}$, and the set $\mathscr{E}_h' = \{e_1, \ldots, e_{M'}\}$ of the internal edges, for which at least one of the two end vertices is internal. We denote by $e_{ij} \in \mathscr{E}_h$ the edge which connects the grid points $\mathbf{x}_i, \mathbf{x}_j \in \mathscr{E}_h$. For each grid point $\mathbf{x}_i$, we introduce the set of indices $I(i)$ of the neighboring grid points, that is, $j \in I(i)$ if and only if $e_{ij} \in \mathscr{X}_h$.

We consider the Dirichlet tessellation $\mathscr{D}_h$, dual to $\mathscr{T}_h$, made of the Dirichlet (or Voronoi) cells of the grid points $\mathscr{X}_h$, and we denote by $\mathscr{D}_h'$ the Dirichlet tessellation corresponding to the internal grid points $\mathscr{X}_h'$. We denote by $V_i \in \mathscr{D}_h$ the Voronoi

cell of the grid point $\mathbf{x}_i \in \mathscr{X}_h$. The Voronoi cell V_i has at most as many faces as the cardinality of $I(i)$, and we use the notation $v_{ij} = V_i \cap V_j$, $j \in I(i)$. The face v_{ij}, whenever the area $|v_{ij}| \neq 0$, is orthogonal to e_{ij} for any $j \in I(i)$, and equidistant from $\mathbf{x}_i$ and $\mathbf{x}_j$, so the external unit normal on v_{ij}, external with respect to V_i, is $\mathbf{n}_{ij} = \frac{\mathbf{x}_j - \mathbf{x}_i}{|\mathbf{x}_j - \mathbf{x}_i|}$, which we have already encountered when discussing the Scharfetter-Gummel discretization.

Now we are ready to apply the Box Integration method to the Poisson equation

$$\nabla \cdot \mathbf{D} = \rho := qN_{\mathrm{bi}} - qn_{\mathrm{i}}\rho_n e^{\phi/V_{\mathrm{th}}} + qn_{\mathrm{i}}\rho_p e^{-\phi/V_{\mathrm{th}}},$$

$$\mathbf{D} = -\epsilon\nabla\phi,$$

with $\rho = \rho(\mathbf{x}, \rho_n, \rho_p, \phi)$. Integrating the first equation on the internal Voronoi cell $V_i \in \mathscr{D}_h'$, and using the divergence theorem, we get:

$$\sum_{j\in I(i)} \int_{v_{ij}} \mathbf{D}\cdot\mathbf{n}_{ij}\,\mathrm{d}\sigma = \int_{V_i} \rho\,\mathrm{d}\mathbf{x}, \qquad i = 1,\ldots,N'. \tag{2.69}$$

These exact equations are approximated as

$$\sum_{j\in I(i)} |v_{ij}| D_{ij} = |V_i|\rho_i, \qquad i = 1,\ldots,N', \tag{2.70}$$

where $D_{ij} := \mathbf{D}\cdot\mathbf{n}_{ij}$ is evaluated on the mid point of the edge e_{ij}, that is, on $\mathbf{x}_{ij} := \frac{1}{2}(\mathbf{x}_i + \mathbf{x}_j)$, and the index i in the source term denotes evaluation on $\mathbf{x}_i$, in all its arguments.

Next, we need to approximate the flux D_{ij}, and this is done by assuming that the electric field is constant along the edge e_{ij}. Then, we can derive the expression

$$D_{ij} = -\epsilon_{ij}\frac{\phi_j - \phi_i}{|e_{ij}|}, \qquad j \in I(i), \quad i = 1,\ldots,N', \tag{2.71}$$

where the dielectric constant is evaluated on $\mathbf{x}_{ij}$, and is generally approximated by $\epsilon_{ij} \approx \frac{1}{2}(\epsilon_i + \epsilon_j)$.

Using (2.71) in (2.70), we find

$$\sum_{j\in I(i)} |v_{ij}|\epsilon_{ij}\frac{\phi_i - \phi_j}{|e_{ij}|} = |V_i|\rho_i, \qquad i = 1,\ldots,N', \tag{2.72}$$

which is a nonlinear system of N' equations for the N unknowns $\phi_1,\ldots,\phi_N$. In compact form, we can write

$$\mathbf{A}_\phi\boldsymbol{\phi} + \mathbf{A}_\phi^\partial\boldsymbol{\phi}^\partial = \mathbf{b}_\phi(\boldsymbol{\phi}, \boldsymbol{\rho}_n, \boldsymbol{\rho}_p), \tag{2.73}$$

with $\boldsymbol{\phi} = (\phi_1, \ldots, \phi_{N'})^\top$, $\boldsymbol{\phi}^\partial = (\phi_{N'+1}, \ldots, \phi_N)^\top$. This equation is the discrete analog of the Poisson equation.

The remaining $N - N'$ equations, needed to determine the unknowns, come from the boundary conditions. We have $N - N' = N_D + N_N$, where N_D is the number of nodes on Γ_D, and N_N the number of nodes on Γ_N. It is simple to impose N_D Dirichlet conditions,

$$\phi_i = \phi_{\mathrm{bi},i} + u_{D,k}, \quad \text{if } \mathbf{x}_i \in \Gamma_{D,k}. \tag{2.74}$$

It is a bit more complicated to impose N_N Neumann conditions, at least in the framework of the Box Integration method. A possible way of doing it, is by using a BDF formula for expressing the normal derivative on a Neumann grid point in terms of inner grid points along the normal direction, possibly with the help of some interpolation. Whatever method we use, we end up with N_N equations of the form

$$\phi_i + \sum_{j=1}^{N'} a_{ij}\phi_j = 0, \quad \text{if } \mathbf{x}_i \in \Gamma_N, \tag{2.75}$$

with many zero coefficients. Combining Eqs. (2.74) and (2.75), we can write them in the compact form

$$\mathbf{A}^\partial \boldsymbol{\phi} + \boldsymbol{\phi}^\partial = \mathbf{b}_\phi^\partial(\mathbf{u}_D). \tag{2.76}$$

We notice that the matrix $\mathbf{A}^\partial$ does not depend on the differential equation but only on the tessellation $\mathscr{T}_h$ and on the formula used for expressing the normal derivative with respect to the internal nodes. Equation (2.76) is the discrete analogue of the boundary conditions for the Poisson equation, and together with (2.73) form a set of equations which can be solved for $\boldsymbol{\phi}$ and $\boldsymbol{\phi}^\partial$.

We can apply the same procedure to the electron continuity equation,

$$\begin{aligned} \frac{\partial n}{\partial t} + \nabla \cdot \mathbf{j}_n &= -R, \\ \mathbf{j}_n &= -D_n n_\mathrm{i} e^{\phi/V_\mathrm{th}} \nabla \rho_n, \end{aligned} \tag{2.77}$$

and to the hole continuity equation,

$$\begin{aligned} \frac{\partial p}{\partial t} + \nabla \cdot \mathbf{j}_p &= -R, \\ \mathbf{j}_p &= -D_p n_\mathrm{i} e^{-\phi/V_\mathrm{th}} \nabla \rho_p, \end{aligned} \tag{2.78}$$

with n, p given in terms of ρ_n, ρ_p and ϕ by (2.62). Using the Scharfetter-Gummel discretization (2.66) and (2.68) for the fluxes, we obtain the discretized equations

$$\begin{aligned} |V_i|\frac{\mathrm{d}n_i}{\mathrm{d}t} + \sum_{j\in I(i)} |v_{ij}| j_{n,ij} &= -|V_i| R_i, \\ j_{n,ij} &= D_{n,ij} n_{\mathrm{i}} e^{\phi_i/V_{\mathrm{th}}} B\left(\frac{\phi_i - \phi_j}{V_{\mathrm{th}}}\right) \frac{\rho_{n,j} - \rho_{n,i}}{|e_{ij}|}, \quad j \in I(i), \end{aligned} \tag{2.79}$$

and

$$\begin{aligned} |V_i|\frac{\mathrm{d}p_i}{\mathrm{d}t} + \sum_{j\in I(i)} |v_{ij}| j_{p,ij} &= -|V_i| R_i, \\ j_{p,ij} &= D_{p,ij} n_{\mathrm{i}} e^{-\phi_i/V_{\mathrm{th}}} B\left(\frac{\phi_j - \phi_i}{V_{\mathrm{th}}}\right) \frac{\rho_{n,i} - \rho_{n,j}}{|e_{ij}|}, \quad j \in I(i), \end{aligned} \tag{2.80}$$

with $i = 1, \ldots, N'$. To these equations we need to add the discrete Dirichlet and Neumann boundary conditions for both equations,

$$\rho_{n,i} = e^{-u_{D,k}/V_{\mathrm{th}}}, \quad \text{if } \mathbf{x}_i \in \Gamma_{D,k}, \tag{2.81}$$

$$\rho_{n,i} + \sum_{j=1}^{N'} a_{ij}\rho_{n,j} = 0, \quad \text{if } \mathbf{x}_i \in \Gamma_N, \tag{2.82}$$

and

$$\rho_{p,i} = e^{u_{D,k}/V_{\mathrm{th}}}, \quad \text{if } \mathbf{x}_i \in \Gamma_{D,k}, \tag{2.83}$$

$$\rho_{p,i} + \sum_{j=1}^{N'} a_{ij}\rho_{p,j} = 0, \quad \text{if } \mathbf{x}_i \in \Gamma_N. \tag{2.84}$$

In compact form, the spatially discrete continuity equations can be written as:

$$\mathbf{A}_0 \frac{\mathrm{d}\boldsymbol{n}(\boldsymbol{\phi}, \boldsymbol{\rho}_n)}{\mathrm{d}t} + \mathbf{A}_n(\boldsymbol{\phi})\boldsymbol{\rho}_n + \mathbf{A}_n^{\partial}(\boldsymbol{\phi})\boldsymbol{\rho}_n^{\partial} = \mathbf{b}_n(\boldsymbol{\phi}, \boldsymbol{\rho}_n, \boldsymbol{\rho}_p), \tag{2.85}$$

$$\mathbf{A}^{\partial}\boldsymbol{\rho}_n + \boldsymbol{\rho}_n^{\partial} = \mathbf{b}_n^{\partial}(\mathbf{u}_D), \tag{2.86}$$

$$\mathbf{A}_0 \frac{\mathrm{d}\boldsymbol{p}(\boldsymbol{\phi}, \boldsymbol{\rho}_p)}{\mathrm{d}t} + \mathbf{A}_p(\boldsymbol{\phi})\boldsymbol{\rho}_p + \mathbf{A}_p^{\partial}(\boldsymbol{\phi})\boldsymbol{\rho}_p^{\partial} = \mathbf{b}_p(\boldsymbol{\phi}, \boldsymbol{\rho}_n, \boldsymbol{\rho}_p), \tag{2.87}$$

$$\mathbf{A}^{\partial}\boldsymbol{\rho}_p + \boldsymbol{\rho}_p^{\partial} = \mathbf{b}_p^{\partial}(\mathbf{u}_D), \tag{2.88}$$

with notation analogous to the one used for the discretized Poisson equation (2.73) and (2.76). Besides the presence of the time derivative, the main difference is that now the matrices corresponding to the elliptic operators, that is, $\mathbf{A}_n$ and $\mathbf{A}_p$, depend nonlinearly on the electric potential.

We notice that, within the Box Integration method framework, other spatial discretizations are possible. In particular, we can start from the drift-diffusion system written for the natural variables ϕ, n, p. In this case, the discrete Poisson equation becomes linear and it is possible to write the Scharfetter-Gummel discretization for $j_{n,ij}$ as a linear combination of n_i, n_j, with coefficients depending nonlinearly on the electric potential,

$$j_{n,ij} = \frac{D_{n,ij}}{|e_{ij}|}\left(B\left(\frac{\phi_j - \phi_i}{V_{\text{th}}}\right)n_j - B\left(\frac{\phi_i - \phi_j}{V_{\text{th}}}\right)n_i\right), \tag{2.89}$$

$$j_{p,ij} = \frac{D_{p,ij}}{|e_{ij}|}\left(B\left(\frac{\phi_i - \phi_j}{V_{\text{th}}}\right)p_j - B\left(\frac{\phi_j - \phi_i}{V_{\text{th}}}\right)p_i\right). \tag{2.90}$$

Then, we obtain a linear ordinary differential equation for $\boldsymbol{n}$, with coefficients depending nonlinearly on the electric potential, and similarly for $\boldsymbol{p}$. This form looks much simpler than the one we have derived above, but it becomes unstable if we try to decouple the three main problems by iteration, as in the Gummel map. Nevertheless it can be used if the system is solved by Newton iteration, without using the Gummel map. For this reason, we will apply it in the next chapter, and we summarize it as follows:

$$\mathbf{A}_\phi \boldsymbol{\phi} + \mathbf{A}_\phi^\partial \boldsymbol{\phi}^\partial = \mathbf{b}_\phi(\boldsymbol{n}, \boldsymbol{p}), \tag{2.91}$$

$$\mathbf{A}^\partial \boldsymbol{\phi} + \boldsymbol{\phi}^\partial = \mathbf{b}_\phi^\partial(\mathbf{u}_D), \tag{2.92}$$

$$\mathbf{A}_0 \frac{\mathrm{d}\boldsymbol{n}}{\mathrm{d}t} + \mathbf{A}_n(\boldsymbol{\phi})\boldsymbol{n} + \mathbf{A}_n^\partial(\boldsymbol{\phi})\boldsymbol{n}^\partial = \mathbf{b}_n(\boldsymbol{n}, \boldsymbol{p}), \tag{2.93}$$

$$\mathbf{A}^\partial \boldsymbol{n} + \boldsymbol{n}^\partial = \mathbf{b}_n^\partial, \tag{2.94}$$

$$\mathbf{A}_0 \frac{\mathrm{d}\boldsymbol{p}}{\mathrm{d}t} + \mathbf{A}_p(\boldsymbol{\phi})\boldsymbol{p} + \mathbf{A}_p^\partial(\boldsymbol{\phi})\boldsymbol{p}^\partial = \mathbf{b}_p(\boldsymbol{n}, \boldsymbol{p}), \tag{2.95}$$

$$\mathbf{A}^\partial \boldsymbol{p} + \boldsymbol{p}^\partial = \mathbf{b}_p^\partial. \tag{2.96}$$

Note that Eqs. (2.94) and (2.96) do not depend on $\mathbf{u}_D$, because the Dirichlet boundary conditions for the variables n, p are now given by (2.55).

2.2.1.7 Space Discretization of the Distributed Model: The Coupling Conditions

The last item to be discussed is the coupling conditions with the network. The network-to-device coupling condition is immediate, because the term $\mathbf{b}_\phi^\partial$ (in the formulation with the Slotboom variables, also $\mathbf{b}_n^\partial$ and $\mathbf{b}_p^\partial$) depends on the applied potentials $\mathbf{u}_D$, which are related to the network node potentials by the coupling relation (2.56). The device-to-network coupling is more delicate, because we need to introduce the discretized current transmitted to the network through the k-th Ohmic contact, $\Gamma_{D,k}$, $k = 1, \ldots, K$.

First, we implement the coupling condition as in (2.57). At this aim, we consider the Voronoi cells V_i corresponding to grid nodes $\mathbf{x}_i$ in $\Gamma_{D,k}$, and we integrate the charge conservation equation on the union of these Voronoi cells, $V_{D,k} = \bigcup_{\mathbf{x}_i \in \Gamma_{D,k}} V_i$:

$$\int_{V_{D,k}} \left[\frac{\partial}{\partial t}(-qn + qp) + \nabla \cdot (-q\mathbf{j}_n + q\mathbf{j}_p) \right] \mathrm{d}\mathbf{x} = 0. \tag{2.97}$$

Using Poisson's equation, we find

$$\frac{\partial}{\partial t}(-qn + qp) = \nabla \cdot \frac{\partial \mathbf{D}}{\partial t}, \qquad \mathbf{D} = \epsilon \mathbf{E} = -\epsilon \nabla \phi.$$

Then, by the divergence theorem, we can write

$$\begin{aligned}
\int_{V_{D,k}} \nabla \cdot \left[\frac{\partial \mathbf{D}}{\partial t} - q\mathbf{j}_n + q\mathbf{j}_p \right] \mathrm{d}\mathbf{x} &= \int_{\partial V_{D,k}} \mathbf{n} \cdot \left[\frac{\partial \mathbf{D}}{\partial t} - q\mathbf{j}_n + q\mathbf{j}_p \right] \mathrm{d}\sigma \\
&= \int_{\partial V_{D,k} \cap \partial \Omega} \mathbf{n} \cdot \left[\frac{\partial \mathbf{D}}{\partial t} - q\mathbf{j}_n + q\mathbf{j}_p \right] \mathrm{d}\sigma \\
&\quad + \int_{\partial V_{D,k} \setminus \partial \Omega} \mathbf{n} \cdot \left[\frac{\partial \mathbf{D}}{\partial t} - q\mathbf{j}_n + q\mathbf{j}_p \right] \mathrm{d}\sigma = 0.
\end{aligned}$$

The first integral is approximately the outer current flux through the Ohmic contact $\Gamma_{D,k}$, that is, with our convention,

$$\int_{\partial V_{D,k} \cap \partial \Omega} \mathbf{n} \cdot \left[\frac{\partial \mathbf{D}}{\partial t} - q\mathbf{j}_n + q\mathbf{j}_p \right] \mathrm{d}\sigma \approx -j_{D,k}.$$

The maximum error in this approximation occurs when the grid points on $\Gamma_{D,k}$ closer to the neighboring Neumann boundary are located on the junction between Dirichlet and Neumann boundary, in which case $\partial V_{D,k} \cap \partial \Omega$ consists of $\Gamma_{D,k}$ bordered with a strip whose thickness is the order of half the diameter of the Voronoi cells. On the other hand, we can write

$$\begin{aligned}
&\int_{\partial V_{D,k} \setminus \partial \Omega} \mathbf{n} \cdot \left[\frac{\partial \mathbf{D}}{\partial t} - q\mathbf{j}_n + q\mathbf{j}_p \right] \mathrm{d}\sigma \\
&\quad = \sum_{\mathbf{x}_i \in \Gamma_{D,k}} \sum_{\substack{j \in I(i) \\ \mathbf{x}_j \notin \Gamma_{D,k}}} \int_{v_{ij}} \mathbf{n}_{ij} \cdot \left[\frac{\partial \mathbf{D}}{\partial t} - q\mathbf{j}_n + q\mathbf{j}_p \right] \mathrm{d}\sigma \\
&\quad \approx \sum_{\mathbf{x}_i \in \Gamma_{D,k}} \sum_{\substack{j \in I(i) \\ \mathbf{x}_j \notin \Gamma_{D,k}}} |v_{ij}| \left[\frac{\mathrm{d}D_{ij}}{\mathrm{d}t} - qj_{n,ij} + qj_{p,ij} \right],
\end{aligned}$$

where D_{ij}, $j_{n,ij}$, $j_{p,ij}$ are defined as in (2.71) and (2.79), (2.80), or (2.89), (2.90). Combining the previous relations we find the approximation

$$j_{D,k} = \sum_{\mathbf{x}_i \in \Gamma_{D,k}} \sum_{\substack{j \in I(i) \\ \mathbf{x}_j \notin \Gamma_{D,k}}} |v_{ij}| \left[\frac{\mathrm{d}D_{ij}}{\mathrm{d}t} - q j_{n,ij} + q j_{p,ij} \right], \tag{2.98}$$

which can be used as device-to-network discrete coupling condition. In short, recalling the definition of the coupling term $\boldsymbol{\lambda}$, we can write

$$\boldsymbol{\lambda} = \mathbf{A}_D \mathbf{i}_D, \quad \mathbf{i}_D = \mathbf{A}^c \frac{\mathrm{d}\boldsymbol{\phi}}{\mathrm{d}t} + \mathbf{A}_n^c(\boldsymbol{\phi})\mathbf{n} + \mathbf{A}_p^c(\boldsymbol{\phi})\mathbf{p}. \tag{2.99}$$

We note that in this coupling condition, the time derivative of D_{ij} occurs, that is, the time derivative of $\boldsymbol{\phi}$, which is an "algebraic variable" for the discretized device equations with no coupling.

Next, we formulate the discrete version of the alternative formulation of the device-to-network coupling conditions (2.59). We need to evaluate the capacitance matrix $\mathbf{C}_D$, defined by (2.60), and to formulate the discrete version of the operator $\mathscr{I}_k(\mathbf{J})$ appearing in (2.59). As for the capacitance matrix, we can write

$$\begin{aligned} C_{D,kl} &= \sum_{i=1}^{N} \int_{V_i} \epsilon \nabla \varphi_k \cdot \nabla \varphi_l \, d\mathbf{x} \\ &= \sum_{i=1}^{N} \left[\int_{\partial V_i} \epsilon \varphi_k \nabla \varphi_l \cdot \mathbf{n} \, \mathrm{d}\sigma - \int_{V_i} \varphi_k \nabla \cdot (\epsilon \nabla \varphi_l) \, d\mathbf{x} \right] \\ &= \sum_{i=1}^{N} \int_{\partial V_i} \epsilon(\varphi_k - \varphi_{k,i}) \nabla \varphi_l \cdot \mathbf{n} \, \mathrm{d}\sigma, \end{aligned}$$

where φ_j are defined by (2.33), and $\varphi_{k,i} = \varphi_k(\mathbf{x}_i)$. The last equality follows because $\nabla \cdot (\epsilon \nabla \varphi_l)$ is identically zero due to the definition of φ_l. If $\mathbf{x}_i \in \mathscr{X}_h'$, this integral can be approximated by

$$\begin{aligned} \int_{\partial V_i} \epsilon(\varphi_k - \varphi_{k,i}) \nabla \varphi_l \cdot \mathbf{n} \, \mathrm{d}\sigma &= \sum_{j \in I(i)} \int_{v_{ij}} \epsilon(\varphi_k - \varphi_{k,i}) \nabla \varphi_l \cdot \mathbf{n}_{ij} \, \mathrm{d}\sigma \\ &\approx \sum_{j \in I(i)} |v_{ij}| \epsilon_{ij} (\varphi_{k,ij} - \varphi_{k,i}) \frac{\varphi_{l,j} - \varphi_{l,i}}{|e_{ij}|}, \end{aligned}$$

with $\epsilon_{ij} = \epsilon(\mathbf{x}_{ij}) \approx \frac{1}{2}(\epsilon_i + \epsilon_j)$, $\varphi_{k,ij} = \varphi_k(\mathbf{x}_{ij}) \approx \frac{1}{2}(\varphi_{k,i} + \varphi_{k,j})$. Then, we find the following approximation:

$$\int_{V_i} \epsilon \nabla\varphi_k \cdot \nabla\varphi_l \, d\mathbf{x} \approx \sum_{j\in I(i)} \frac{|v_{ij}|}{2|e_{ij}|}\epsilon_{ij}(\varphi_{k,j} - \varphi_{k,i})(\varphi_{l,j} - \varphi_{l,i}). \tag{2.100}$$

If $\mathbf{x}_i \in \mathscr{X}_h \cap \partial\Omega$, we have

$$\begin{aligned}\int_{\partial V_i} \epsilon(\varphi_k - \varphi_{k,i})\nabla\varphi_l \cdot \mathbf{n}\,\mathrm{d}\sigma = &\sum_{j\in I(i)} \int_{v_{ij}} \epsilon(\varphi_k - \varphi_{k,i})\nabla\varphi_l \cdot \mathbf{n}_{ij}\,\mathrm{d}\sigma \\ &+ \int_{\partial V_i\cap\partial\Omega} \epsilon(\varphi_k - \varphi_{k,i})\nabla\varphi_l \cdot \mathbf{n}\,\mathrm{d}\sigma.\end{aligned}$$

The second integral vanishes because either $\nabla\varphi_l \cdot \mathbf{n} = 0$, if V_i touches the Neumann boundary, or $\varphi_k - \varphi_{k,i} = 0$, if V_i touches a Dirichlet boundary, so we are led to the same approximation (2.100).

In conclusion, the capacitance matrix is approximated by

$$\tilde{C}_{D,kl} = \sum_{i=1}^{N} \sum_{j\in I(i)} \frac{|v_{ij}|}{2|e_{ij}|}\epsilon_{ij}(\varphi_{k,j} - \varphi_{k,i})(\varphi_{l,j} - \varphi_{l,i}). \tag{2.101}$$

In a similar way, we can approximate $\mathscr{I}_k(\mathbf{J})$. We can write

$$\begin{aligned}\mathscr{I}_k(\mathbf{J}) &= -\sum_{i=1}^{N} \int_{V_i} \nabla\varphi_k \cdot \mathbf{J}\, d\mathbf{x} \\ &= -\sum_{i=1}^{N} \left[\int_{\partial V_i} \varphi_k \mathbf{J}\cdot\mathbf{n}\,\mathrm{d}\sigma - \int_{V_i} \varphi_k \nabla\cdot\mathbf{J}\, d\mathbf{x}\right] \\ &\approx -\sum_{i=1}^{N} \int_{\partial V_i} (\varphi_k - \varphi_{k,i})\mathbf{J}\cdot\mathbf{n}\,\mathrm{d}\sigma,\end{aligned}$$

so an approximation is given by

$$\tilde{\mathscr{I}}_k = -\sum_{i=1}^{N} \sum_{j\in I(i)} \frac{|v_{ij}|}{2}(\varphi_{k,j} - \varphi_{k,i})(-qj_{n,ij} + qj_{p,ij}). \tag{2.102}$$

In short, the coupling conditions can be written as:

$$\begin{aligned} \boldsymbol{\lambda} &= \mathbf{A}_D \frac{\mathrm{d}\mathbf{q}_D}{\mathrm{d}t} + \mathbf{A}_D \tilde{\mathscr{I}}_D, \quad \tilde{\mathscr{I}}_D = \mathbf{A}_n^c(\boldsymbol{\phi})\mathbf{n} + \mathbf{A}_p^c(\boldsymbol{\phi})\mathbf{p}, \\ \mathbf{q}_D &= \tilde{\mathbf{C}}_D \mathbf{v}_D \equiv \tilde{\mathbf{C}}_D \mathbf{A}_D^\top \mathbf{u}. \end{aligned} \tag{2.103}$$

2.2.2 Electro-Thermal Effects at the System Level

The typical trend associating new technology generations with a reduced power consumption has been reversed in the last decade making an accurate electro-thermal analysis of ICs a necessity for a reliable and cost-effective design. To support this need computer aided design (CAD) tools must provide dependable means to simulate coupled electro-thermal effects.

The development of a robust algorithm for this purpose requires a high degree of integration inside usual industrial design flows to be effectively usable, and the possibility to account for 2D/3D heat diffusion to properly describe thermal effects at the system level. In particular it should allow an efficient handling of the space-time multiscale effects associated with the problem at hand. Figure 2.1 shows a brief sketch of a new strategy (originally proposed in [20]) to automatically perform system level electro-thermal simulations inside an industrial design flow.

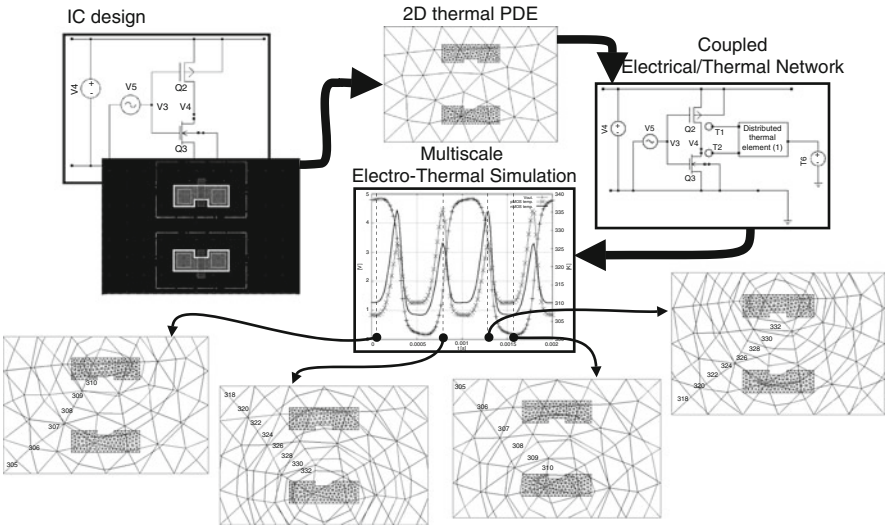

Fig. 2.1 Automated design flow for the electro-thermal simulation of ICs. A thermal element model is automatically constructed from available circuit schematic and design layout, permitting the set-up and simulation of an electro-thermal network that accounts for heat diffusion at the system level

In this approach the electrical behavior of possibly each circuit element is modeled by standard compact models with an added temperature node. Mutual heating is then accounted for by a *novel circuital element* embedding a 2D or 3D diffusion-reaction partial differential equation (PDE) in its constitutive relations to describe heat-diffusion on a distributed domain. By imposing suitable integral conditions this element is casted in a form analogous to that of usual electrical circuit elements, so that its use in a standard circuit simulator requires only the implementation of a new element evaluator, but no modification to the main structure of the solver. This permits the automatic set-up and simulation of an electro-thermal network that accounts for heat diffusion at the system level.

2.2.2.1 Definition of the PDE-Based Thermal Element Model

A suitable thermal element balancing power fluxes at junction temperature nodes is required to extend a purely electrical description of a circuit to an electro-thermal one. In the following it is shown how a multiscale model that fits such a purpose can be derived starting from information that are readily available during IC design phase, i.e. 2D or 3D layout geometry and possibly 3D package geometry.

As sketched in Fig. 2.2 this information is used to describe the overall physical region where to simulate thermal effects as an open, bounded domain:

$$\Omega \subset \mathbb{R}^d \quad (d = 2, 3),$$

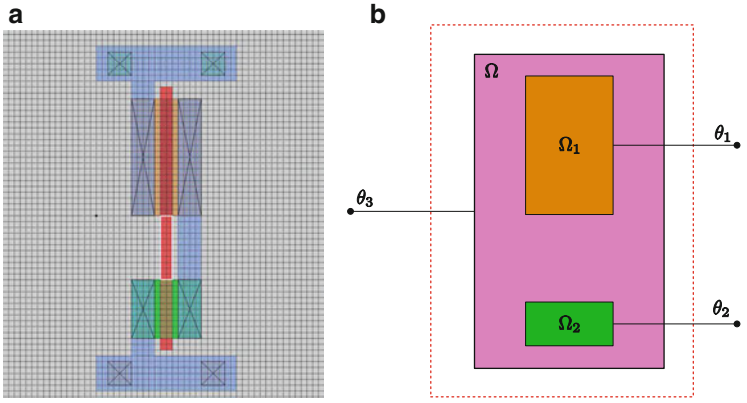

Fig. 2.2 Layout or package information from IC design are automatically converted into a geometrical description of the domains in which suitable PDEs describing heat diffusion at the system level are casted. Notice that while θ_1 and θ_2 refer to mean temperature values over Ω_1 and Ω_2 respectively, θ_3 represents ambient temperature. (**a**) Inverter layout. (**b**) Extracted geometry

and to associate each thermally active device with a subset related to its layout positioning:

$$\Omega_k \subset \Omega \text{ for } k = 1, \ldots, K$$

where its power flux is supposed to be dissipated. Each subset is required one to fulfill the following properties:

$$\begin{aligned} \texttt{int}(\Omega_k) &\neq \emptyset \qquad && \forall k = 1, \ldots, K, \\ \bar{\Omega}_k &\subset \Omega \qquad && \forall k = 1, \ldots, K, \\ \bar{\Omega}_k \cap \bar{\Omega}_j &= \emptyset \ \forall j, k = 1, \ldots, K, \quad k \neq j. \end{aligned}$$

Furthermore it is supposed for either Ω and Ω_k $(k = 1, \ldots, K)$ to have Lipschitz boundary. The unknowns considered in the thermal element model are the junction temperature vector:

$$\boldsymbol{\theta} = [\theta_1, \ldots, \theta_{K+1}]^T ,$$

where the first K components are associated with each subset region while the last one represents ambient temperature, the power density vector:

$$\mathbf{p} = [p_1, \ldots, p_K]^T ,$$

where each component represents the Joule power per unit area dissipated in each region and the distributed temperature field $T(\mathbf{x}, t)$ on Ω.

Assuming $(\cdot, \cdot)$ to denote the usual $\mathbb{L}^2(\Omega)$ scalar product and $\mathbf{1}_{\Omega_k}$ to denote the indicator function of the set Ω_k, then the distributed temperature field $T(\mathbf{x}, t)$ is linked to junction temperature nodes through:

$$\frac{1}{|\Omega_k|}(T, \mathbf{1}_{\Omega_k}) = \theta_k \text{ for } k = 1, \ldots, K,$$

i.e. θ_k represents the mean value over Ω_k of $T(\mathbf{x}, t)$. In the same way the power flux entering each node is related to the Joule power per unit area via:

$$(p_k, \mathbf{1}_{\Omega_k}) = p_k |\Omega_k| = P_k \text{ for } k = 1, \ldots, K.$$

The total power P_k dissipated over Ω_k is thus equal, for every fixed time instant, to the product of a mean power density p_k times the area of each active region $|\Omega_k|$. Finally the power flux to ambient temperature node is defined to be:

$$P_{K+1} = -\sum_{k=1}^{K} p_k |\Omega_k|.$$

to ensure energy conservation inside the thermal element. Though the decisions to uniformly distribute the dissipated power P_k inside Ω_k and define θ_k as the mean temperature over Ω_k are somehow arbitrary, they constitute a sound physical approximation at a macro-scale level, if it is considered that usually:

$$\text{diam}(\Omega_k) \ll \text{diam}(\Omega) \text{ for } k = 1, \ldots, K.$$

Anyhow, other shapes for the power distribution inside Ω_k, as well as any other means to define junction temperatures starting from the distributed field $T(\mathbf{x}, t)$ may have been adopted in principle.

If packaging information is available, then heat-diffusion on a 3D domain is supposed to be modeled by a quasi-linear PDE:

$$c_V(T, \mathbf{x}) \frac{\partial T(\mathbf{x}, t)}{\partial t} + \mathscr{L}_3 T(\mathbf{x}, t) = \sum_{k=1}^{K} p_k(t) \mathbf{1}_{\Omega_k}(\mathbf{x}) \qquad \text{in } \Omega, \tag{2.104}$$

where:

$$\mathscr{L}_3 T(\mathbf{x}, t) := -\sum_{i,j=1}^{3} D_i \Big[\kappa_{ij}(T, \mathbf{x}) D_j T(\mathbf{x}, t) \Big], \quad D_i := \frac{\partial}{\partial x_i}. \tag{2.105}$$

In (2.104) the term $c_V(T, \mathbf{x})$ represents the distributed thermal capacitance of the material, while in (2.105) the terms $\kappa_{ij}(T, \mathbf{x})$ $(i, j = 1, \ldots, 3)$ account for possibly anisotropic heat-diffusion. A common assumption, stemming from physical considerations, is that:

$$\kappa_{ij}(T, \mathbf{x}) = \kappa_{ji}(T, \mathbf{x}),$$

so that the associated tensor results to be symmetric. This PDE has to be complemented by suitable boundary conditions that are, here and in the following, assumed to be of Robin type:

$$\frac{\partial T(\mathbf{x}, t)}{\partial \mathbf{n}_{\mathscr{L}}} = R(T, \theta_{K+1}) \quad \text{on } \partial\Omega. \tag{2.106}$$

In (2.106) the term $\dfrac{\partial T(\mathbf{x}, t)}{\partial \mathbf{n}_{\mathscr{L}}}$ denotes the conormal derivative of $T(\mathbf{x}, t)$ on $\partial\Omega$ and is defined as:

$$\frac{\partial T(\mathbf{x}, t)}{\partial \mathbf{n}_{\mathscr{L}}} := \sum_{i,j=1}^{3} n_i \kappa_{ij} D_j T(\mathbf{x}, t) \,,$$

where n_i is the i-th component of the normal outward oriented unit vector on $\partial\Omega$.

In the case that only layout information is available, or that package temperature field is not of interest, then heat diffusion can be modeled by a quasi-linear PDE similar to the one used in the 3D case:

$$\hat{c}_V(T,\mathbf{x})\frac{\partial T(\mathbf{x},t)}{\partial t} + \mathscr{L}_2\, T(\mathbf{x},t) = \sum_{k=1}^{K} p_k(t)\,\mathbf{1}_{\Omega_k}(\mathbf{x}) \qquad \text{in } \Omega,$$

the only difference being that now the operator $\mathscr{L}_2$, defined as:

$$\mathscr{L}_2\, T(\mathbf{x},t) := -\sum_{i,j=1}^{2} D_i\Big[\hat{\kappa}_{ij}(T,\mathbf{x})D_j T(\mathbf{x},t)\Big] + \hat{c}(T,\mathbf{x})T(\mathbf{x},t),$$

embodies a reaction term $\hat{c}(T,\mathbf{x})$ to model heat loss in the missing third direction. Suitable boundary conditions are needed also in this case to close the model.

2.2.2.2 Analysis of the Thermal Element Model

The well-posedness of the thermal element model when externally controlled by independent sources fixing the Joule power per unit area stems directly from its definition in Sect. 2.2.2.1. The reader interested in a broader treatment of this subject is referred to [20, Chapter 3]. Existence and uniqueness of a solution can also be proven in the case where the external independent sources fix the average temperature over a region. In particular, a result of this type is given in this section.

In the case at hand heat-diffusion processes are restricted to the case of the linear operator:

$$\mathscr{L}\, T(\mathbf{x}) := -\sum_{i,j=1}^{d} D_i\Big[\kappa_{ij}(\mathbf{x})D_j T(\mathbf{x})\Big] + c(\mathbf{x})T(\mathbf{x}), \tag{2.107}$$

where $\kappa_{ij}(\mathbf{x}), c(\mathbf{x}) \in \mathbb{L}^\infty(\Omega)$ and:

$$\begin{aligned} c(\mathbf{x}) &\geq 0 \qquad \text{a.e. in } \Omega\ , \\ \kappa_{ij}(\mathbf{x}) &= \kappa_{ji}(\mathbf{x})\ i,j = 1,\ldots,d\ . \end{aligned}$$

Furthermore it is assumed for $\mathscr{L}$ to be uniformly elliptic in Ω, i.e. it exists $\tau > 0$ such that:

$$\sum_{i,j=1}^{d} \kappa_{ij}(\mathbf{x})\xi_j\xi_i \geq \tau\,|\boldsymbol{\xi}|^2\,, \tag{2.108}$$

for each $\boldsymbol{\xi} \in \mathbb{R}^d$ and almost every $\mathbf{x} \in \Omega$. The PDE employed to describe thermal effects is enforced in a weak formulation that reads:

$$\frac{d}{dt}(T, v) + a(T, v) + \hat{\alpha}(T - \theta_{K+1}, v)_{\partial\Omega} = \sum_{k=1}^{K} p_k(\mathbf{1}_{\Omega_k}, v) \,, \tag{2.109}$$

where:

$$a(T, v) := \int_{\Omega} \Big(\sum_{i,j=1}^{d} \kappa_{ij}(\mathbf{x})\, D_j T\, D_i v \Big)\, d\mathbf{x} + \int_{\Omega} c(\mathbf{x})\, T\, v\, d\mathbf{x}. \tag{2.110}$$

is the bilinear form associated with $\mathscr{L}$, while $(\cdot,\cdot)_{\partial\Omega}$ denote the $\mathbb{L}^2(\partial\Omega)$ scalar product. Under these hypothesis it is possible to prove the following:

Theorem 2.1 *Given:*

1. $T_0 \in \mathbb{L}^2(\Omega)$,
2. $\theta_k \in \mathbb{C}^0[0, \mathrm{t}_1]$ *and* $\theta_k(0)$ *consistent with* T_0 $(k = 1, \ldots, K)$,
3. $\theta_{K+1} \in \mathbb{C}^0[0, \mathrm{t}_1]$,

there exist unique:

1. $T \in \mathbb{C}^0\big([0, \mathrm{t}_1]; \mathbb{L}^2(\Omega)\big) \cap \mathbb{L}^2\big((0, \mathrm{t}_1); \mathbb{H}^1(\Omega)\big)$,
2. $p_k \in \mathbb{C}^0[0, \mathrm{t}_1]$ $(k = 1, \ldots, K)$,

such that:

$$\begin{aligned} \frac{d}{dt}(T, v) + a(T, v) + (\hat{\alpha} T, v)_{\partial\Omega} &= \sum_{k=1}^{K} p_k(\mathbf{1}_{\Omega_k}, v) + (\hat{\alpha}\theta_{K+1}, v)_{\partial\Omega} \\ &\qquad \text{for all } v \in \mathbb{H}^1(\Omega), \\ T(\mathbf{x}, 0) &= T_0(\mathbf{x}), \\ (T, \mathbf{1}_{\Omega_k}) &= \theta_k(t)|\Omega_k| \quad \text{for } k = 1, \ldots, K. \end{aligned}$$

Readers interested in the proof of this theorem are referred to [20, Chapter 3.2], where further considerations on the practical role played by Theorem 2.1 and its elliptic counterpart are also given.

2.2.2.3 Evaluation of the Thermal Element Model

The structure most commonly adopted in the design of a software package for transient circuit simulation is usually based upon a set of *element evaluators* that provide a non-linear solver with the local Jacobian matrices and residuals needed to assemble the linearized system corresponding to each Newton iteration. These

local contributions, commonly referred to as *stamps*, completely define the behavior of each circuit element and are usually represented in a table-like format [20, Chapter 5]. In the following the stamp associated with the thermal element model defined in Sect. 2.2.2.1 will be given.

Introduce to this aim the vectors:

$$\begin{aligned}\boldsymbol{\theta}_k &= [\theta_1(t_k), \ldots, \theta_{K+1}(t_k)]^T,\\ \mathbf{p}_k &= [p_1(t_k), \ldots, p_K(t_k)]^T,\\ \mathbf{T}_k &= \left[\mathbf{T}_C(t_k), \mathbf{T}_1(t_k), \ldots, \mathbf{T}_K(t_k)\right]^T,\end{aligned}$$

associated with the thermal element unknowns at the time instant t_k. The particular structure of the vector $\mathbf{T}_k$ stems from the space discretization of the distributed temperature field $T(\mathbf{x}, t)$ with the patches of finite elements methods [34]. If the linear operator (2.107) is assumed to properly describe heat-diffusion effects, and a p-step linear multi-step method of the form:

$$\dot{y}(t_k) + f(y(t_k), t_k) \approx \sum_{j=0}^{p} \alpha_j\, y(t_{k-j}) + h \sum_{j=0}^{p} \beta_j\, f(y(t_{k-j}), t_{k-j})\,,$$

is supposed to be used for time-discretization purposes, then the stamp associated with the thermal element reads:

	$\boldsymbol{\theta}_k$	$\mathbf{r}_k$	
	$\mathbb{J}_{k,\boldsymbol{\theta}}$	$\mathbb{J}_{k,\mathbf{r}}$	$\mathbf{F}_k$,
	$\mathbb{Q}_{k,\boldsymbol{\theta}}$	$\mathbb{Q}_{k,\mathbf{r}}$	$\mathbf{G}_k$,

where:

$$\mathbf{r}_k = \begin{bmatrix}\mathbf{p}_k\\ \mathbf{T}_k\end{bmatrix}.$$

Assuming $\mathbf{T}$ to have n_T components, and defining:

$$\boldsymbol{\Omega} \in \mathbb{R}^{K+1\times K} \quad \text{such that} \quad \boldsymbol{\Omega} := \begin{bmatrix} |\Omega_1| & \cdots & 0\\ \vdots & \ddots & \vdots\\ 0 & \cdots & |\Omega_K|\\ -|\Omega_1| & \cdots & -|\Omega_K| \end{bmatrix},$$

then it is possible to provide an explicit formulation for the entries referring to the first line of the stamp:

$$\mathbb{J}_{k,\boldsymbol{\theta}} \in \mathbb{R}^{K+1\times K+1} \quad \text{with } \mathbb{J}_{k,\boldsymbol{\theta}} := \left[0\right] ,$$

$$\mathbb{J}_{k,\mathbf{r}} \in \mathbb{R}^{K+1\times K+n_T} \text{ with } \mathbb{J}_{k,\mathbf{r}} := \left[\boldsymbol{\Omega}\ 0\right] ,$$

$$\mathbf{F}_k \in \mathbb{R}^{K+1} \qquad \text{with } \quad \mathbf{F}_k := \boldsymbol{\Omega}\ \mathbf{p}_k .$$

The definition of the remaining entries results to be a bit more involved. Assume $\{\phi_j, j = 1,\dots,n_T\}$ to represent the full basis set associated with the space discretized vector $\mathbf{T}$ and define:

$$M_{\boldsymbol{\theta}} \in \mathbb{R}^{K\times K+1} \text{ with } \quad M_{\boldsymbol{\theta}} := \begin{bmatrix} 1 \cdots 0\ 0 \\ \vdots \ddots \vdots\ 0 \\ 0 \cdots 1\ 0 \end{bmatrix} ,$$

$$M_{\mathbf{T}} \in \mathbb{R}^{K\times n_T} \quad \text{with } [M_{\mathbf{T}}]_{ij} := \frac{1}{|\Omega_i|}(\phi_j, \mathbf{1}_{\Omega_i}) .$$

The space discretized counterpart of the relation linking junction temperatures and distributed temperature field reads then:

$$M_{\boldsymbol{\theta}}\boldsymbol{\theta} - M_{\mathbf{T}}\mathbf{T} = 0 .$$

Denote with:

$$B \in \mathbb{R}^{n_T\times K+1} \text{ with } \quad B := \begin{bmatrix} 0 \cdots 0\ \ b_1 \\ \vdots \ddots \vdots\ \ \vdots \\ 0 \cdots 0\ b_{n_T} \end{bmatrix} ,$$

$$P \in \mathbb{R}^{n_T\times K} \quad \text{with } [P]_{ij} := (\mathbf{1}_{\Omega_j}, \phi_i) ,$$

the matrices accounting for the PDE boundary conditions and heat generation terms, respectively. Notice that only the last column of B has non-zero entries, as boundary conditions depend only on the environment temperature. Assume finally A and C to be the stiffness and mass matrix stemming from patches of finite element method (for more insight on the construction of these matrices the interested reader is referred to [20, Chapter 4]). The space discretized formulation of the heat-diffusion equation reads then:

$$C\dot{\mathbf{T}} + A\mathbf{T} + P\mathbf{p} + B\boldsymbol{\theta} = 0 .$$

Applying the linear multi-step time discretization introduced before it is possible to write the Jacobian contributions as:

$$\mathbb{Q}_{k,\boldsymbol{\theta}} \in \mathbb{R}^{K+n_T \times K+1} \quad \text{with } \mathbb{Q}_{k,\boldsymbol{\theta}} := \begin{bmatrix} M_{\boldsymbol{\theta}} \\ h\beta_0 B \end{bmatrix},$$

$$\mathbb{Q}_{k,\mathbf{r}} \in \mathbb{R}^{K+n_T \times K+n_T} \text{ with } \mathbb{Q}_{k,\mathbf{r}} := \begin{bmatrix} 0 & M_{\mathbf{T}} \\ h\beta_0 P & (\alpha_0 C + h\beta_0 A) \end{bmatrix},$$

while defining:

$$\mathbf{g}_k = \sum_{j=1}^{p} \alpha_j C \mathbf{T}_{k-j} + h \sum_{j=1}^{p} \beta_j \left(A\mathbf{T}_{k-j} + P\mathbf{p}_{k-j} + B\boldsymbol{\theta}_{k-j} \right),$$

gives the following expression for the residual $\mathbf{G}_k \in \mathbb{R}^{K+n_T}$:

$$\mathbf{G}_k = -\begin{bmatrix} 0 \\ h\beta_0 B\boldsymbol{\theta}_k + h\beta_0 P\mathbf{p}_k + (\alpha_0 C + h\beta_0 A)\mathbf{T}_k + \mathbf{g}_k \end{bmatrix}.$$

2.2.2.4 Analysis of the Coupled System

To conclude this section the existence and uniqueness of a solution to the whole electro-thermal system is discussed. This result is of major importance to show that under non-restrictive assumptions the extended electro-thermal netlist introduced in Fig. 2.1 enjoys the same smoothness of the original electrical netlist, that is here formalized as:

$$\begin{aligned} A_C \frac{d\mathbf{q}}{dt} + A_R \mathbf{r}(A_R^T \mathbf{e}, \boldsymbol{\theta}) + A_L \mathbf{i}_L + A_V \mathbf{i}_V + A_I \mathbf{i}(A_C^T \mathbf{e}, \boldsymbol{\theta}) &= 0, \\ \frac{d\boldsymbol{\phi}}{dt} - A_L^T \mathbf{e} &= 0, \\ A_V^T \mathbf{e} - \mathbf{v}(t) &= 0, \\ \mathbf{q} - \mathbf{q}_C(A_C^T \mathbf{e}) &= 0, \\ \boldsymbol{\phi} - \boldsymbol{\phi}_L(\mathbf{i}_L) &= 0. \end{aligned} \tag{2.111}$$

Notice that an additional dependence on junction temperatures is assumed for resistors and controlled current sources. The electrical part has then to be complemented by the balance of Joule power at the thermal network nodes:

$$|\Omega_k| p_k - W_k(\boldsymbol{\theta}, \mathbf{e}) = 0 \text{ for } k = 1, \ldots, K, \tag{2.112}$$

by the thermal element interface conditions:

$$|\Omega_k|\theta_k - (T, \mathbf{1}_{\Omega_k}) = 0 \text{ for } k = 1, \ldots, K, \tag{2.113}$$

and by the PDE describing heat diffusion:

$$\frac{d}{dt}(T, v) + a(T, v) + \hat{\alpha}(T, v)_{\partial\Omega} - \sum_{k=1}^{K} p_k(\mathbf{1}_{\Omega_k}, v) - \hat{\alpha}(g_k, v)_{\partial\Omega} = 0 \quad \forall v \in \mathbb{H}^1(\Omega). \tag{2.114}$$

The electrical part (2.111) is supposed in the following to be index-1 for any given $\boldsymbol{\theta} \in \mathbb{C}^0[0, \mathrm{t}_1]$. Defining Q_C to be the orthogonal projector onto the kernel of A_C^T and P_C to be its complement, then sufficient conditions to fulfill the index-1 requirement are [24]:

1. $\ker(A_C, A_R, A_V)^T = \{0\}$, $\ker Q_C^T A_V = \{0\}$,
2. $\mathbf{i}(A_C^T \mathbf{e}, \boldsymbol{\theta})$ uniformly continuous in $\boldsymbol{\theta}$ and Lipschitz continuous in $A_C^T \mathbf{e}$,
3. $\mathbf{V}(\cdot)$ continuous,
4. $\boldsymbol{\phi}_L(\cdot)$ and $\mathbf{q}_C(\cdot)$ differentiable functions of their arguments,
5. $\dfrac{\partial \mathbf{q}_C(A_C^T \mathbf{e})}{\partial (A_C^T \mathbf{e})}$, $\dfrac{\partial \boldsymbol{\phi}_L(\mathbf{i}_L)}{\partial (\mathbf{i}_L)}$ positive definite,
6. $\mathbf{r}(A_R^T \mathbf{e}, \boldsymbol{\theta})$ uniformly continuous in $\boldsymbol{\theta}$ and differentiable in $A_R^T \mathbf{e}$,
7. $\dfrac{\partial \mathbf{r}(A_R^T \mathbf{e}, \boldsymbol{\theta})}{\partial (A_R^T \mathbf{e})}$ positive definite and uniformly continuous in $\boldsymbol{\theta}$.

Under these assumptions the existence and uniqueness of a global solution to an initial value problem with consistent initial conditions on $[0, \mathrm{t}_1]$ follows from standard results [35, Theorem 15]. Furthermore, for each component of the solution in the time interval $[0, \mathrm{t}_1]$ a bound of the form:

$$|x(t)| \leq |d_A(\boldsymbol{\theta}(t))| + \int_0^t |d_D(\boldsymbol{\theta}(\tau))| d\tau \,, \tag{2.115}$$

holds, where $d_A(\cdot)$ and $d_D(\cdot)$ are continuous functions. Notice that the form of (2.115) is due to the index-1 condition, thanks to which the time-derivatives of $\boldsymbol{\theta}(t)$ do not appear in the bound. In this case also the following a-priori bound, uniformly in $\boldsymbol{\theta}$, can be shown to hold:

$$|x(t)| \leq \max_{\mathscr{G}} |d_A(\boldsymbol{\theta})| + |t| \max_{\mathscr{G}} |d_D(\boldsymbol{\theta})| \,, \tag{2.116}$$

where $\mathscr{G}$ is a closed set, such that:

$$\mathscr{F} := \left\{ \mathbf{s} \in \mathbb{R}^K : |\mathbf{s}| \leq \max_{t \in [0, \mathrm{t}_1]} |\boldsymbol{\theta}(t)| \right\} \subseteq \mathscr{G} \subseteq \mathbb{R}^K \,. \tag{2.117}$$

The assumptions made on the thermal part of the system are:

1. $g(\mathbf{x}, t) \in \mathbb{C}^0\left([0, \mathrm{t}_1], \mathbb{L}^2(\partial\Omega)\right)$,
2. $W_k(\cdot, \cdot)$ continuous function of its arguments ($k = 1, \ldots, K$),

To provide system (2.111)–(2.114) with consistent initial conditions it is possible to prescribe arbitrarily $T(\mathbf{x}, 0) := T_0(\mathbf{x}) \in \mathbb{L}^2(\Omega)$, $P_C\mathbf{e}(0)$ and $\mathbf{i}_L(0)$. Then $\boldsymbol{\theta}(0)$ is obtained from (2.113), $Q_C\mathbf{e}(0)$, $\mathbf{i}_V(0)$, $\boldsymbol{\phi}(0)$, $\mathbf{q}(0)$ are computed from the algebraic constraints of (2.111) once $\boldsymbol{\theta}(0)$ is known, and $\mathbf{p}(0)$ is finally determined from (2.112).

The existence and uniqueness of a solution to (2.111)–(2.114) in a given time interval $t \in [0, \mathrm{t}_1]$ is investigated in the next:

Theorem 2.2 *Consider system (2.111)–(2.114) with the further hypothesis that:*

1. *There exist* $C_{\mathbf{W}} > 0$ *such that* $|W_k(\boldsymbol{\theta}, \mathbf{e})| \leq C_{\mathbf{W}}$ *for* $k = 1, \ldots, K$.

Suppose furthermore that the assumptions outlined in the previous paragraphs on the electrical and thermal part of the network are fulfilled. Then, given consistent initial conditions, there exist a unique solution to an initial value problem on a given time interval $[0, \mathrm{t}_1]$ *and:*

1. $P_C\mathbf{e}$, $\mathbf{i}_L$, $\mathbf{q}$ *and* $\boldsymbol{\phi}$ *are differentiable,*
2. $Q_C\mathbf{e}$, $\mathbf{i}_V$, $\boldsymbol{\theta}$ *and* $\mathbf{p}$ *are continuous,*
3. *The regularity of the PDE solution is at least:*

$$T \in \mathbb{L}^2\left((0, \mathrm{t}_1), \mathbb{H}^1(\Omega)\right) \cap \mathbb{C}^0\left([0, \mathrm{t}_1], \mathbb{L}^2(\Omega)\right) ,$$

while:

$$\frac{\partial T}{\partial t} \in \mathbb{L}^2\left((0, \mathrm{t}_1), \mathbb{H}^{-1}(\Omega)\right) ,$$

4. *The energy estimate:*

$$\|T(\mathbf{x}, t)\|^2_{\mathbb{L}^2(\Omega)} + \eta \int_0^t \|T(\mathbf{x}, \tau)\|^2_{\mathbb{H}^1(\Omega)} \, d\tau \leq \|T_0(\mathbf{x})\|^2_{\mathbb{L}^2(\Omega)} + \frac{1}{\eta} \int_0^t S^2 d\tau ,$$

holds for each $t \in [0, \mathrm{t}_1]$ *where:*

$$S = S(C_{\mathbf{W}}, \hat{\alpha}, \Omega_k, g) := C_{\mathbf{W}} \sum_{k=1}^{K} \sqrt{|\Omega_k|} + \hat{\alpha} \, \|g(t)\|_{\mathbb{L}^2(\partial\Omega)} .$$

Proof In the following the so-called Faedo-Galerkin method is exploited to construct a sequence of DAE systems that approximate the PDAE system (2.111)–(2.114). The line followed stems directly from the one usually employed to prove the well posedness of parabolic PDEs casted in a weak formulation (see [52, Chapter 11, Theorem 11.1.1]).

That being said, since $\mathbb{H}^1(\Omega)$ is a separable Hilbert space it admits a complete orthonormal basis $\{\phi_j\}_{j\geq 1}$. Define then:

$$V^N := \text{span}\{\phi_1, \ldots, \phi_N\} .$$

Substitute the PDE appearing in (2.111)–(2.114) with the approximate problem:

$$\frac{d}{dt}(T^N, v) + a(T^N, v) + \hat{\alpha}(T^N, v)_{\partial\Omega} - \sum_{k=1}^{K} p_k^N (\mathbf{1}_{\Omega_k}, v) - \hat{\alpha}(g, v)_{\partial\Omega} = 0 \qquad (2.118)$$

for all $v \in V^N$, where $N \geq K$ in order to fulfill the constraints imposed by (2.113). Writing:

$$T^N(\mathbf{x}, t) := \sum_{s=1}^{N} c_s^N(t)\phi_s(\mathbf{x}) , \qquad (2.119)$$

then (2.118) results to be equivalent to:

$$M\frac{d\mathbf{c}^N}{dt} + A\mathbf{c}^N - B\mathbf{p}^N - \mathbf{F}^N(t) = 0 . \qquad (2.120)$$

where the stiffness and mass matrices are defined as:

$$M \in \mathbb{R}^{N\times N} \text{ with } \left[M_{ij}\right] := [(\phi_i, \phi_j)] ,$$

$$A \in \mathbb{R}^{N\times N} \text{ with } [A_{ij}] := [a(\phi_j, \phi_i) + \hat{\alpha}(\phi_j, \phi_i)_{\partial\Omega}] ,$$

$$B \in \mathbb{R}^{N\times K} \text{ with } [B_{ij}] := [(\mathbf{1}_{\Omega_k}, \phi_i)] ,$$

while the known vector $\mathbf{F}^N$ reads:

$$\mathbf{F}^N \in \left[\mathbb{C}^0[0, \mathrm{t}_1]\right]^N \text{ with } [F_i^N] := [\hat{\alpha}(g, \phi_i)_{\partial\Omega}] .$$

Finally the unknown vectors in (2.120) are:

$$\mathbf{p}^N(t) := [p_1^N(t), \ldots, p_K^N(t)]^T ,$$

$$\mathbf{c}^N(t) := [c_1^N(t), \ldots, c_N^N(t)]^T .$$

Similarly it is possible to substitute (2.119) in (2.113) and obtain the equivalent system:

$$\boldsymbol{\Omega}\boldsymbol{\theta}^N - B^T\mathbf{c}^N = 0 , \qquad (2.121)$$

where:

$$\boldsymbol{\Omega} \in \mathbb{R}^{K\times K} \text{ with } \boldsymbol{\Omega} := \text{diag}(|\Omega_1|, \ldots, |\Omega_K|) \,,$$

and:

$$\boldsymbol{\theta}^N(t) := [\theta_1^N(t), \ldots, \theta_K^N(t)]^T \,.$$

Reformulating (2.112) in matrix notation:

$$\boldsymbol{\Omega}\,\mathbf{p}^N - \mathbf{W}(\boldsymbol{\theta}^N, \mathbf{e}^N) = 0 \,, \tag{2.122}$$

with:

$$\boldsymbol{W}(\boldsymbol{\theta}^N, \mathbf{e}^N) := [W_1(\boldsymbol{\theta}^N, \mathbf{e}^N), \ldots, W_K(\boldsymbol{\theta}^N, \mathbf{e}^N)]^T \,,$$

it is possible to write the DAE system approximating (2.111)–(2.114) as:

$$\begin{aligned}
A_C \frac{d\mathbf{q}^N}{dt} + A_R\mathbf{r}(A_R^T\mathbf{e}^N, \boldsymbol{\theta}^N) + A_L\mathbf{i}_L^N + A_V\mathbf{i}_V^N + A_I\mathbf{i}(A_C^T\mathbf{e}^N, \boldsymbol{\theta}^N) &= 0 \,,\\
\frac{d\boldsymbol{\phi}^N}{dt} - A_L^T\mathbf{e}^N &= 0 \,,\\
A_V^T\mathbf{e}^N - \mathbf{V}(t) &= 0 \,,\\
\mathbf{q}^N - \mathbf{q}_C(A_C^T\mathbf{e}^N) &= 0 \,,\\
\boldsymbol{\phi}^N - \boldsymbol{\phi}_L(\mathbf{i}_L^N) &= 0 \,,\\
\boldsymbol{\Omega}\,\mathbf{p}^N - \mathbf{W}(\boldsymbol{\theta}^N, \mathbf{e}^N) &= 0 \,,\\
\boldsymbol{\Omega}\,\boldsymbol{\theta}^N - B^T\mathbf{c}^N &= 0 \,,\\
M\frac{d\mathbf{c}^N}{dt} + A\mathbf{c}^N - B\mathbf{p}^N - \mathbf{F}^N(t) &= 0 \,.
\end{aligned} \tag{2.123}$$

Notice that M can be inverted as it is positive definite. Thus (2.120) defines an explicit differential equation for the variable $\mathbf{c}^N$:

$$\frac{d\mathbf{c}^N}{dt} = -M^{-1}\left[A\mathbf{c}^N - B\mathbf{p}^N - \mathbf{F}^N(t)\right] \,. \tag{2.124}$$

From (2.121) it holds:

$$\boldsymbol{\theta}^N = \boldsymbol{\Omega}^{-1}B^T\mathbf{c}^N \,, \tag{2.125}$$

due to the regularity of $\boldsymbol{\Omega}$. Differentiating (2.125) and taking into account (2.124) the following explicit differential equation is obtained for $\boldsymbol{\theta}^N$:

$$\frac{d\boldsymbol{\theta}^N}{dt} = \boldsymbol{\Omega}^{-1} B^T \frac{d\mathbf{c}^N}{dt} = -\boldsymbol{\Omega}^{-1} B^T M^{-1} \left[A\mathbf{c}^N - B\mathbf{p}^N - \mathbf{F}^N(t) \right] .$$

Substituting (2.125) into (2.111) reads:

$$\begin{aligned} A_C \frac{d\mathbf{q}}{dt} + A_R \hat{\mathbf{r}}(A_R^T \mathbf{e}, \mathbf{c}^N) + A_L \mathbf{i}_L + A_V \mathbf{i}_V + A_I \hat{\mathbf{i}}(A_C^T \mathbf{e}, \mathbf{c}^N) &= 0, \\ \frac{d\boldsymbol{\phi}}{dt} - A_L^T \mathbf{e} &= 0, \\ A_V^T \mathbf{e} - \mathbf{V}(t) &= 0, \\ \mathbf{q} - \mathbf{q}_C(A_C^T \mathbf{e}) &= 0, \\ \boldsymbol{\phi} - \boldsymbol{\phi}_L(\mathbf{i}_L) &= 0, \end{aligned} \tag{2.126}$$

where:

$$\hat{\mathbf{r}}(A_R^T \mathbf{e}, \mathbf{c}^N) := \mathbf{r}(A_R^T \mathbf{e}, \boldsymbol{\Omega}^{-1} B^T \mathbf{c}^N) ,$$

$$\hat{\mathbf{i}}(A_C^T \mathbf{e}, \mathbf{c}^N) := \mathbf{i}(A_C^T \mathbf{e}, \boldsymbol{\Omega}^{-1} B^T \mathbf{c}^N) .$$

The assumptions on the electrical part of the system ensure that only one differentiation of (2.126) is needed to derive, through appropriate algebraic manipulations, a set of explicit differential equations for the variables $\mathbf{e}$, $\mathbf{q}$, $\boldsymbol{\phi}$, $\mathbf{i}_L$ and $\mathbf{i}_V$. Finally from (2.122) it stems:

$$\mathbf{p}^N = \boldsymbol{\Omega}^{-1} \mathbf{W}(\boldsymbol{\theta}^N, \mathbf{e}^N) .$$

Even here only one differentiation is necessary to derive an explicit differential equation for $\mathbf{p}^N$. The index of system (2.123) results then to be one.

Defining the orthogonal projection:

$$P_N : \mathbb{L}^2(\Omega) \to V^N ,$$

it is possible to derive a set of consistent initial conditions for (2.123). In fact, it just suffices to define the initial conditions for the approximate problem (2.118) as:

$$T_0^N := P_N(T_0) , \tag{2.127}$$

and proceed as done in the original PDAE system. Notice that the initial condition for system (2.120) equivalent to (2.127) is given by the solution of the linear system:

$$(M\mathbf{c}^N(0))_j = (T_0, \phi_j) \text{ for } j = 1, \ldots, N .$$

As consistent initial conditions have been obtained, then (2.123) admits a unique global solution [35].

To proceed with the Faedo-Galerkin method it is necessary at this point to recover, for all the variables in (2.123), upper bounds in $\mathbb{L}^2(0,\mathrm{t}_1)$ that are independent of N. These bounds will be employed afterwards to pass to the weak-limit $N \to \infty$ and determine then a solution to the initial PDAE system. Due to the hypothesis made on the boundedness of $|W_k(\cdot,\cdot)|$ it is convenient to start from the thermal part of the network, noticing that:

$$p_k^N \in \mathbb{C}^0[0,\mathrm{t}_1] \subset \mathbb{L}^2(0,\mathrm{t}_1)\ k = 1,\ldots,K,$$

$$c_k^N \in \mathbb{C}^1[0,\mathrm{t}_1] \subset \mathbb{H}^1(0,\mathrm{t}_1)\ k = 1,\ldots,K,$$

hold, from which it follows naturally:

$$T^N \in \mathbb{H}^1\left((0,\mathrm{t}_1),\mathbb{H}^1(\Omega)\right)\ .$$

Choosing T^N as a test function in (2.118) gives:

$$\left(\frac{d}{dt}T^N, T^N\right) + a(T^N,T^N) + \hat{\alpha}(T^N,T^N)_{\partial\Omega} \tag{2.128}$$

$$= \sum_{k=1}^{K} p_k^N(\mathbf{1}_{\Omega_k}, T^N) + \hat{\alpha}(g,T^N)_{\partial\Omega}\ . \tag{2.129}$$

Exploiting the coercivity of the bilinear form it is possible to obtain:

$$\frac{1}{2}\frac{d}{dt}\left\|T^N\right\|^2_{\mathbb{L}^2(\Omega)} + \eta\left\|T^N\right\|^2_{\mathbb{H}^1(\Omega)} \tag{2.130}$$

$$\leq \left(\frac{d}{dt}T^N, T^N\right) + a(T^N,T^N) + \hat{\alpha}(T^N,T^N)_{\partial\Omega}\ , \tag{2.131}$$

while from the continuity of the right-hand side in (2.128) and the hypothesis on the boundedness of $|W_k(\cdot,\cdot)|$ $(k = 1,\ldots,K)$ follows:

$$\begin{aligned}&\sum_{k=1}^{K} p_k^N(\mathbf{1}_{\Omega_k}, T^N) + \hat{\alpha}(g,T^N)_{\partial\Omega}\\ &\leq \left(C_{\mathbf{W}}\sum_{k=1}^{K}\sqrt{|\Omega_k|} + \hat{\alpha}\left\|g(t)\right\|_{\mathbb{L}^2(\partial\Omega)}\right)\left\|T^N(t)\right\|_{\mathbb{L}^2(\Omega)}\ .\end{aligned} \tag{2.132}$$

Recapitulating the definition of $S(C_{\mathbf{W}}, \hat{\alpha}, \Omega_k, g) := C_{\mathbf{W}} \sum_{k=1}^{K} \sqrt{|\Omega_k|} + \hat{\alpha} \|g(t)\|_{\mathbb{L}^2(\partial\Omega)}$, and combining (2.130) with (2.132) it is possible to obtain:

$$\frac{1}{2}\frac{d}{dt}\left\|T^N(t)\right\|^2_{\mathbb{L}^2(\Omega)} + \eta\left\|T^N(t)\right\|^2_{\mathbb{H}^1(\Omega)} \leq S(C_{\mathbf{W}}, \hat{\alpha}, \Omega_k, g)\left\|T^N(t)\right\|_{\mathbb{L}^2(\Omega)} .$$

Integrating over $(0, t)$ with $t \in (0, \mathrm{t}_1)$, employing Young's inequality and taking into account that:

$$\|T_0^N\|_{\mathbb{L}^2(\Omega)} \leq \|T_0\|_{\mathbb{L}^2(\Omega)} ,$$

as T_0^N is a projection of T_0 onto a finite dimensional space, it follows then:

$$\left\|T^N(t)\right\|^2_{\mathbb{L}^2(\Omega)} + \eta\int_0^t \left\|T^N(\tau)\right\|^2_{\mathbb{H}^1(\Omega)} d\tau \leq \|T_0\|^2_{\mathbb{L}^2(\Omega)} + \frac{1}{\eta}\int_0^t S^2 d\tau . \tag{2.133}$$

The sequence T^N is thus bounded in $\mathbb{L}^2\left((0, \mathrm{t}_1), \mathbb{H}^1(\Omega)\right) \cap \mathbb{L}^\infty\left((0, \mathrm{t}_1), \mathbb{L}^2(\Omega)\right)$ and from (2.112) it is trivial to infer that also $\mathbf{p}^N$ is bounded in the $\mathbb{L}^2(0, \mathrm{t}_1)$ sense. From (2.113) it is possible to obtain, after some algebra:

$$|\theta_k^N(t)|^2 \leq \frac{1}{|\Omega_k|^2}\|T^N(t)\|^2_{\mathbb{L}^2(\Omega)} \quad k = 1, \ldots, K,$$

and derive an upper bound in $\mathbb{L}^2(0, \mathrm{t}_1)$ for $\boldsymbol{\theta}^N$ by means of (2.133):

$$|\theta_k^N(t)|^2 \leq \frac{1}{|\Omega_k|^2}\left[\|T_0\|^2_{\mathbb{L}^2(\Omega)} + \frac{1}{\eta}\int_0^{\mathrm{t}_1} S^2 d\tau\right] \quad k = 1, \ldots, K.$$

Also this bound does not depend on N. It is now possible to define:

$$C_{\boldsymbol{\theta}} := \max_{k=1,\ldots,K}\left(\frac{1}{|\Omega_k|^2}\left[\|T_0\|^2_{\mathbb{L}^2(\Omega)} + \frac{1}{\eta}\int_0^{\mathrm{t}_1} S^2 d\tau\right]\right),$$

and then:

$$\mathscr{G} := \left\{\mathbf{s} \in \mathbb{R}^K : |s| \leq \sqrt{C_{\boldsymbol{\theta}}}\right\} .$$

As $\mathscr{G}$ does not depend on N and fulfills condition (2.117) then the bound on the variables of the electrical part is derived from (2.116). Notice that this is possible in our framework due to the index-1 hypothesis made on (2.111). Finally, due to the

continuity of the non-linear functions in (2.123) also the terms:

$$\mathbf{r}^N := \mathbf{r}(A_R^T \mathbf{e}^N, \boldsymbol{\theta}^N) \ , \quad \mathbf{i}^N := \mathbf{i}(A_C^T \mathbf{e}^N, \boldsymbol{\theta}^N) \ ,$$
$$\mathbf{q}_C^N := \mathbf{q}_C(A_C^T \mathbf{e}^N) \quad , \boldsymbol{\phi}_L^N := \boldsymbol{\phi}_L(\mathbf{i}_L^N) \quad ,$$
$$\mathbf{W}^N := \mathbf{W}(\boldsymbol{\theta}^N, \mathbf{e}^N) \quad ,$$

are bounded in the $\mathbb{L}^2(0, \mathrm{t}_1)$ norm by a constant that is independent of N. At this point upper bounds for every entity in (2.123) have been determined. Hence it is possible to select a subsequence (still denoted with the N super-script) in which (see e.g. [42]):

- T^N converges in the weak* topology of $\mathbb{L}^\infty\left((0, \mathrm{t}_1), \mathbb{L}^2(\Omega)\right)$,
- T^N converges weakly in $\mathbb{L}^2\left((0, \mathrm{t}_1), \mathbb{H}^1(\Omega)\right)$,
- $\mathbf{e}^N, \mathbf{i}_L^N, \mathbf{q}^N, \boldsymbol{\phi}^N, \mathbf{i}_V^N, \mathbf{p}^N$ and $\boldsymbol{\theta}^N$ converge weakly in the $\mathbb{L}^2(0, \mathrm{t}_1)$ sense,
- $\mathbf{r}^N, \mathbf{i}^N, \mathbf{q}_C^N, \boldsymbol{\phi}_L^N$ and $\mathbf{W}^N$ converge weakly in the $\mathbb{L}^2(0, \mathrm{t}_1)$ sense.

Anyhow, to exploit weak convergence properties in order to construct a solution to the original PDAE system it is still necessary to prove that:

$$\mathbf{r}^N \rightharpoonup \mathbf{r}(A_R^T \mathbf{e}, \boldsymbol{\theta}) \ , \quad \mathbf{i}^N \rightharpoonup \mathbf{i}(A_C^T \mathbf{e}, \boldsymbol{\theta}) \ ,$$
$$\mathbf{q}_C^N \rightharpoonup \mathbf{q}_C(A_C^T \mathbf{e}) \quad , \boldsymbol{\phi}_L^N \rightharpoonup \boldsymbol{\phi}_L(\mathbf{i}_L) \quad ,$$
$$\mathbf{W}^N \rightharpoonup \mathbf{W}(\boldsymbol{\theta}, \mathbf{e}) \quad ,$$

when:

$$\mathbf{e}^N \rightharpoonup \mathbf{e} \ , \ \mathbf{i}_L^N \rightharpoonup \mathbf{i}_L \ , \ \boldsymbol{\theta}^N \rightharpoonup \boldsymbol{\theta} \ .$$

This will be shown in the following taking advantage of regularity results that hold for the PDE part of this system. Indeed it will turn out that the convergence of the DAE part of (2.111)–(2.114) is to be intended at least pointwise.

Let us start then multiplying the first term at the left hand side in (2.118) by:

$$\Psi \in \mathbb{C}^1([0, \mathrm{t}_1]) \ , \ \Psi(\mathrm{t}_1) = 0 \ ,$$

and integrating by parts ($j = 1, \ldots, N$):

$$\int_0^{\mathrm{t}_1} \left(\frac{dT^N}{dt}(\tau), \phi_j \right) \Psi(\tau) d\tau = -\int_0^{\mathrm{t}_1} \left(T^N(\tau), \phi_j\right) \frac{d\Psi}{dt}(\tau) d\tau - (T_0^N, \phi_j)\Psi(0) \ .$$

Passing to the limit in (2.118), choosing an arbitrary $N_0 \geq K$ and recalling that T_0^N converges in $\mathbb{L}^2(\Omega)$ to T_0 while p_k^N converges in $\mathbb{L}^2(0, \mathrm{t}_1)$ to p_k, it is finally

obtained:

$$
\begin{aligned}
&-\int_0^{t_1}\left(T(\tau),\phi_j\right)\frac{d\Psi}{dt}(\tau)d\tau\,-\,(T_0,\phi_j)\Psi(0)+\int_0^{t_1}a(T,\phi_j)\Psi(\tau)d\tau\\
&+\int_0^{t_1}\hat{\alpha}(T(\tau),\phi_j)_{\partial\Omega}\Psi(\tau)d\tau=\int_0^{t_1}\sum_{k=1}^{K}p_k(\mathbf{1}_{\Omega_k},\phi_j)\Psi(\tau)d\tau\\
&\quad+\int_0^{t_1}\hat{\alpha}(g,\phi_j)_{\partial\Omega}\Psi(\tau)d\tau\qquad j=1,\ldots,N_0.
\end{aligned}
\tag{2.134}
$$

Since the linear combinations of ϕ_j are dense in $\mathbb{H}^1(\Omega)$, then (2.134) can be written equivalently testing on each $v\in\mathbb{H}^1(\Omega)$. Thus:

$$
T(\mathbf{x},t)\in\mathbb{L}^2\left((0,t_1),\mathbb{H}^1(\Omega)\right)\cap\mathbb{L}^\infty\left((0,t_1),\mathbb{L}^2(\Omega)\right)\,, \tag{2.135}
$$

fulfills (2.114) with p_k $(k=1,\ldots,K)$ as source terms. From (2.135) it follows also:

$$
T(\mathbf{x},t)\in\mathbb{L}^2\left((0,t_1),\mathbb{H}^1(\Omega)\right)\cap\mathbb{H}^1\left((0,t_1),\mathbb{H}^{-1}(\Omega)\right)\,, \tag{2.136}
$$

and using the arguments in [52, Chapter 11, p.369] and [43, p.23]:

$$
T\in\mathbb{C}^0\left([0,t_1],\mathbb{L}^2(\Omega)\right)\quad,\quad\frac{\partial T}{\partial t}\in\mathbb{L}^2\left((0,t_1),\mathbb{H}^{-1}(\Omega)\right)\,.
$$

Define:

$$
\Delta T^N(t):=T^N(t)-T(t)\quad,\quad\Delta p_k^N(t):=p_k^N(t)-p_k(t)\,.
$$

Subtracting (2.114) from (2.118) and choosing $\Delta T^N(t)$ as a test function reads:

$$
\frac{1}{2}\frac{d}{dt}\|\Delta T^N\|^2_{\mathbb{L}^2(\Omega)}+a(\Delta T^N,\Delta T^N)+\hat{\alpha}\|\Delta T^N\|^2_{\mathbb{L}^2(\partial\Omega)}=\sum_{k=1}^{K}\Delta p_k^N(\mathbf{1}_{\Omega_k},\Delta T^N)\,.
$$

Integrating over $(0,t)$ and exploiting the coercivity of the bilinear form it is then possible to obtain the following inequality:

$$
\left\|\Delta T^N(t)\right\|^2_{\mathbb{L}^2(\Omega)}\le\Delta K^N(t)\xrightarrow{N\to\infty}0\,, \tag{2.137}
$$

with:

$$
\Delta K^N(t):=\left\|\Delta T^N(0)\right\|^2_{\mathbb{L}^2(\Omega)}+2\sum_{k=1}^{K}\left[\int_0^t\Delta p_k^N(\tau)(\mathbf{1}_{\Omega_k},\Delta T^N(\tau))d\tau\right].
$$

As both sides of (2.137) are continuous, this inequality holds also in the form:

$$\max_{t\in[0,t_1]} \left\| \Delta T^N(t) \right\|^2_{\mathbb{L}^2(\Omega)} \leq \max_{t\in[0,t_1]} \Delta K^N(t) \xrightarrow{N\to\infty} 0\,.$$

Introducing $\Delta\theta_k^N := \theta_k^N(t) - \theta_k(t)$ and noticing that:

$$\max_{t\in[0,t_1]} |\Delta\theta_k^N(t)|^2 \leq \frac{1}{|\Omega_k|^2} \max_{t\in[0,t_1]} \left\| \Delta T^N(t) \right\|^2_{\mathbb{L}^2(\Omega)} \qquad k = 1,\ldots,K,$$

it follows that the convergence of $\boldsymbol{\theta}^N$ to $\boldsymbol{\theta}$ is not only weak, but uniform. Then, due to the stability properties of (2.111) the electrical variables also converge to their limit uniformly and not only weakly. In particular it can be inferred that:

- $P_C\mathbf{e}$, $\mathbf{i}_L$, $\mathbf{q}$ and $\boldsymbol{\phi}$ are differentiable,
- $Q_C\mathbf{e}$ and $\mathbf{i}_V$ are continuous.

As at this point $\mathbf{e}$ and $\boldsymbol{\theta}$ are known to be continuous, then it follows that $\mathbf{W}^N$ converges to $\mathbf{W}$ pointwise and thus $\mathbf{p}$ is also continuous.

Finally it remains to show that $T(\mathbf{x},0) = T_0(\mathbf{x})$ in order to prove that the constructed solution actually solves the initial value problem prescribed in the beginning. Multiplying (2.114) by:

$$\Psi \in \mathbb{C}^1([0,t_1])\,,\ \Psi(t_1) = 0\,,$$

and integrating by parts it follows:

$$\begin{aligned} &-\int_0^{t_1} (T(\tau),v)\,\frac{d\Psi}{dt}(\tau)d\tau - (T(0),v)\Psi(0) + \int_0^{t_1} a(T,v)\Psi(\tau)d\tau \\ &+\int_0^{t_1} \hat{\alpha}(T(\tau),v)_{\partial\Omega}\Psi(\tau)d\tau = \int_0^{t_1} \sum_{k=1}^{K} p_k(\mathbf{1}_{\Omega_k},v)\Psi(\tau)d\tau \\ &\quad+\int_0^{t_1} \hat{\alpha}(g,v)_{\partial\Omega}\Psi(\tau)d\tau \qquad \forall v\in\mathbb{H}^1(\Omega), \end{aligned}$$

thus, taking $\Psi(0) = 1$:

$$(T(0) - T_0, v) = 0 \quad \forall v \in \mathbb{H}^1(\Omega)\,.$$

This implies $T(\mathbf{x},0) = T_0(\mathbf{x})$, and proves the existence and uniqueness of a solution to a prescribed initial value problem for system (2.111)–(2.114).

2.2.3 Multiphysics Modeling via Maxwell's Equations

The mathematical model of circuit analysis is given by element relations connected by Kirchhoff's laws, yielding a system of DAEs. Each relation originates from Maxwell's equations, but typically it is simplified to avoid the simulation of PDEs, where it is not necessary. But if an application demands distributed field effects, e.g. eddy currents, those effects need to be reintroduced by a PDE, in which some conducting parts are identified by circuit branches. We consider here two examples, that are especially important in the analysis of magnetoquasistatic fields, the *solid* and *stranded conductor* models. Finally the coupling of the networks DAEs with the (magnetoquasistatic) field PDEs yields a system of PDAEs.

Let us start with the network model of circuits, as introduced in system (2.1). [26], that yields a system of DAEs. We extend the current balance equation by two additional vectors $\mathbf{i}_{\text{sol}} \in \mathbb{R}^{N_{\text{sol}}}$ and $\mathbf{i}_{\text{str}} \in \mathbb{R}^{N_{\text{str}}}$, that describe the unknown currents through N_{sol} solid and N_{str} stranded conductors

$$\begin{aligned} \mathbf{A}_{\text{C}} \frac{\mathrm{d}}{\mathrm{d}t} \mathbf{q} + \mathbf{A}_{\text{R}} r(\mathbf{A}_{\text{R}}^{\top} \mathbf{u}, t) + \mathbf{A}_{\text{L}} \mathbf{i}_{\text{L}} + \mathbf{A}_{\text{V}} \mathbf{i}_{\text{V}} + \mathbf{A}_{\text{I}} \mathbf{i}(t) + \mathbf{A}_{\text{str}} \mathbf{i}_{\text{str}} + \mathbf{A}_{\text{sol}} \mathbf{i}_{\text{sol}} &= \mathbf{0}, \\ \frac{\mathrm{d}}{\mathrm{d}t} \boldsymbol{\phi} - \mathbf{A}_{\text{L}}^{\top} \mathbf{u} = \mathbf{0}, \qquad \mathbf{A}_{\text{V}}^{\top} \mathbf{u} - \mathbf{v}(t) &= \mathbf{0}, \\ \mathbf{q} - \mathbf{q}_{\text{C}}(\mathbf{A}_{\text{C}}^{\top} \mathbf{u}, t) = \mathbf{0}, \quad \boldsymbol{\phi} - \boldsymbol{\phi}_{\text{L}}(\mathbf{i}_{\text{L}}, t) &= \mathbf{0}, \end{aligned}$$

with consistent initial values for the node potentials $\mathbf{u}$, charges $\mathbf{q}$, fluxes $\boldsymbol{\phi}$, and currents $\mathbf{i}_{\text{L}}$, $\mathbf{i}_{\text{V}}$. We will address the whole system in the following more abstractly by the semi-explicit initial-value problem

$$\begin{aligned} \dot{\mathbf{y}}_1 &= \mathbf{f}_1(\mathbf{y}_1, \mathbf{z}_1, \mathbf{z}_{2b}), \quad \text{with} \quad \mathbf{y}_1(0) = \mathbf{y}_{1,0} \\ \mathbf{0} &= \mathbf{g}_1(\mathbf{y}_1, \mathbf{z}_1, \mathbf{z}_{2b}), \end{aligned} \tag{2.138}$$

with the unknowns

$$\mathbf{y}_1 := (\mathbf{q}, \boldsymbol{\phi})^{\top}, \quad \mathbf{z}_1 := (\mathbf{u}, \mathbf{i}_{\text{L}}, \mathbf{i}_{\text{V}})^{\top} \quad \text{and} \quad \mathbf{z}_{2b} := (\mathbf{i}_{\text{str}}, \mathbf{i}_{\text{sol}})^{\top}.$$

We assume that System (2.138) is an index-1 DAE, i.e., $\partial \mathbf{g}_1 / \partial \mathbf{z}_1$ nonsingular, which is the case if several topological conditions are fulfilled, [24]. The field PDE will describe a relation between the unknown currents $\mathbf{z}_{2b}$ and the voltage drops

$$\mathbf{v}_{\text{str}} := \mathbf{A}_{\text{str}}^{\top} \mathbf{u} \qquad \text{and} \qquad \mathbf{v}_{\text{sol}} := \mathbf{A}_{\text{sol}}^{\top} \mathbf{u}\,,$$

that will serve as an external excitement of Maxwell's Equations.

2.2.3.1 Maxwell's Equations

Maxwell's equations can be applied to describe a wide range of electromagnetic devices; in our focus are device parts that are typically embedded in electrical circuits exhibiting significant magnetic effects and dissipation losses, but with a disregardable displacement current. This kind of application is covered by the *magnetoquasistatic* (MQS) subset of Maxwell's Equations, [39], that is given by the partial differential equations

$$\begin{aligned} \nabla \times \boldsymbol{E} &= -\frac{\mathrm{d}\boldsymbol{B}}{\mathrm{d}t}\,, & \nabla \times \boldsymbol{H} &= \boldsymbol{J}\,, \\ \nabla \cdot \boldsymbol{D} &= \boldsymbol{\rho}\,, & \nabla \cdot \boldsymbol{B} &= 0\,, \end{aligned} \tag{2.139a}$$

with algebraic material relations

$$\boldsymbol{J} = \sigma \boldsymbol{E}\,, \qquad \boldsymbol{D} = \varepsilon_0\, \varepsilon_r \boldsymbol{E} = \varepsilon \boldsymbol{E}\,, \qquad \boldsymbol{B} = \mu_0\, \mu_r \boldsymbol{H} = \mu \boldsymbol{H}\,, \tag{2.139b}$$

on a domain Ω and typically with the *flux wall* boundary condition

$$\boldsymbol{B} \cdot \mathbf{n}_\perp = 0 \quad \text{on } \partial\Omega\,, \tag{2.139c}$$

where $\boldsymbol{E} = \boldsymbol{E}(\mathbf{r}, t)$ is the electric field strength, depending on its location in space $\mathbf{r} = (x, y, z)^\top$ and time t, similarly $\boldsymbol{B} = \boldsymbol{B}(\mathbf{r}, t)$ is the magnetic flux density, whose normal component is vanishing at the boundary, since the vector $\mathbf{n}_\perp$ defines here the outer normal at the boundary. $\boldsymbol{H} = \boldsymbol{H}(\mathbf{r}, t)$ denotes the magnetic field strength, $\boldsymbol{D} = \boldsymbol{D}(\mathbf{r}, t)$ the electric flux density, $\boldsymbol{\rho} = \boldsymbol{\rho}(\mathbf{r}, t)$ the electric charge density and $\boldsymbol{J} = \boldsymbol{D}(\mathbf{r}, t)$ the electric current density. The material parameters $\varepsilon = \varepsilon(\mathbf{r})$, $\sigma = \sigma(\mathbf{r})$, $\mu = \mu(\mathbf{r}, \boldsymbol{H})$ are rank-2 tensors describing the permittivity, conductivity and permeability; the first two tensors are assumed constant but the permeability may depend nonlinearly on the field strength. If we neglect furthermore hysteresis, the Jacobian $\partial \boldsymbol{B} / \partial \boldsymbol{H}$ is symmetric positive definite, [38], and we can derive from the second relation of (2.139b) the *HB-characteristic*

$$\boldsymbol{H} = \nu \boldsymbol{B}$$

with the (nonlinear) reluctivity $\nu = \nu(\mathbf{r}, \boldsymbol{B})$ acting as the inverse of the permeability. Now when expressing the magnetic flux and the electric field in terms of the magnetic vector potential $\boldsymbol{A} = \boldsymbol{A}(\mathbf{r}, t)$ and the electric scalar potential $\boldsymbol{\varphi} = \boldsymbol{\varphi}(\mathbf{r}, t)$

$$\boldsymbol{B} = \nabla \times \boldsymbol{A}\,, \qquad \boldsymbol{E} = -\nabla \boldsymbol{\varphi} - \frac{\mathrm{d}\boldsymbol{A}}{\mathrm{d}t}\,, \tag{2.140}$$

Ampère's Law may be equivalently given as the *curl-curl* equation

$$\nabla \times (\nu \nabla \times \boldsymbol{A}) = \boldsymbol{J} \ . \tag{2.141}$$

The curl-curl equation does not determine the potentials uniquely, because the definitions (2.140) are still fulfilled after a gauge transformation. Typically one defines a representant from the class of equivalent potentials as the desired solution by enforcing an additional gauge condition, for example *Coulomb's gauge*

$$\nabla \cdot \boldsymbol{A} = 0 \ , \tag{2.142}$$

which ensures on simply connected domains a unique solution of the problem in the vector potential formulation, [14].

In the 2D case, where a planar model is embedded in an 3D environment both, the magnetic vector potential $\boldsymbol{A}$ and the source current density $\boldsymbol{J}$ exhibit only components in z-direction, which are perpendicular to the planar model in the $x-y$ plane, i.e.,

$$\boldsymbol{A} = \begin{pmatrix} 0 & 0 & \boldsymbol{A}_z \end{pmatrix}^\top \qquad \text{and} \qquad \boldsymbol{J} = \begin{pmatrix} 0 & 0 & \boldsymbol{J}_z \end{pmatrix}^\top .$$

Thus the potential $\boldsymbol{A}$ fulfills automatically the Coulomb gauge

$$\nabla \cdot \boldsymbol{A} = \frac{\partial \boldsymbol{A}_x}{\partial x} + \frac{\partial \boldsymbol{A}_y}{\partial y} + \frac{\partial \boldsymbol{A}_z}{\partial z} = 0 \ ,$$

since $\boldsymbol{A}_x = \boldsymbol{A}_y = 0$ is trivial and $\boldsymbol{A}_z$ is independent of z and therefore the potential is uniquely defined without enforcing a gauge explicitly; this is in contrast to the 3D case.

2.2.3.2 Conductor Models

In the following the models for the *solid* and *stranded conductor* are derived, whose characteristics are determined by Maxwell's Equations (2.139), but on the other hand allow us to identify parts of the field domain Ω as branches in a circuit using voltages $\mathbf{v}_{\text{sol}}$, $\mathbf{v}_{\text{str}}$ and currents $\mathbf{i}_{\text{sol}}$, $\mathbf{i}_{\text{str}}$, [13]. We denote the corresponding parts of the domain by

$$\Omega_{\text{sol},l} \subset \Omega \qquad \text{and} \qquad \Omega_{\text{str},k} \subset \Omega \qquad \text{for } 1 \le l \le N_{\text{sol}},\ 1 \le k \le N_{\text{str}}$$

and assume furthermore that they are mutually non-overlapping.

The solid conductor model describes the behavior of a massive bar of conducting material, as shown in Fig. 2.3b. For high frequencies there is a tendency for the current density in the core of those conductor to be smaller than near the surface, [39]. This phenomenon is called *skin effect*. It causes the resistance of the conductor

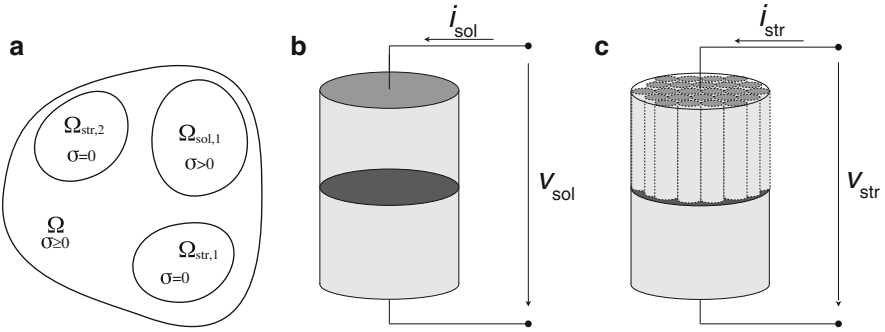

Fig. 2.3 Conductors Models. (**a**) Sketch of a 2D domain with two stranded and one solid conductor, (**b**) solid conductor made of massive conducting material causing eddy currents and (**c**) stranded conductor made of thin strands

to increase with the frequency of the current. A similar phenomenon appears in a solid conductor when localized in the neighborhood of other current carrying conductors. Also then, eddy currents and eddy-current losses appear in the solid conductor. These effects are to be simulated in the following: the solid conductor will serve as the device in a electrical circuit, where skin- and proximity effects are considered.

The voltage drop along each solid conductor is applied as the potential difference between two electrodes, i.e.,

$$-\nabla\boldsymbol{\varphi} = \sum_{l=1}^{N_{\mathrm{sol}}} \boldsymbol{\chi}_{\mathrm{sol},l}\,(\mathbf{v}_{\mathrm{sol}})_l$$

where $\boldsymbol{\chi}_{\mathrm{sol},l}$ is the *potential distribution* function of the l-th solid conductor with $\operatorname{supp}\boldsymbol{\chi}_{\mathrm{sol},l} = \Omega_{\mathrm{sol},l}$. Inserting the voltage drop into Ohm's Law, first equation in (2.139b), and applying it as the only excitement of the curl-curl equation yields (2.141)

$$\sigma\frac{\mathrm{d}\boldsymbol{A}}{\mathrm{d}t} + \nabla\times(\nu\nabla\times\boldsymbol{A}) = \sum_{l=1}^{N_{\mathrm{sol}}}\sigma\boldsymbol{\chi}_{\mathrm{sol},l}\,(\mathbf{v}_{\mathrm{sol}})_l \ . \tag{2.143a}$$

The current through the solid conductor is found by integrating the current density over the electrodes. This is equivalent to integrating the quantity $\boldsymbol{\chi}_{\mathrm{sol}}\cdot\boldsymbol{J}$ over the whole computational domain, i.e.,

$$(\mathbf{i}_{\mathrm{sol}})_l = \int_{\Omega}\boldsymbol{\chi}_{\mathrm{sol},l}\cdot\boldsymbol{J}\ \mathrm{d}\Omega = (\mathbf{G}_{\mathrm{sol}})_{l,l}\,(\mathbf{v}_{\mathrm{sol}})_l - \int_{\Omega}\sigma\boldsymbol{\chi}_{\mathrm{sol},l}\cdot\frac{\mathrm{d}\boldsymbol{A}}{\mathrm{d}t}\ \mathrm{d}\Omega\ , \tag{2.143b}$$

for $l = 1, \ldots, N_{\text{sol}}$, where each entry of the positive definite diagonal matrix

$$(\mathbf{G}_{\text{sol}})_{l,l} = \int_{\Omega} \sigma \boldsymbol{\chi}_{\text{sol},l} \cdot \boldsymbol{\chi}_{\text{sol},l} \, \mathrm{d}\Omega \, . \tag{2.143c}$$

corresponds to the lumped DC conductivity of a solid conductor.

In contrast to the solid conductor, the stranded conductor is not built of a single solid material, but consists of thin individual strands wound to form a coil, as depicted in Fig. 2.3c. Each strand does not exhibit significant eddy currents because of its cross section, which is assumed to be substantially smaller than the skin depth related to the frequencies occurring in the model, hence the conductivity, which introduces eddy current effects in the curl-curl equation, is assumed to vanish within stranded conductors

$$\sigma \frac{\mathrm{d}\boldsymbol{A}}{\mathrm{d}t}\Big|_{\Omega_{\text{str},k}} = \mathbf{0} \quad \text{with } k = 1, \ldots, N_{\text{str}}. \tag{2.144}$$

We assume furthermore windings with constant cross-section and thus a homogeneous current distribution holds in the conductor domain, i.e.,

$$\boldsymbol{J} = \sum_{k=1}^{N_{\text{str}}} \boldsymbol{\chi}_{\text{str},k} \, (\mathbf{i}_{\text{str}})_k$$

where $\boldsymbol{\chi}_{\text{str},k}$ is the *winding function* for the k-th stranded conductor with $\operatorname{supp} \boldsymbol{\chi}_{\text{str},l} = \Omega_{\text{str},l}$, such that the curl-curl equation becomes

$$\nabla \times (\nu \nabla \times \boldsymbol{A}) = \sum_{k=1}^{N_{\text{str}}} \boldsymbol{\chi}_{\text{str},k} \, (\mathbf{i}_{\text{str}})_k \, . \tag{2.145a}$$

The flux linked with the winding is given by

$$\psi_k = \int_{\Omega} \boldsymbol{\chi}_{\text{str},k} \cdot \boldsymbol{A} \, \mathrm{d}\Omega$$

and the total voltage drop along the stranded conductor consists of this induced part and a resistive part, i.e.,

$$(\mathbf{v}_{\text{str}})_k = (\mathbf{R}_{\text{str}})_{k,k} \, (\mathbf{i}_{\text{str}})_k + \frac{\mathrm{d}\psi_k}{\mathrm{d}t} \, , \tag{2.145b}$$

where the diagonal DC resistance matrix $\mathbf{R}_{\text{str}}$ can be computed from the model by

$$(\mathbf{R}_{\text{str}})_{k,k} = \int_{\Omega} \frac{1}{f_{\text{str}}} \sigma^{-1} \boldsymbol{\chi}_{\text{str},k} \cdot \boldsymbol{\chi}_{\text{str},k} \, \mathrm{d}\Omega \, , \tag{2.145c}$$

and $f_{\text{str}} \in (0, 1]$ is the fill factor accounting for the cross-sectional fraction of conductive versus insulating materials; in this equation the σ^{-1} is only evaluated

in the domains $\Omega_{\mathrm{str},k}$ $(k = 1, \ldots, N_{\mathrm{str}})$, where $\sigma > 0$but anywhere else in Ω the inverse is not necessarily well defined due to non-conducting materials.

Now summing up all excitements for solid and stranded conductors, i.e., Eqs. (2.143)–(2.145), and putting everything together, we obtain the following PDE system

$$\sigma \frac{\mathrm{d}\boldsymbol{A}}{\mathrm{d}t} + \nabla \times (\nu \nabla \times \boldsymbol{A}) = \sum_k \boldsymbol{\chi}_{\mathrm{str},k} \, (\mathbf{i}_{\mathrm{str}})_k + \sum_l \sigma \boldsymbol{\chi}_{\mathrm{sol},l} \, (\mathbf{v}_{\mathrm{sol}})_l \tag{2.146a}$$

$$\int_{\Omega} \boldsymbol{\chi}_{\mathrm{str},k} \cdot \frac{\mathrm{d}\boldsymbol{A}}{\mathrm{d}t} \, \mathrm{d}\Omega = (\mathbf{v}_{\mathrm{str}})_k - (\mathbf{R}_{\mathrm{str}})_{k,k} \cdot (\mathbf{i}_{\mathrm{str}})_k \,, \tag{2.146b}$$

$$\int_{\Omega} \sigma \boldsymbol{\chi}_{\mathrm{sol},l} \cdot \frac{\mathrm{d}\boldsymbol{A}}{\mathrm{d}t} \, \mathrm{d}\Omega = (\mathbf{G}_{\mathrm{sol}})_{l,l} \cdot (\mathbf{v}_{\mathrm{sol}})_l - (\mathbf{i}_{\mathrm{sol}})_l \,, \tag{2.146c}$$

with Coulomb gauging, flux wall boundary and initial conditions

$$\nabla \cdot \boldsymbol{A} = 0, \qquad \boldsymbol{A} \times \mathbf{n}_{\perp} = 0 \text{ on } \partial\Omega, \qquad \boldsymbol{A}(\mathbf{r}, t_0) = \boldsymbol{A}_0 \text{ at } t = t_0. \tag{2.146d}$$

Finally the coupling of the field PDE (2.146) and the circuit DAE (2.138) yields the full field/circuit PDAE problem.

2.2.3.3 Discretization

Following the method of lines, a spatial discretization of the PDE has to be applied first and a time discretization of the overall system in the second step. For spatial discretization we apply the Finite Integration Technique (FIT), [63], which translates the continuous Maxwell equations one by one into a space-discrete set, called the Maxwell grid equations (MGE). The topology is approximated by a finite number of cells $\mathbf{V}(n)$ for $1 \leq n \leq N$. In 3D those cells are hexahedra when applying the simplest mesh, such that the scheme is equivalent to the finite-difference time-domain method proposed by Yee, [66]. Other methods (FEM) are analoguously, see [15].

The hexahedra discretization yields a cell complex $\mathbf{G}$, composed of intervals defined by equidistant distributed coordinates x_i, y_j and z_k

$$\begin{aligned}\mathbf{G} := \{ &\mathbf{V}(n) := \mathbf{V}(i,j,k) \mid \mathbf{V}(i,j,k) = [x_i, x_{i+1}] \times [y_j, y_{j+1}] \times [z_k, z_{k+1}]; \\ &i = 1, \ldots, I-1; j = 1, \ldots, J-1; k = 1, \ldots, K-1\},\end{aligned}$$

where the three indices i, j and k are combined into one space index, which allows us to number the elements consecutively:

$$n = n(i,j,k) = i + (j-1) \cdot I + (k-1) \cdot I \cdot J \,, \tag{2.147}$$

such that $n \leq N := I \cdot J \cdot K$.

The intersection of two volumes is by construction either empty for non-neighboring volumes or one of the following p-cells, where $p \in \{0, 1, 2, 3\}$ denotes the dimension of the geometrical object and $w \in \{x, y, z\}$ a direction in space:

- 0-cell: a simple point $\mathbf{P}(n)$,
- 1-cell: an edge $\mathbf{L}_w(n)$,
- 2-cell: a facet $\mathbf{A}_w(n)$,
- 3-cell: a volume $\mathbf{V}(n)$.

Every object is associated with its smallest numbered connected point $\mathbf{P}(n)$. An edge $\mathbf{L}_w(n)$ connects two in w-direction neighbored points $\mathbf{P}(n)$ and $\mathbf{P}(n')$ $(n < n')$ and is always directed from $\mathbf{P}(n)$ towards $\mathbf{P}(n')$. A facet $\mathbf{A}_w(n)$ is defined by $\mathbf{P}(n)$ and the direction w, in which its normal vector points.

The basic idea of FIT is the usage of two grids, the primary grid $\mathbf{G}$ is supported by the dual grid $\tilde{\mathbf{G}}$, which is identically but shifted in x-, y- and z-direction by half of a cell length, see Fig. 2.4a. The definition of the dual p-cells, i.e., edges $\tilde{\mathbf{L}}_w(n)$, facets $\tilde{\mathbf{A}}_w(n)$ and volumes $\tilde{\mathbf{V}}(n)$ is analogous to the primary grid $(w \in \{x, y, z\})$. In the following each primary p-cell of $\mathbf{G}$ will be related to one $(3 - p)$-cell of $\tilde{\mathbf{G}}$.

As state variables of the FIT, we introduce electric and magnetic voltages and fluxes. They are defined as integrals of the electric and magnetic field strengths and flux densities over geometrical objects of the computational grid, with respect to the directions $w \in \{x, y, z\}$. The state variables are assigned diacritics $(\hat{\cdot})$ according to their dimension p of the underlying object. The grid voltages over the edges read as

$$\hat{\mathbf{e}}_w(n) = \int_{\mathbf{L}_w(n)} \boldsymbol{E}\ \mathrm{d}\mathbf{s}\,, \qquad \hat{\mathbf{a}}_w(n) = \int_{\mathbf{L}_w(n)} \boldsymbol{A}\ \mathrm{d}\mathbf{s}\,, \qquad \text{and} \qquad \hat{\mathbf{h}}_w(n) = \int_{\tilde{\mathbf{L}}_w(n)} \boldsymbol{H}\ \mathrm{d}\mathbf{s}\,.$$

The fluxes are located on the grid facets and read

$$\hat{\tilde{\mathbf{b}}}_w(n) = \int_{\mathbf{A}_w(n)} \boldsymbol{B}\ \mathrm{d}\mathbf{A}\,, \qquad \hat{\tilde{\mathbf{d}}}_w(n) = \int_{\tilde{\mathbf{A}}_w(n)} \boldsymbol{D}\ \mathrm{d}\mathbf{A}\,, \qquad \text{and} \qquad \hat{\tilde{\mathbf{j}}}_w(n) = \int_{\tilde{\mathbf{A}}_w(n)} \boldsymbol{J}\ \mathrm{d}\mathbf{A}\,.$$

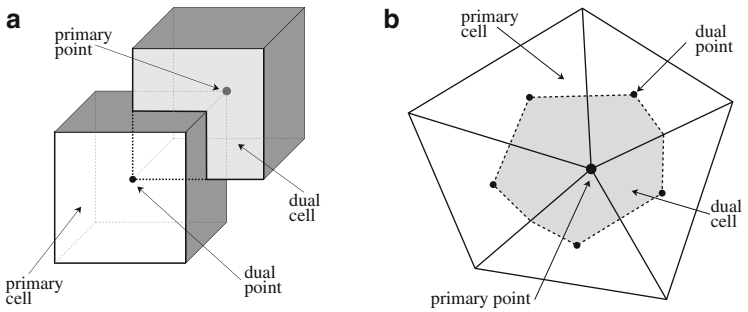

Fig. 2.4 Examples for primary and dual grid cells in 3D and 2D discretizations. (**a**) Staggered hexahedra. (**b**) Barycentric triangulation

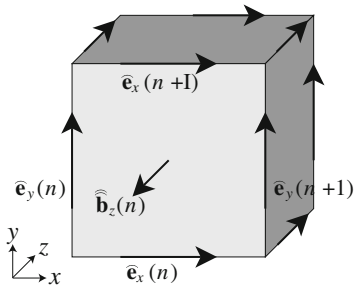

Fig. 2.5 Discretization of Faradays Law

To simplify the notation we will build augmented vectors for each of the newly defined quantities with a length of $3N$, including every spatial direction. For example the discrete electric field strengths are collected in

$$\widehat{\mathbf{e}} = (\bar{\mathbf{e}}_x(1), \ldots, \bar{\mathbf{e}}_x(N), \bar{\mathbf{e}}_y(1), \ldots, \bar{\mathbf{e}}_y(N), \bar{\mathbf{e}}_z(1), \ldots, \bar{\mathbf{e}}_z(N))^\top \,. \tag{2.148}$$

The remaining vectors $\widehat{\mathbf{a}}$, $\widehat{\mathbf{h}}$, $\widehat{\widehat{\mathbf{b}}}$, $\widehat{\widehat{\mathbf{d}}}$ and $\widehat{\widehat{\mathbf{j}}}$ are defined analogously.

Using these notations we are able to discretize Maxwell's Equations (2.139) in terms of FIT. For example, Faraday's law, Fig. 2.5, for a single grid facet $A_z(n)$ can be written discretely as

$$\bar{\mathbf{e}}_x(n) + \bar{\mathbf{e}}_y(n+1) - \bar{\mathbf{e}}_x(n+I) - \bar{\mathbf{e}}_y(n) = -\frac{\mathrm{d}}{\mathrm{d}t}\widehat{\widehat{\mathbf{b}}}_z(n) \,, \tag{2.149}$$

which exploits the new order of numbering and is easily generalized to all facets. The relations for all grid facets are collected in the matrix equation

$$\underbrace{\begin{pmatrix} \vdots \\ \cdots 1 \cdots -1 \cdots -1 \;\; 1 \cdots \\ \vdots \end{pmatrix}}_{\mathbf{C}} \underbrace{\begin{pmatrix} \vdots \\ \widehat{\mathbf{e}}_x(n) \\ \vdots \\ \widehat{\mathbf{e}}_x(n+I) \\ \vdots \\ \widehat{\mathbf{e}}_y(n) \\ \widehat{\mathbf{e}}_y(n+1) \\ \vdots \end{pmatrix}}_{\widehat{\mathbf{e}}} = -\frac{\mathrm{d}}{\mathrm{d}t} \underbrace{\begin{pmatrix} \vdots \\ \widehat{\widehat{\mathbf{b}}}_z(n) \\ \vdots \end{pmatrix}}_{\widehat{\widehat{\mathbf{b}}}} \,. \tag{2.150}$$

Applying this procedure to all continuous MQS equations yields the MQS *Maxwell's Grid Equations*, where the differential operators are represented by

the discrete curl operators $\mathbf{C}$, $\tilde{\mathbf{C}} = \mathbf{C}^\top$ and divergence operators $\mathbf{S}$, $\tilde{\mathbf{S}}$, which live on the primary and dual grid, respectively

$$\begin{aligned} \mathbf{C}\widehat{\mathbf{e}} &= -\frac{\mathrm{d}}{\mathrm{d}t}\widehat{\widetilde{\mathbf{b}}}\,, & \tilde{\mathbf{C}}\widehat{\mathbf{h}} &= \widehat{\widetilde{\mathbf{j}}}\,, \\ \tilde{\mathbf{S}}\widehat{\widetilde{\mathbf{d}}} &= \mathbf{q}\,, & \mathbf{S}\widehat{\widetilde{\mathbf{b}}} &= \mathbf{0}\,, \end{aligned} \tag{2.151}$$

with the vector $\mathbf{q}$ containing the electrical charges allocated at the dual grid cells, resembles closely the continuous system (2.139) and maintains several of its properties.

The laws of the continuous magnetic vector potential (2.140) transfer to

$$\mathbf{C}\widehat{\mathbf{a}} = \widehat{\widetilde{\mathbf{b}}} \qquad \text{and} \qquad \widehat{\mathbf{e}} = -\frac{\mathrm{d}}{\mathrm{d}t}\widehat{\mathbf{a}} - \mathbf{S}^\top\phi\,, \tag{2.152}$$

with the discrete electric scalar potential ϕ. The discrete potentials are not uniquely defined, similar to the continuous ones, because the curl matrix $\mathbf{C}$ has a non-trivial nullspace.

Working towards a complete discretization of Maxwell's Equations, the material relations (2.139b) have to be given in terms of the discrete quantities. This relates the fluxes on the primary grid $\mathbf{G}$ to the voltages on the dual analogon $\tilde{\mathbf{G}}$ and vice versa. Hence, the material relations establish a coupling between both grids, but their construction requires approximations through averaging processes and here lies the fundamental difference between the various discretization approaches, e.g. FEM and FIT, [15]. FIT has the advantage, that for isotropic and anisotropic materials, whose principal directions coincide with the mesh directions, the material matrices are always diagonal.

For example the magnetic flux density $\boldsymbol{B}$ is related to the magnetic field strength $\boldsymbol{H}$ through the permeability μ. In coherence with our earlier requirements we will assume that there are local permeabilities $\mu(n)$ for each grid volume $\mathbf{V}(n)$. When we start with the definition of the discrete magnetic field strength in conjunction with constitutive relation and averaging its value over the facet $\mathbf{A}_w(n)$ to $|\boldsymbol{B}|$, we get the integral quantity

$$\begin{aligned} \widehat{\mathbf{h}}_w(n) &= \int_{\tilde{\mathbf{L}}_w(n)} \boldsymbol{H}\cdot\mathrm{d}\boldsymbol{s} = \int_{\tilde{\mathbf{L}}_w(n)} \mu^{-1}\boldsymbol{B}\cdot\mathrm{d}\boldsymbol{s} \\ &= \bar{\mu}^{-1}(n)\,|\tilde{\mathbf{L}}_w(n)|\cdot|\boldsymbol{B}| + \mathscr{O}(h^l) \qquad (2.153) \\ &\doteq \bar{\mu}^{-1}(n)\,|\tilde{\mathbf{L}}_w(n)|\cdot|\boldsymbol{B}|\,, \qquad (2.154) \end{aligned}$$

with averaged permeabilities $\bar{\mu}(n)$ that gives an error, whose order l depends on the used discretization grid (in this particular case of a Cartesian grid $l = 2$) and

the maximum length of the cell edges $h := \max \mathbf{L}_w(n)$, with $w \in \{x, y, z\}$ and $1 \leq n \leq N$. In a similar manner, we derive for the magnetic flux density

$$\begin{aligned}\hat{\tilde{\mathbf{b}}}_w(n) &= \int_{\mathbf{A}_w(n)} \boldsymbol{B} \cdot \mathrm{d}\mathbf{A} \\ &= |\mathbf{A}_w(n)| \cdot |\boldsymbol{B}| + \mathscr{O}(h^{l+1}) \\ &\doteq |\mathbf{A}_w(n)| \cdot |\boldsymbol{B}|. \end{aligned} \tag{2.155}$$

Both Eqs. (2.154) and (2.155) contain the averaged magnetic flux density $|\boldsymbol{B}|$, which is unknown. Eliminating this unknown through inserting one equation into the other leads to

$$\hat{\tilde{\mathbf{b}}}_w(n) = \underbrace{\bar{\mu}(n) \frac{|\mathbf{A}_w(n)|}{|\tilde{\mathbf{L}}_w(n)|}}_{=:\bar{\mu}_w(n)} \cdot \hat{\mathbf{h}}_w(n) \ ,$$

finally arranging of these permeabilities as a matrix gives

$$\mathbf{M}_\mu := \mathrm{diag}\left(\bar{\mu}_x(1), \ldots, \bar{\mu}_x(N), \bar{\mu}_y(1), \ldots, \bar{\mu}_y(N), \bar{\mu}_z(1), \ldots, \bar{\mu}_z(N)\right).$$

Similarly the other two material matrices are obtained, such that the laws can be given as

$$\hat{\tilde{\mathbf{j}}} = \mathbf{M}_\sigma \hat{\mathbf{e}} \ , \qquad \hat{\tilde{\mathbf{d}}} = \mathbf{M}_\varepsilon \hat{\mathbf{e}} \ , \qquad \hat{\mathbf{h}} = \mathbf{M}_\nu \hat{\tilde{\mathbf{b}}} \ ,$$

where $\mathbf{M}_\sigma$, $\mathbf{M}_\varepsilon$ and $\mathbf{M}_\mu$ are the (diagonal) matrices of conductivities, permittivities and reluctivities. As before in the continuous case the first two matrices are assumed to be constant, and the reluctivity matrix $\mathbf{M}_\nu = \mathbf{M}_\nu(\hat{\tilde{\mathbf{b}}})$ may depend nonlinearly on the magnetic flux. Furthermore the matrices of permittivities and reluctivities (for all $\hat{\tilde{\mathbf{b}}}$) are positive definite, while the conductivity matrix is only positive semi-definite, due to vanishing conductances in electrical insulators.

2.2.3.4 Discrete Vector Potential Formulation

Now having obtained a discrete version of Maxwell's Equations, we can deduce the discrete curl-curl equation with the same steps we used to derive the continuous

formulation. The PDE (2.146) becomes the following space-discrete DAE

$$\mathbf{M}_\sigma \frac{\mathrm{d}}{\mathrm{d}t}\widehat{\mathbf{a}} + \tilde{\mathbf{C}}\mathbf{M}_\nu \mathbf{C}\widehat{\mathbf{a}} = \mathbf{Q}_{\mathrm{str}}\mathbf{i}_{\mathrm{str}} + \mathbf{M}_\sigma \mathbf{Q}_{\mathrm{sol}}\mathbf{v}_{\mathrm{sol}} \,, \tag{2.156a}$$

$$\mathbf{Q}_{\mathrm{str}}^\top \frac{\mathrm{d}}{\mathrm{d}t}\widehat{\mathbf{a}} = \mathbf{v}_{\mathrm{str}} - \mathbf{R}_{\mathrm{str}}\mathbf{i}_{\mathrm{str}} \,, \tag{2.156b}$$

$$\mathbf{Q}_{\mathrm{sol}}^\top \mathbf{M}_\sigma \frac{\mathrm{d}}{\mathrm{d}t}\widehat{\mathbf{a}} = \mathbf{G}_{\mathrm{sol}}\mathbf{v}_{\mathrm{sol}} - \mathbf{i}_{\mathrm{sol}} \,, \tag{2.156c}$$

where the matrix $\mathbf{Q} = [\mathbf{Q}_{\mathrm{sol}}, \mathbf{Q}_{\mathrm{str}}]$ is the discrete analogue to the characteristic functions χ in the continuous model: each column of this matrix corresponds to a conductor model and imposes currents/voltages onto edges of the grid, while each row in the transposed matrix $\mathbf{Q}^\top$ corresponds to the integration of the vector potential over the domain Ω in system (2.146). The conductor domains shall not overlap and we assume this to be true even after the spatial discretization, which affects the coupling matrix as follows

$$(\mathbf{Q})_{k,m}\,(\mathbf{Q})_{m,l} = 0 \text{ for all } m \text{ and } k \neq l. \tag{2.157}$$

Additionally we find especially for the stranded conductor coupling matrix

$$(\mathbf{M}_\sigma)_{k,m}\,(\mathbf{Q}_{\mathrm{str}})_{m,l} = 0 \text{ for all } m, k \text{ and } l, \tag{2.158}$$

which is a consequence of the disregard of eddy currents in stranded conductors, see Eq. (2.144). The matrices of lumped resistances and conductivities are extracted from the model, as explained in Eqs. (2.143c) and (2.145c) and they read in their discrete form as

$$\mathbf{R}_{\mathrm{str}} := \mathbf{Q}_{\mathrm{str}}^\top \mathbf{M}_{\sigma,\mathrm{str}}^{+} \mathbf{Q}_{\mathrm{str}} \qquad \text{and} \qquad \mathbf{G}_{\mathrm{sol}} := \mathbf{Q}_{\mathrm{sol}}^\top \mathbf{M}_\sigma \mathbf{Q}_{\mathrm{sol}} \,, \tag{2.159}$$

where $\mathbf{M}_{\sigma,\mathrm{str}}^{+}$ is the pseudo-inverse of the conductivity matrix with conductivities only in the stranded conductor domains, hence

$$(\mathbf{M}_{\sigma,\mathrm{str}})_{k,m}\,(\mathbf{Q}_{\mathrm{sol}})_{m,l} = 0 \text{ for all } m, k, l \qquad \text{and} \qquad \mathbf{M}_\sigma \mathbf{M}_{\sigma,\mathrm{str}}^{+} = \mathbf{0} \,, \tag{2.160}$$

where $\mathbf{M}_{\sigma,\mathrm{str}}^{+}$ is the pseudo-inverse of $\mathbf{M}_{\sigma,\mathrm{str}}$.

2.2.3.5 Gauging of the Curl-Curl Equation

In 3D the curl-curl equation (2.156a) has no unique solution since both the conductivity matrix $\mathbf{M}_\sigma$ and the curl operator $\mathbf{C}$ have non-trivial nullspaces, and

thus the matrix pencil

$$\lambda \mathbf{M}_\sigma + \tilde{\mathbf{C}}\mathbf{M}_\nu \mathbf{C} \text{ for } \lambda \in \mathbb{R}$$

is in general only positive semi-definite, but a gauging, can enforce positive definiteness. For example a special Coulomb gauging, see (2.142), which applies only to the non-conducting parts of the problem, is proposed in [18]

$$\tilde{\mathbf{S}}\mathbf{M}_{\hat{\sigma}}\,\hat{\mathbf{a}} = \mathbf{0}\,,$$

where $\mathbf{M}_{\hat{\sigma}}$ is a special material matrix with artificial conductivities on the diagonal, if the entry corresponds to a non-conducting material, such that all its columns are in the nullspace of $\mathbf{M}_\sigma$. Using a Schur complement the restriction can by integrated into the curl-curl matrix, which becomes for example

$$\mathbf{K}_\nu := \tilde{\mathbf{C}}\mathbf{M}_\nu \mathbf{C} - \mathbf{M}_{\hat{\sigma}}\tilde{\mathbf{S}}^\top \mathbf{N}\tilde{\mathbf{S}}\mathbf{M}_{\hat{\sigma}}$$

and gives the grad-div regularization, [19]. Finally the matrix pencil $\lambda\mathbf{M}_\sigma + \mathbf{K}_\nu$ is positive definite for a simply connected domain Ω (without cavities), if the matrix $\mathbf{N}$ is negative definite, [18].

The positive definiteness of the gauged matrix pencil can still be enforced, if nonlinear reluctivities are considered, i.e., $\mathbf{M}_\nu = \mathbf{M}_\nu(\hat{\hat{\mathbf{b}}})$. The structure and hence the kernel of the nonlinear curl-curl matrix remain unchanged, as the following derivative shows

$$\frac{\mathrm{d}}{\mathrm{d}\hat{\mathbf{a}}}\left(\tilde{\mathbf{C}}\mathbf{M}_\nu(\hat{\hat{\mathbf{b}}})\mathbf{C}\hat{\mathbf{a}}\right) = \tilde{\mathbf{C}}\frac{\mathrm{d}}{\mathrm{d}\hat{\hat{\mathbf{b}}}}\left(\mathbf{M}_\nu(\hat{\hat{\mathbf{b}}})\mathbf{C}\hat{\mathbf{a}}\right)\frac{\mathrm{d}\hat{\hat{\mathbf{b}}}}{\mathrm{d}\hat{\mathbf{a}}} = \tilde{\mathbf{C}}\frac{\mathrm{d}}{\mathrm{d}\hat{\hat{\mathbf{b}}}}\left(\mathbf{M}_\nu(\hat{\hat{\mathbf{b}}})\hat{\hat{\mathbf{b}}}\right)\mathbf{C} = \tilde{\mathbf{C}}\frac{\mathrm{d}\hat{\mathbf{h}}}{\mathrm{d}\hat{\hat{\mathbf{b}}}}\mathbf{C}\,,$$

where both the reluctivity matrix $\mathbf{M}_\nu(\hat{\hat{\mathbf{b}}})$ and the differential reluctivity matrix $\mathbf{M}_{\nu,\mathrm{d}} := \mathrm{d}\hat{\mathbf{h}}/\mathrm{d}\hat{\hat{\mathbf{b}}}$ are still positive definite, [33]. In any case only the (constant) nullspace of the curl-operator has to be covered by the gauging and thus it is assumed in the following that

$$\lambda\mathbf{M}_\sigma + \mathbf{K}_\nu(\hat{\hat{\mathbf{b}}}) \qquad \text{and} \qquad \lambda\mathbf{M}_\sigma + \frac{\mathrm{d}}{\mathrm{d}\hat{\mathbf{a}}}\left(\mathbf{K}_\nu(\hat{\hat{\mathbf{b}}})\hat{\mathbf{a}}\right)$$

are positive definite for a $\lambda \in \mathbb{R}$.

2.2.3.6 Structure of the Coupled System

Having now transformed the field PDE into a uniquely solvable DAE, we discuss in the following the coupling of the subproblems using a more abstract formulation.

Lemma 2.1 *The field system* (2.156) *is equivalent to the semi-explicit initial value problem*

$$\begin{aligned} \dot{\mathbf{y}}_2 &= \mathbf{f}_2(\mathbf{y}_2, \mathbf{z}_{2a}, \mathbf{v}_1), \quad \textit{with} \quad \mathbf{y}_2(0) = \mathbf{y}_{2,0}, \\ \mathbf{0} &= \mathbf{g}_{2a}(\mathbf{y}_2, \mathbf{z}_{2a}), \\ \mathbf{0} &= \mathbf{g}_{2b}(\mathbf{y}_2, \mathbf{z}_{2a}, \mathbf{z}_{2b}), \end{aligned} \tag{2.161}$$

where $\mathbf{y}_2 := \mathscr{P}_\sigma \widehat{\mathbf{a}}$, $\mathbf{z}_{2a} := \mathscr{Q}_\sigma \widehat{\mathbf{a}}$, $\mathbf{z}_{2b} := (\mathbf{i}_{\mathrm{str}}, \mathbf{i}_{\mathrm{sol}})^\top$ *and* $\mathbf{v}_1 := (\mathbf{v}_{\mathrm{str}}, \mathbf{v}_{\mathrm{sol}})^\top$

Proof In a first step system (2.156) is reformulated, such that there are no dependencies on derivatives in the two solid and stranded conductor coupling equations (2.156c) and (2.156b). In a second step the curl-curl equation (2.156a) is split into equations coming from conductive materials and non-conductive materials, since only the first materials did yield a differential term $\frac{\mathrm{d}}{\mathrm{d}t}\widehat{\mathbf{a}}$.

Equation (2.156b) is left-multiplied by $\mathbf{Q}_{\mathrm{str}}\mathbf{R}_{\mathrm{str}}^{-1}$ and added to Eq. (2.156a), which yields

$$\left(\mathbf{M}_\sigma + \mathbf{Q}_{\mathrm{str}}\mathbf{R}_{\mathrm{str}}^{-1}\mathbf{Q}_{\mathrm{str}}^\top\right)\frac{\mathrm{d}}{\mathrm{d}t}\widehat{\mathbf{a}} + \mathbf{K}_\nu(\widehat{\widehat{\mathbf{b}}})\widehat{\mathbf{a}} = \mathbf{Q}_{\mathrm{str}}\mathbf{R}_{\mathrm{str}}^{-1}\mathbf{v}_{\mathrm{str}} + \mathbf{M}_\sigma\mathbf{Q}_{\mathrm{sol}}\mathbf{v}_{\mathrm{sol}}\,, \tag{2.162a}$$

where the new mass matrix $\mathbf{M}_\sigma + \mathbf{Q}_{\mathrm{str}}\mathbf{R}_{\mathrm{str}}^{-1}\mathbf{Q}_{\mathrm{str}}^\top$ is still symmetric positive semi-definite and can be interpreted as a special conductivity matrix, but it is obviously less sparse.

Left-multiplying Eq. (2.162a) by $\mathbf{Q}_{\mathrm{str}}^\top\mathbf{M}_{\sigma,\mathrm{str}}^+$ and adding to Eq. (2.156b) gives

$$\mathbf{i}_{\mathrm{str}} - \mathbf{R}_{\mathrm{str}}^{-1}\mathbf{Q}_{\mathrm{str}}^\top\mathbf{M}_{\sigma,\mathrm{str}}^+\mathbf{K}_\nu(\widehat{\widehat{\mathbf{b}}})\widehat{\mathbf{a}} = \mathbf{0}\,, \tag{2.162b}$$

because the conductors do not overlap $\mathbf{M}_{\sigma,\mathrm{str}}^+\mathbf{M}_\sigma = \mathbf{0}$, see Eq. (2.160) and due to the definition of the lumped resistance matrix for stranded conductors $\mathbf{Q}_{\mathrm{str}}^\top\mathbf{M}_{\sigma,\mathrm{str}}^+\mathbf{Q}_{\mathrm{str}} = \mathbf{R}_{\mathrm{str}}$ in Eq. (2.145c). Similarly a left-multiplication of Eq. (2.156a) by $\mathbf{Q}_{\mathrm{sol}}^\top$ added to Eq. (2.156c) gives

$$\mathbf{i}_{\mathrm{sol}} - \mathbf{Q}_{\mathrm{sol}}^\top\mathbf{K}_\nu(\widehat{\widehat{\mathbf{b}}})\widehat{\mathbf{a}} = \mathbf{0}\,, \tag{2.162c}$$

because of the definition of the lumped solid conductor conductances $\mathbf{G}_{\mathrm{sol}} = \mathbf{Q}_{\mathrm{sol}}^\top\mathbf{M}_\sigma\mathbf{Q}_{\mathrm{sol}}$.

Let us now split the curl-curl Equation (2.162a) according to the conductivity of the materials. The symmetric positive semi-definiteness of the mass matrix guarantees an orthogonal matrix $\mathscr{T}$ that transforms the mass matrix into its Jordan Normal Form

$$\mathscr{T}\left(\mathbf{M}_\sigma + \mathbf{Q}_{\mathrm{str}}\mathbf{R}_{\mathrm{str}}^{-1}\mathbf{Q}_{\mathrm{str}}^\top\right)\mathscr{T}^\top = \begin{pmatrix} \mathbf{J}_\sigma & \\ & \mathbf{0} \end{pmatrix},$$

where $\mathbf{J}_\sigma$ is a diagonal matrix consisting of the (positive) eigenvalues of $\mathbf{M}_\sigma$ and $\mathbf{Q}_{\text{str}}\mathbf{R}_{\text{str}}^{-1}\mathbf{Q}_{\text{str}}^\top$. This transformation depends only on the topology, there is neither a dependence on the vector potential nor on the time. Thus its application to the whole Eq. (2.162a) gives automatically a splitting of the vector potential $\hat{\mathbf{a}}$ into differential and algebraic parts, that is constant in time

$$\mathbf{y}_2 := \mathscr{P}_\sigma \hat{\mathbf{a}} := \begin{pmatrix}\mathbf{I} & \mathbf{0}\end{pmatrix} \mathscr{T} \hat{\mathbf{a}} \qquad \text{and} \qquad \mathbf{z}_{2a} := \mathscr{Q}_\sigma \hat{\mathbf{a}} := \begin{pmatrix}\mathbf{0} & \mathbf{I}\end{pmatrix} \mathscr{T} \hat{\mathbf{a}} \,,$$

such that $\hat{\mathbf{a}} = \mathscr{P}_\sigma^\top \mathbf{y}_2 + \mathscr{Q}_\sigma^\top \mathbf{z}_{2a}$, while the currents are just collected in an additional algebraic variable

$$\mathbf{z}_{2b} := (\mathbf{i}_{\text{str}}, \mathbf{i}_{\text{sol}})^\top \,.$$

The application of $\mathscr{T}$ to the right hand side of (2.162a) yields

$$\begin{aligned}
&\mathscr{T}\left(\mathbf{Q}_{\text{str}}\mathbf{R}_{\text{str}}^{-1}\mathbf{v}_{\text{str}} + \mathbf{M}_\sigma \mathbf{Q}_{\text{sol}}\mathbf{v}_{\text{sol}}\right) \\
=&\mathscr{T}\left(\mathbf{M}_\sigma + \mathbf{Q}_{\text{str}}\mathbf{R}_{\text{str}}^{-1}\mathbf{Q}_{\text{str}}^\top\right)\mathscr{T}^\top \mathscr{T}\left(\mathbf{Q}_{\text{str}}(\mathbf{Q}_{\text{str}}^\top\mathbf{Q}_{\text{str}})^{-1}\mathbf{v}_{\text{str}} + \mathbf{Q}_{\text{sol}}\mathbf{v}_{\text{sol}}\right) \\
=&\begin{pmatrix}\mathbf{J}_\sigma & \\ & \mathbf{0}\end{pmatrix} \mathscr{T}\left(\mathbf{Q}_{\text{str}}(\mathbf{Q}_{\text{str}}^\top\mathbf{Q}_{\text{str}})^{-1}\mathbf{v}_{\text{str}} + \mathbf{Q}_{\text{sol}}\mathbf{v}_{\text{sol}}\right)
\end{aligned}$$

by just utilizing the properties (2.157)–(2.159) and thus the transformation of Eq. (2.162a) using the new variables read

$$\begin{aligned}
\mathbf{J}_\sigma \frac{\mathrm{d}}{\mathrm{d}t}\mathbf{y} &= -\mathscr{P}_\sigma \mathbf{K}_\nu \mathscr{P}_\sigma^\top \mathbf{y}_2 - \mathscr{P}_\sigma \mathbf{K}_\nu \mathscr{Q}_\sigma^\top \mathbf{z}_{2a} + \mathscr{P}_\sigma\left(\mathbf{Q}_{\text{str}}\mathbf{R}_{\text{str}}^{-1}\mathbf{v}_{\text{str}} + \mathbf{M}_\sigma \mathbf{Q}_{\text{sol}}\mathbf{v}_{\text{sol}}\right) \\
\mathbf{0} &= \mathscr{Q}_\sigma \mathbf{K}_\nu \mathscr{P}_\sigma^\top \mathbf{y}_2 + \mathscr{Q}_\sigma \mathbf{K}_\nu \mathscr{Q}_\sigma^\top \mathbf{z}_{2a} \,. \qquad (2.163)
\end{aligned}$$

The first equation defines the function $\mathbf{f}_2$ after a left-multiplication by the inverse $\mathbf{J}_\sigma^{-1}$ of the Jordan Normal Form, while the second Eq. (2.163) defines the first algebraic constraint $\mathbf{g}_{2a}$. Finally the definition of the additional algebraic constraint $\mathbf{g}_{2b}$ follows immediately from Eqs. (2.162b) and (2.162c).

Using the new abstract notation, the field/circuit coupled problem consists of the two subsystems (2.138) and (2.161), i.e.,

$$\begin{aligned}
\dot{\mathbf{y}}_1 &= \mathbf{f}_1(\mathbf{y}_1, \mathbf{z}_1, \boxed{\mathbf{z}_2}), \qquad \text{and} \qquad \dot{\mathbf{y}}_2 = \mathbf{f}_2(\mathbf{y}_2, \mathbf{z}_2, \boxed{\mathbf{z}_1}), \\
\mathbf{0} &= \mathbf{g}_1(\mathbf{y}_1, \mathbf{z}_1, \boxed{\mathbf{z}_2}), \qquad\qquad \mathbf{0} = \mathbf{g}_2(\mathbf{y}_2, \mathbf{z}_2),
\end{aligned}$$

where the coupling terms are highlighted by boxes. Note, that the notation was abused slightly, since the algebraic variables $\mathbf{z}_1$ and $\mathbf{z}_2$ contain more than the actually needed node potentials $\mathbf{u}$ and the currents $\mathbf{i}_{\text{sol}}$ and $\mathbf{i}_{\text{str}}$ through solid and stranded conductors.

The coupled problems from electromagnetics are considered again in Chap. 2.

2.2.4 Thermal and Quantum Effects in Semiconductors

In semiconductor technology, the miniaturization of devices is more and more progressing. As a consequence, the simulation of the today nanoscale semiconductor devices requires advanced transport models that take into account also quantum effects and the heating of the crystal. These effects are not very relevant in micrometer devices, but they are crucial for the electric performance in the nanoscale case.

At semiclassical kinetic level the thermal effects are modeled by describing the energy transport in solids with a phonon gas obeying the Peierls kinetic equation while the charge transport is described by the Boltzmann equation, coupled to the Poisson equation for the electric potential. However such a complex system is very difficult to face from a numerical point of view and the simulations require long CPU times not suitable for CAD purposes in electrical engineering. For this reason simpler macroscopic models are warranted in order to use them in the design of electrical devices. A physically sound way for getting macroscopic models is to consider the moment system associated with the transport equations and obtain the closure relations with the maximum entropy principle (hereafter MEP) [9, 53, 54].

Concerning the quantum effects, the typical physical situation we want to describe is the case when the main contribution to the charge transport is semiclassical while the quantum effects enter as small perturbations. For example, this is reasonable for MOSFETs of characteristic length in the range of 10–20 nanometers under strong electric field. Now the semiclassical Boltzmann equation for electrons is replaced with the Wigner equation and a singular perturbation approach is used with a Chapman-Enskog expansion in the high field scaling.

What follows is based on [56] and [57].

2.2.4.1 The Electron-Phonon System

At semiclassical kinetic level, the transport of energy inside the crystal is modeled through quasi-particles called phonons (Fig. 2.6).

The electron-phonon system is described by the Boltzmann-Peierls equations for the distribution functions of electrons and phonons, coupled to the Poisson equation for the electric potential

$$\frac{\partial f}{\partial t} + \mathbf{v}(\mathbf{k}) \cdot \nabla_x f - \frac{e\,\mathbf{E}}{\hbar} \cdot \nabla_k f = C[f, g^{(ac)}, g^{(np)}], \tag{2.164}$$

$$\frac{\partial g^{(ac)}}{\partial t} + \frac{\partial \omega^{(ac)}}{\partial q^i} \frac{\partial g^{(ac)}}{\partial x^i} = S^{(ac)}[g^{(ac)}, g^{(np)}, f], \tag{2.165}$$

$$\frac{\partial g^{(np)}}{\partial t} = S^{(np)}[g^{(np)}, g^{(ac)}, f], \tag{2.166}$$

$$\mathbf{E} = -\nabla_x \Phi, \quad \nabla(\epsilon \nabla \Phi) = -e(C_D(x) - n), \tag{2.167}$$

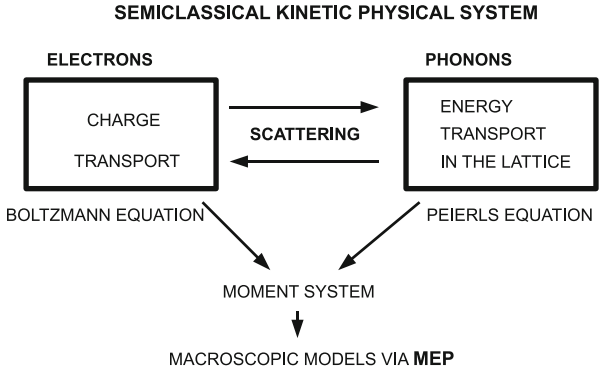

Fig. 2.6 Schematic representation of the electron-phonon system describing the coupling between the charge transport and the crystal thermal effect in a semiconductor and general strategy for getting macroscopic models

where *ac* and *np* stand for acoustic and non-polar optical phonons. $f(\mathbf{x}, \mathbf{k}, t)$ is the electron distribution function which depends on the position $\mathbf{x} \in \mathbb{R}^3$, time t and wave vector $\mathbf{k}$. $C[f, g^{(ac)}, g^{(np)}]$ is the collision operator of electrons with phonons and impurities. We will neglect electron-electron interaction because it is relevant only at very high density, usually not reached in the most common electron devices. e represents the absolute value of the elementary charge. ∇_x and ∇_k denote the nabla operator with respect to $\mathbf{x}$ and $\mathbf{k}$, respectively.

We assume that the conduction bands of semiconductor are described by Kane's dispersion relation

$$\mathscr{E}(k) = \frac{1}{2\alpha}\left[-1 + \sqrt{1 + 4\alpha\frac{\hbar^2 k^2}{2m^*}}\right], \qquad \mathbf{k} \in \mathbb{R}^3,$$

with $\mathscr{E}(k)$ the energy measured from the valley minimum, m^* the effective electron mass, $\hbar\mathbf{k}$ the crystal momentum and α the non parabolicity parameter (for Silicon $\alpha = 0.5eV^{-1}$). Consequently, according to the quantum relation $\mathbf{v} = \frac{1}{\hbar}\nabla_{\mathbf{k}}\mathscr{E}(k)$, the electron velocity is given by the relation $\mathbf{v} = \dfrac{\hbar\mathbf{k}}{m^*\sqrt{1 + 4\alpha\frac{\hbar^2 k^2}{2m^*}}}$.

$g^{(A)} \equiv g(\mathbf{x}, t, \mathbf{q}^{(A)})$ is the phonon distribution of type A (acoustic or non polar optical) which depends on the position $\mathbf{x}$, time t and the wave vector $\mathbf{q}^{(A)}$. $S^{(A)}[g^{(ac)}, g^{(np)}, f]$ is the collision operator of phonons with electrons. The phonon-phonon interaction is described by the relaxation time approximation.

The phonon energy $\hbar\omega^{(A)}$ is related to $\mathbf{q}^{(A)}$ by the dispersion relation. Here we will consider a simplified isotropic model $\omega = \omega(q)$, q being the modulus of $\mathbf{q}$. In particular in the acoustic branch the Debye approximation $\omega = c\,q$ will be adopted

with c the Debye velocity, while in the optical branch the Einstein approximation $\omega = \text{const}$ will be used. Moreover we assume that the non-polar optical phonons are described by the Bose-Einstein distribution.

$C_D(x)$ is the doping density, considered as a known function of the position, ϵ is the dielectric constant and $n(x,t)$ the electron number density

$$n(x,t) = \int_{\mathbb{R}^3} f \, \mathrm{d}^3 \mathbf{k}.$$

The direct solution of the system (2.164), (2.167) is very expensive from a computational point of view (for a deterministic numerical solution see [16, 30]) and not practical for electron device design. An alternative approach is to replace the transport equations with a macroscopic model deduced as moment equations of (2.164)–(2.166). These are obtained by multiplying (2.164) with a weight function $\psi(\mathbf{k})$, (2.165) and (2.166) with a weight function $\eta(\mathbf{q})$ and integrating over the first Brillouin zone.

We will consider the 8-moment electron system comprising the balance equations for the electron density, average crystal momentum, energy and energy-flux

$$\frac{\partial n}{\partial t} + \frac{\partial \left(nV^i\right)}{\partial x^i} = 0, \tag{2.168}$$

$$\frac{\partial \left(nP^i\right)}{\partial t} + \frac{\partial \left(nU^{ij}\right)}{\partial x^i} + neE^i = nC_p^i, \tag{2.169}$$

$$\frac{\partial \left(nW\right)}{\partial t} + \frac{\partial \left(nS^j\right)}{\partial x^i} + neV_k E^k = nC_W, \tag{2.170}$$

$$\frac{\partial \left(nS^i\right)}{\partial t} + \frac{\partial \left(nF^{ij}\right)}{\partial x^i} + neE_j G^{ij} = nC_W^i, \tag{2.171}$$

coupled to the 9-moment phonon system comprising the balance equation for the phonon energy, average momentum density and the deviatoric part of its flux

$$\frac{\partial u}{\partial t} + Q_k = P_u, \tag{2.172}$$

$$\frac{\partial p_i}{\partial t} + \frac{1}{3}\frac{\partial u}{\partial x_i} + \frac{\partial N_{\langle jk\rangle}}{\partial x_k} = P_i, \tag{2.173}$$

$$\frac{\partial N_{\langle ij\rangle}}{\partial t} + \frac{\partial M_{\langle ij\rangle k}}{\partial x_k} = P_{\langle ij\rangle}. \tag{2.174}$$

The basic quantities entering the electron equations are defined in the kinetic framework as follows (the density has been already defined above)

$$V^i = \frac{1}{n}\int_{\mathbb{R}^3} f v^i \,\mathrm{d}^3\mathbf{k} \quad \text{is the average electron velocity,}$$

$$W = \frac{1}{n}\int_{\mathbb{R}^3} \mathscr{E}(k) f \,\mathrm{d}^3\mathbf{k} \quad \text{is the average electron energy,}$$

$$S^i = \frac{1}{n}\int_{\mathbb{R}^3} f v^i \mathscr{E}(k)\mathrm{d}^3\mathbf{k} \quad \text{is the energy flux,}$$

$$P^i = \frac{1}{n}\int_{\mathbb{R}^3} f\hbar k^i \mathrm{d}^3\mathbf{k} = m^*\left(V^i + 2\alpha S^i\right) \text{ is the average crystal momentum.}$$

The other electron quantities including production terms are given by

$$U^{ij} = \frac{1}{n}\int_{\mathbb{R}^3} f v^i \hbar k^j \mathrm{d}^3\mathbf{k}, \quad G^{ij} = \frac{1}{n}\int_{\mathbb{R}^3} \frac{1}{\hbar} f \frac{\partial}{\partial k_j}(\mathscr{E} v_i)\mathrm{d}^3\mathbf{k},$$

$$F^{ij} = \frac{1}{n}\int_{\mathbb{R}^3} f v^i v^j \mathscr{E}(k)\mathrm{d}^3\mathbf{k}$$

$$nC_W = \int_{\mathbb{R}^3} C[f, g^{(ac)}, g^{(np)}]\mathscr{E}(k)\,\mathrm{d}^3\mathbf{k}, \quad nC_p^i = \int_{\mathbb{R}^3} C[f, g^{(ac)}, g^{(np)}]\hbar k^i \,\mathrm{d}^3\mathbf{k},$$

$$nC_W^i = \int_{\mathbb{R}^3} C[f, g^{(ac)}, g^{(np)}] v^i \mathscr{E}(k)\,\mathrm{d}^3\mathbf{k}.$$

The basic quantities entering the phonon equations are defined as follows

$$u = \int_{\mathbb{R}^3} \hbar\omega\, g \,\mathrm{d}^3\mathbf{q} \text{ is the phonon energy density,}$$

$$Q_k = \int_{\mathbb{R}^3} \hbar\omega \frac{\partial\omega}{\partial q_k}\, g \,\mathrm{d}^3\mathbf{q} \text{ is the phonon energy density flux,}$$

$$p_i = \hbar\int_{\mathbb{R}^3} q_i\, g \,\mathrm{d}^3\mathbf{q} \text{ is the phonon momentum density,}$$

$$N_{ik} = \int_{\mathbb{R}^3} \frac{\hbar\omega}{q^2} q_i q_k\, g \,\mathrm{d}^3\mathbf{q} \text{ is the momentum flux density.}$$

Phonon momentum flux can be decomposed into an isotropic part and a deviatoric part $N_{ik} = \dfrac{u}{3}\,\delta_{ik} + N_{\langle ik\rangle}$. The deviatoric part of the momentum flux $N_{\langle ik\rangle}$, and its flux are represented by

$$N_{\langle ij\rangle} = \int_{\mathbb{R}^3} \frac{\hbar\omega}{q^2} q_{<i} q_{j>}\, g \,\mathrm{d}^3\mathbf{q}, \quad M_{\langle ij\rangle k} = \int_{\mathbb{R}^3} \frac{\hbar\omega^2}{q^4} q_{<i} q_{j>} q_k\, g \,\mathrm{d}^3\mathbf{q}.$$

The phonon production terms are given by

$$P_u = \int_{\mathbb{R}^3} \hbar\omega\, S[g^{(ac)}, g^{(np)}, f]\, \mathrm{d}^3\,\mathbf{q}, \quad P_i = \int_{\mathbb{R}^3} \hbar q_i\, S[g^{(ac)}, g^{(np)}, f]\, \mathrm{d}^3\,\mathbf{q},$$
$$P_{\langle ij\rangle} = \int_{\mathbb{R}^3} \frac{\hbar\omega}{q^2} q_{<i} q_{j>}\, S[g^{(ac)}, g^{(np)}, f]\, \mathrm{d}^3\,\mathbf{q}.$$

2.2.4.2 The Maximum Entropy Principle

The set of balance equations (2.168)–(2.174) does not form a closed system since more unknowns appear than the number of equations. Therefore the problem of prescribing suitable closure relations arises.

The maximum entropy principle (hereafter MEP) gives a systematic way for obtaining constitutive relations. In the information theory framework the principle has been formalized by Shannon [61]. In statistical physics, it has been introduced in [22, 41] (see also [65] for a review). In [7–9, 49, 53, 54] the approach has been applied to charge transport in semiconductors considering the phonons as a thermal bath. Here the phonons are no longer supposed to be at equilibrium and therefore one has to maximize the phonon distribution.

In the case under investigation, since it is assumed that the non-polar optical phonons are described by Bose-Einstein distribution

$$g_{BE} = \left[\exp\left(\frac{\hbar\omega^{(op)}}{k_B T_L}\right) - 1\right]^{-1},$$

with T_L the lattice temperature, MEP can be formulated as follows. If a given number of moments $M_A^{(f)}$, $A = 1, \ldots, N$ of f as well as a given number of moments $M_B^{(g)}$, $B = 1, \ldots, M$ of $g = g^{(ac)}$ are known, the distribution functions which can be used to evaluate the unknown moments of f and g, correspond to the maximum, (f_{ME}, g_{ME}), of the entropy functional

$$s(f,g) = -k_B \left[\int_{\mathbb{R}^3} f(\log f - 1)\mathrm{d}^3\,\mathbf{k} + \int_{\mathbb{R}^3} \left(g \ln\frac{g}{y} - (y+g)\ln\left(1+\frac{g}{y}\right)\right)\mathrm{d}^3\,\mathbf{q}\right]$$

under the constraints

$$\int_{\mathbb{R}^3} \Psi_A^{(e)}(\mathbf{k})\, f_{ME}\mathrm{d}^3\,\mathbf{k} = M_A^{(f)}, \quad \int_{\mathbb{R}^3} \Psi_B^{(p)}(\mathbf{q}) g_{ME}\mathrm{d}^3\,\mathbf{q} = M_B^{(g)},$$

where $\Psi_A^{(e)}(\boldsymbol{k})$ and $\Psi_B^{(p)}(\boldsymbol{q})$ are electrons and phonons weight functions, respectively, relative to the basic moments $M_A^{(f)}$ and $M_B^{(g)}$. k_B is Boltzmann constant and $y = \dfrac{3}{8\pi^3}$.

From a statistical point of view, f_{ME} and g_{ME} represent the least biased estimators of f and g that can be obtained using only the knowledge of a finite number of moments of f and g. Assuming as fundamental variables for electrons, the density n, the velocity $\mathbf{V}$, the energy W and the energy-flux $\mathbf{S}$, this procedure leads for electrons to the non-equilibrium distribution (see [9, 53])

$$f_{ME} = \exp\left(-\frac{\lambda}{k_B} - \lambda^W \mathscr{E}(k)\right)[1-\chi],$$

with[1] $\chi = \lambda_i^V v^i + \lambda_i^S v_i\ \mathscr{E}(k)$ where Lagrange multipliers associated with the density, the momentum and the energy flux have the expressions

$$\frac{\lambda}{k_B} = -\log\frac{n\hbar^3}{4\pi m^*\sqrt{2m^* d_0}},\ \lambda_i^V = b_{11}V_i + b_{12}S_i,\ \lambda_i^S = b_{12}V_i + b_{22}S_i$$

while λ^W is the Lagrange multiplier related to the energy. It depends on W and it is obtained by inverting the relation

$$W = \frac{\int_0^\infty \mathscr{E}\sqrt{\mathscr{E}(1+\alpha\mathscr{E})}(1+2\alpha\mathscr{E})\exp\left(-\lambda^W\mathscr{E}\right)\mathrm{d}\mathscr{E}}{\int_0^\infty \sqrt{\mathscr{E}(1+\alpha\mathscr{E})}(1+2\alpha\mathscr{E})\exp\left(-\lambda^W\mathscr{E}\right)\mathrm{d}\mathscr{E}}.$$

The coefficients b_{ij} are given by $b_{11} = \frac{a_{22}}{\Delta},\ b_{12} = -\frac{a_{12}}{\Delta},\ b_{22} = \frac{a_{11}}{\Delta}$ with

$$a_{11} = -\frac{2p_0}{3m^* d_0},\ a_{12} = -\frac{2p_1}{3m^* d_0},\ a_{22} = -\frac{2p_2}{3m^* d_0}, \Delta = a_{11}a_{22} - a_{12}^2,$$

including d_k and p_k defined by

$$d_k = \int_0^\infty \mathscr{E}^k\sqrt{\mathscr{E}(1+\alpha\mathscr{E})}(1+2\alpha\mathscr{E})\exp\left(-\lambda^W\mathscr{E}\right)\mathrm{d}\mathscr{E},$$

$$p_k = \int_0^\infty \frac{[\mathscr{E}(1+\alpha\mathscr{E})]^{3/2}\mathscr{E}^k}{1+2\alpha\mathscr{E}}\exp\left(-\lambda^W\mathscr{E}\right)\mathrm{d}\mathscr{E}.$$

For acoustic phonons, assuming as fundamental variables the energy u, the momentum $\mathbf{p}$ and the deviatoric part of the momentum flux $N_{\langle ij\rangle}$, the following phonon non-equilibrium distribution has been deduced as in [23]

$$g_{ME} \equiv g_{ME}^{(ac)} = g_{BE} + g_{BE}^+\left[\frac{3c^2\hbar q}{4uk_B T_L}p_i l_i + \frac{15\hbar cq}{8uk_B T_L}\left(N_{ij}l_i l_j - \frac{u}{3}\right)\right],$$

[1] Einstein's convention is used: summation with respect repeated dummy indices is understood.

where

$$g_{BE}^{+} = \frac{\exp\left(\frac{\hbar c q}{k_B T_L}\right)}{\left(\exp\left(\frac{\hbar c q}{k_B T_L}\right) - 1\right)^2},$$

and $\mathbf{l} = (l_1, l_2, l_3)$ belongs to S^2, the unit sphere of $\mathbb{R}^3$. We assume as definition of T_L, the Debye relation $u = \sigma\, T_L^4$.

The previous acoustic phonon distribution is valid up to first order in the deviation from the equilibrium.

Putting f_{ME} and g_{ME} into the kinetic definition of the variables appearing in the balance equations (2.168)–(2.174), one gets the desired closure relation in terms of the fundamental variables n, $\mathbf{V}$, W, $\mathbf{S}$, u, $\mathbf{p}$ and $N_{\langle ij\rangle}$.

2.2.4.3 Closure Relations: Phonon Subsystem

Each term is given by the sum of two contributions: one due to the acoustic and another due to the non-polar optical phonons. The details can be found in [56]. Concerning the energy-flux one has $Q_k^{(ac)} = c^2\, p_k^{(ac)}$, $Q_k^{(np)} = 0$ wherefrom

$$Q_k = c^2\, p_k,$$

since $p_k^{(np)} = 0$. Similarly, concerning the divergence of the deviatoric part, one has

$$\frac{\partial M_{\langle ij\rangle k}}{\partial x_k} = c^2 \frac{2}{5} \frac{\partial p_{\langle i}}{\partial x_{j\rangle}}.$$

The production of the energy and the production of the deviatoric part of the momentum flux due to interaction between acoustic phonons and electrons vanishes $P_u^{(ac)} = 0$, $P_{\langle ij\rangle}^{(ac)} = 0$ while the production of momentum for this scattering mechanism is given by

$$\begin{aligned} P_i^{(ac)} = &-n I V_i \frac{4\pi\hbar}{3} \int_0^\infty g_{BE}(q)\,(A_0(q)\, b_{11}(W) + A_1(q)\, b_{12}(W))\; q^4\, \mathrm{d}q \\ &-n I S_i \frac{4\pi\hbar}{3} \int_0^\infty g_{BE}(q)\,(A_0(q)\, b_{12}(W) + A_1(q)\, b_{22}(W))\; q^4\, \mathrm{d}q, \end{aligned} \tag{2.175}$$

where $I = \dfrac{D_A^2 \hbar^2}{16\pi^2 \rho_S v_s \sqrt{2}(m^*)^{3/2} d_0}$, with D_A^2 the deformation potential, ρ_S the silicon density, v_s the longitudinal sound speed and

$$A_0(q) = \int_{\frac{q}{2}}^{\infty} k \exp\left(-\lambda^W \mathscr{E}\right) \mathrm{d}k, \quad A_1(q) = \int_{\frac{q}{2}}^{\infty} k \mathscr{E} \exp\left(-\lambda^W \mathscr{E}\right) \mathrm{d}k.$$

Since the non-polar optical phonons are described by the Bose-Einstein, the production of momentum is zero along with the deviatoric part of the momentum flux: $P_i^{(np)} = 0, \quad P_{\langle ij \rangle}^{(np)} = 0$.

The energy production can be easily obtained by taking into account that the total energy of the electron-phonon system must be conserved. Since the energy production vanishes in the case of acoustic phonons, we have $P_u^{(np)} = P_u = -nC_W$, where C_W is the electron energy production.

The production terms of energy, momentum and the deviatoric part of the momentum flux arising from the phonon-phonon (ph) acoustic interaction are given by

$$P_u^{(ph)} = 0, \quad P_i^{(ph)} = -\frac{1}{\tau_R} p_i, \quad P_{\langle ij \rangle}^{(ph)} = -\frac{1}{\tau} N_{\langle ij \rangle},$$

where τ_R is the relaxation time for resistive processes and τ is total relaxation time.

Summing up the above relations the production terms read as follows. The production of energy, momentum and deviatoric part of the momentum flux read as

$$\begin{aligned} P_u &= -nC_W, \\ P_i &= n\, c_{11}^{(p)}(W, T_L)\; V_i + n\, c_{12}^{(p)}(W, T_L)\; S_i - \frac{p_i}{\tau_R}, \\ P_{\langle ij \rangle} &= -\frac{N_{\langle ij \rangle}}{\tau}, \end{aligned}$$

where the coefficients $c_{11}^{(p)}(W, T_L)$ and $c_{12}^{(p)}(W, T_L)$ originate from Eq. (2.175).

2.2.4.4 Closure Relations for Electrons

The general expression of the production term for acoustic phonons based on f_{ME} reads as

$$C_{\psi^{(e)}}^{(ac)} = I \int_{\mathbb{R}^3} \int_0^{2k} \psi^{(e)}(\mathbf{k}) \left[2g_{BE} + 1\right] \exp\left(-\lambda^W \mathscr{E}\right) \frac{q^4}{2k^2} \left(\lambda_i^V l^i + \lambda_i^S l_i \; \mathscr{E}(k)\right) \mathrm{d}q \; \mathrm{d}^3\mathbf{k}.$$

The production of the energy is zero since the scattering is considered in the elastic approximation $C_W^{(ac)} = 0$. The production of the crystal momentum is given by

$$C_p^{i\ (ac)} = \frac{2\pi I}{3} V_i \int_0^\infty \hbar k\ C\ (k) \exp\left(-\lambda^W \mathscr{E}\right) (b_{11}(W) + \mathscr{E} b_{12}(W))\, \mathrm{d}k$$
$$+ \frac{2\pi I}{3} S_i \int_0^\infty \hbar k\ C\ (k) \exp\left(-\lambda^W \mathscr{E}\right) (b_{12}(W) + \mathscr{E} b_{22}(W))\, \mathrm{d}k, \qquad (2.176)$$

where $C\ (k) = \int_0^{2k} q^4\, (2 g_{BE} + 1)\, \mathrm{d}q$.

The production of the energy flux has the same structure

$$C_W^{i\ (ac)} = \frac{2\pi I}{3} V_i \int_0^\infty \frac{\hbar k}{m^*} \frac{\mathscr{E}\ C\ (k) \exp\left(-\lambda^W \mathscr{E}\right)}{\sqrt{1 + 4\alpha \frac{\hbar^2 k^2}{2m^*}}} (b_{11}(W) + \mathscr{E} b_{12}(W))\, \mathrm{d}k$$
$$+ \frac{2\pi I}{3} S_i \int_0^\infty \frac{\hbar k}{m^*} \frac{\mathscr{E}\ C\ (k) \exp\left(-\lambda^W \mathscr{E}\right)}{\sqrt{1 + 4\alpha \frac{\hbar^2 k^2}{2m^*}}} (b_{12}(W) + \mathscr{E} b_{22}(W))\, \mathrm{d}k. \qquad (2.177)$$

In the case of electron–non-polar optical phonon scattering we have the same expressions already found in [9, 53] but with the lattice temperature which is no longer constant.

Summing up the above results, the production terms in the electron moment system can be written in general forms as the sum of terms due to productions of acoustic and non-polar phonon–electron scattering (electron-electron scattering is negligible). In particular, the production of energy, momentum and energy-flux read

$$C_W = C_W^{(e)},$$
$$C_p^i = c_{11}^{(e)}(W, T_L) V_i + c_{12}^{(e)}(W, T_L) S_i,$$
$$C_W^i = c_{21}^{(e)}(W, T_L) V_i + c_{22}^{(e)}(W, T_L) S_i.$$

where the coefficients $c_{11}^{(e)}(W, T_L)$, $c_{12}^{(e)}(W, T_L)$, $c_{21}^{(e)}(W, T_L)$ and $c_{22}^{(e)}(W, T_L)$ originate from Eqs. (2.176) and (2.177).

2.2.4.5 Limiting Energy Transport and Lattice Heating Model

Under an appropriate scaling, an energy-transport model for electrons coupled to the crystal energy balance equation can be derived. Such a model comprises three balance equations: one for the electron density, one for the electron energy density and one for the crystal temperature. This allows a comparison with the existing

models, already known in the literature, for the lattice heating in presence of a charge flow. We assume long time and diffusion scaling, that is with spatial variation on large scale,

$$t = \mathscr{O}\left(\frac{1}{\delta^2}\right),\ x_k = \mathscr{O}\left(\frac{1}{\delta}\right),$$

and that the variables vanishing at equilibrium are of first order

$$\mathbf{V} = \mathscr{O}(\delta),\ \mathbf{S} = \mathscr{O}(\delta),\ \mathbf{p} = \mathscr{O}(\delta),\ \mathbf{N}_{\langle ij\rangle} = \mathscr{O}(\delta),$$

δ being a formal small parameter which is related to the anisotropic part of f_{ME} (see [53]). Moreover we suppose that

$$C_W = \mathscr{O}\left(\frac{1}{\delta^2}\right) \quad \text{and} \quad \tau = \mathscr{O}\left(\frac{1}{\delta^2}\right). \tag{2.178}$$

The last assumptions have the following meaning. If we introduce the energy relaxation time τ_W, one can write $C_W = -\dfrac{W - \frac{3}{2}k_B T_L}{\tau_W}$. Therefore relation $(2.178)_1$ is equivalent to require a long energy relaxation time. Since the experimental data indicates $\tau \geq \tau_W$, it is quite natural to assume also $(2.178)_2$.

By proceedings formally as in [53], we write

$$t = \delta^2 \tilde{t},\ x = \delta \tilde{x},\ \mathbf{V} = \delta\,\tilde{\mathbf{V}},\ \mathbf{S} = \delta\,\tilde{\mathbf{S}},\ \mathbf{p} = \delta\,\tilde{\mathbf{p}},\ \mathbf{N}_{\langle ij\rangle} = \delta\,\tilde{\mathbf{N}}_{\langle ij\rangle},$$

and substitute into relations (2.168)–(2.174).

By eliminating the tilde for simplifying the notation, observing that C_P^i and C_W^i are of order δ and by putting equal to zero the coefficients of the various powers of δ in the previous system, one gets again the balance equations (3.72) and (3.74) of density and energy, and moreover

$$\begin{aligned}
&\frac{\partial}{\partial t} n V^i = 0, \quad \frac{\partial}{\partial t} n S^i = 0,\\
&\frac{1}{n}\frac{\partial}{\partial x^j}\, n U^{(0)} = -eE^i + c_{11}^{(e)} V^i + c_{12}^{(e)} S^i,\\
&\frac{1}{n}\frac{\partial}{\partial x^j} n F^{(0)} \delta_{ij} = -eE^i G^{(0)} + c_{21}^{(e)} V^i + c_{22}^{(e)} S^i.
\end{aligned}$$

The last two relations allow to express $\mathbf{V}$ and $\mathbf{S}$ as functions of n, W, T_L and ϕ.

Concerning the phonon part, solving the previous compatibility conditions at each order in δ gives

$$\frac{\partial u}{\partial t} + \frac{\partial c^2 p_k}{\partial x_k} = -n\, C_W, \tag{2.179}$$

$$p_i = -\frac{1}{3}\,\tau_R\,\frac{\partial u}{\partial x_i} + \tau_R\,\left(n\, c_{11}^{(p)}\, V_i + n\, c_{12}^{(p)}\, S_i\right), \tag{2.180}$$

$$\frac{\partial N_{\langle ik\rangle}}{\partial t} = -\frac{\partial N_{\langle ik\rangle}}{\tau}, \tag{2.181}$$

$$\frac{\partial p_{\langle i}}{\partial x_{j\rangle}} = 0. \tag{2.182}$$

We remark that, as expected in a diffusive regime, only the resistive processes are relevant and that neglecting the convective part due to the electron flow $\tau_R\,\left(n\, c_{11}^{(p)}\, V_i + n\, c_{12}^{(p)}\, S_i\right)$ in (2.180) leads to the well known Peierls relation $Q_k = -\frac{1}{3}\, c^2\, \tau_R\, \frac{\partial u}{\partial x_k}$.

Collecting all the previous results, the following *energy transport model for electrons coupled to the lattice energy equation* is obtained

$$\frac{\partial n}{\partial t} + \operatorname{div}(n\mathbf{V}) = 0, \tag{2.183}$$

$$\frac{\partial (nW)}{\partial t} + \operatorname{div}(n\mathbf{S}) - ne\mathbf{V}\cdot\nabla\phi = nC_W, \tag{2.184}$$

$$\rho c_V\,\frac{\partial T_L}{\partial t} - \operatorname{div}\left[k(T_L)\nabla T_L\right] = H, \tag{2.185}$$

where $\rho\, c_V = \dfrac{\partial u}{\partial T_L}$ with c_V specific heat in Silicon at constant volume, $k(T_L) = \frac{1}{3}\rho\, c_V\, c^2\, \tau_R$ is the thermal conductivity and

$$H = -nC_W - c^2 \operatorname{div}\left(\tau_R\, n c_{11}^{(p)}\mathbf{V} + \tau_R n c_{12}^{(p)}\mathbf{S}\right) \tag{2.186}$$

is the crystal energy production.

The electron velocity and energy-flux have the same expression as in [54] but with a lattice temperature which is not kept at equilibrium

$$\mathbf{V} = D_{11}(W, T_L)\,\nabla \log n + D_{12}(W, T_L)\,\nabla W + D_{13}(W, T_L)\,\nabla\phi, \tag{2.187}$$

$$\mathbf{S} = D_{21}(W, T_L)\,\nabla \log n + D_{22}(W, T_L)\nabla\, W + D_{23}(W, T_L)\,\nabla\phi, \tag{2.188}$$

where

$$D_{11}(W,T_L) = D_V\left[c_{12}^{(e)}F - c_{22}^{(e)}U\right], \quad D_{12}(W,T_L) = D_V\left[c_{12}^{(e)}F' - c_{22}^{(e)}U'\right],$$
$$D_{13}(W,T_L) = D_V\left[c_{22}^{(e)}e - c_{12}^{(e)}eG\right], \quad D_V(W,T_L) = \frac{1}{c_{12}^{(e)}c_{21}^{(e)} - c_{22}^{(e)}c_{11}^{(e)}},$$
$$D_{21}(W,T_L) = D_S\left[c_{11}^{(e)}F - c_{21}^{(e)}U\right], \quad D_{22}(W,T_L) = D_S\left[c_{11}^{(e)}F' - c_{21}^{(e)}U'\right],$$
$$D_{23}(W,T_L) = D_S\left[c_{21}^{(e)}e - c_{11}^{(e)}eG\right], \quad D_S(W,T_L) = \frac{1}{c_{22}^{(e)}c_{11}^{(e)} - c_{12}^{(e)}c_{21}^{(e)}}.$$

The explicit form of the coefficients can be easily obtained when taking into the account expressions reported in [9, 53].

In the literature several expressions of H have been proposed (see for more details [60]). In [32] only the Joule effect has been included $H = -e\,n\,\mathbf{V}\cdot\mathbf{E}$, while in [1] the following formulation was suggested $H = -\mathrm{div}\,(E_C\,n\,\mathbf{V})$, with E_C the conduction band edge energy. A different model has been given in [17] $H = -e\,n\,\mathbf{V}\cdot\nabla\phi_n$, with ϕ_n the quasi-Fermi electron potential. It is evident that the previous models can cover only part of the effects present in (2.186).

In order to compare our results with those reported in [62], we sum up Eqs. (3.74) and (3.75), obtaining the balance equation for the total energy

$$\frac{\partial\,(nW)}{\partial t} + \rho c_V\,\frac{\partial T_L}{\partial t} + \mathrm{div}\,(n\mathbf{S} - k(T_L)\nabla T_L) = -\mathbf{J}\cdot\mathbf{E} - c^2\mathrm{div}\left(\tau_R\,n c_{11}^{(p)}\mathbf{V} + \tau_R n c_{12}^{(p)}\mathbf{S}\right), \quad (2.189)$$

where $\mathbf{J} = -en\mathbf{V}$ is the current density. The production terms in Eq. (2.189) are given by a Joule heating term and a divergence term. The argument of the divergence operator can be written as

$$-P_n\,\mathbf{J} - P_S\,n\,\mathbf{S},$$

with $P_n = \dfrac{c^2\,\tau_R\,c_{11}^{(p)}}{e}$ and $P_S = -c^2\,\tau_R\,c_{12}^{(p)}$ a kind of thermoelectric power coefficients. The main difference with [62] (eq. 31 therein, without holes and recombination-generation term), is that $n\,\mathbf{S}$ is not neglected. Moreover, P_n and P_S have an explicit expression directly related to the scattering parameters, and both electrons and lattice have different temperatures.

2.2.4.6 Quantum Corrections

Besides the crystal heating, also quantum effects must been included in the simulation of nanoscale devices. What follows is based on [57]. The starting point is the single particle Wigner-Poisson system in the effective mass approximation which represents the quantum analogous of the semiclassical Boltzmann-Poisson system. In the following the explicit dependence on the lattice temperature will be not written since the results does not change with respect to T_L.

In the effective mass approximation the Wigner-Poisson system reads as

$$\frac{\partial w}{\partial t} + \mathbf{v} \cdot \nabla_x w + \frac{e}{m^*} \Theta[\Phi] w = \mathscr{C}[w], \tag{2.190}$$

$$\operatorname{div}(\epsilon \nabla \Phi_S) = -e(C_D(x) - n). \tag{2.191}$$

where the unknown function $w(\mathbf{x}, \mathbf{v}, t)$, depending on the position, velocity and time, is the Wigner quasi distribution, defined as

$$w(\mathbf{x}, \mathbf{v}, t) = \mathscr{F}^{-1}[\rho(\mathbf{x} + \frac{\hbar}{2m^*}\boldsymbol{\eta}, \mathbf{x} - \frac{\hbar}{2m^*}\boldsymbol{\eta}, t)](\mathbf{v}) =$$
$$\frac{1}{(2\pi)^3} \int_{\mathbb{R}^3} \rho(\mathbf{x} + \frac{\hbar}{2m^*}\boldsymbol{\eta}, \mathbf{x} - \frac{\hbar}{2m^*}\boldsymbol{\eta}, t)\ e^{i\mathbf{v}\cdot\boldsymbol{\eta}}\, \mathrm{d}^3\, \boldsymbol{\eta}.$$

Here $\rho(\mathbf{x}, \mathbf{y})$ is the density matrix, which is related to the wave function $\psi(\mathbf{x}, t)$ by

$$\rho(\mathbf{x}, \mathbf{y}) = \overline{\psi(\mathbf{x}, t)}\, \psi(\mathbf{y}, t).$$

$\mathscr{F}$ denotes the Fourier transform, given for function $g(\mathbf{v}) \in L^1(\mathbb{R}^3)$ by

$$\mathscr{F}[g(\mathbf{v})](\eta) = \int_{\mathbb{R}^3_v} g(\mathbf{v})\, \mathrm{e}^{-i\mathbf{v}\cdot\eta}\, \mathrm{d}^3\, \mathbf{v},$$

and $\mathscr{F}^{-1}$ the inverse Fourier transform

$$\mathscr{F}^{-1}[h(\boldsymbol{\eta})] = \frac{1}{(2\,\pi)^3} \int_{\mathbb{R}^3_\eta} h(\boldsymbol{\eta})\, \mathrm{e}^{i\mathbf{v}\cdot\boldsymbol{\eta}}\, \mathrm{d}^3\, \boldsymbol{\eta}.$$

The potential Φ is usually given by the sum of a self-consistent term Φ_S, solution of the Poisson equation (2.191), and an additional term Φ_B which models the potential barriers in hetero-junctions and is a prescribed function of the position.

As well known, $w(\mathbf{x}, \mathbf{v}, t)$ is not in general positive definite. However it is possible to calculate the macroscopic quantities of interest as expectation values

(moments) of $w(\mathbf{x}, \mathbf{v}, t)$ in the same way of the semiclassical case, e.g.

$$\text{density} \quad n(\mathbf{x}, t) = \int_{\mathbb{R}^3} w(\mathbf{x}, \mathbf{v}, t)\, \mathrm{d}^3\, \mathbf{v},$$

$$\text{velocity} \quad V(\mathbf{x}, t) = \frac{1}{n(\mathbf{x}, t)} \int_{\mathbb{R}^3} \mathbf{v}\, w(\mathbf{x}, \mathbf{v}, t)\, \mathrm{d}^3\, \mathbf{v},$$

$$\text{energy} \quad W(\mathbf{x}, t) = \frac{1}{n(\mathbf{x}, t)} \int_{\mathbb{R}^3} \frac{1}{2}\, m^*\, v^2\, w(\mathbf{x}, \mathbf{v}, t)\, \mathrm{d}^3\, \mathbf{v},$$

$$\text{energy-flux} \quad S(\mathbf{x}, t) = \frac{1}{n(\mathbf{x}, t)} \int_{\mathbb{R}^3} \frac{1}{2}\, m^*\, \mathbf{v}\, v^2\, w(\mathbf{x}, \mathbf{v}, t)\, \mathrm{d}^3\, \mathbf{v}.$$

It is worth to mention that the previous definition of energy and energy flux are valid only in the parabolic band, consistently with the effective mass approximation.

$\Theta[\Phi]$ represents the pseudo-differential operator

$$\Theta[\Phi] w(\mathbf{x}, \mathbf{v}, t) = \frac{i m^*}{\hbar (2\pi)^3} \int_{\mathbb{R}^3_\eta \times \mathbb{R}^3_{v'}} \left[\Phi\left(\mathbf{x} + \frac{\hbar}{2m^*}\boldsymbol{\eta},\, t\right) - \Phi\left(\mathbf{x} - \frac{\hbar}{2m^*}\boldsymbol{\eta},\, t\right) \right]$$
$$w(\mathbf{x}, \mathbf{v}', t)\, \mathrm{e}^{-i(\mathbf{v}'-\mathbf{v})\cdot\boldsymbol{\eta}}\, \mathrm{d}^3\, \mathbf{v}'\, \mathrm{d}^3\, \boldsymbol{\eta}.$$

$\mathscr{C}[w]$ is the quantum collision term. Its formulation is itself an open problem. Some attempts can be found in [10, 28], but a derivation suitable for application in electron devices is still lacking. Here we propose an expression which is a perturbation of the semiclassical collision term, useful for the formulation of macroscopic models.

As general guideline $\mathscr{C}[w]$ should drive the system towards the equilibrium. If we consider the electrons in a thermal bath at the lattice temperature $T_L = 1/k_B\beta$, the equilibrium Wigner function w_{eq} has been found in [64].

For our purposes we *locally* parameterize the equilibrium Wigner function in terms of the electron density. Up to first order in $\hbar^2$ on has

$$w_{eq} = w_{eq}^{(0)} + \hbar^2\, w_{eq}^{(1)} + \mathscr{O}(\hbar^4) = n(\mathbf{x}, t) \left(\frac{m^*\beta}{2\,\pi}\right)^{3/2} \mathrm{e}^{-\beta\,\mathscr{E}} \times$$
$$\left\{ 1 + \frac{\hbar^2 \beta^2 e}{24} \left[\frac{\Delta\, \Phi}{m^*} - \beta\; v_r\, v_s\, \frac{\partial^2 \Phi}{\partial\, x_r\, \partial\, x_s} \right] \right\} + \mathscr{O}(\hbar^4),$$

where

$$w_{eq}^{(0)} = n(\mathbf{x}, t) \left(\frac{m^*\beta}{2\,\pi}\right)^{3/2} \mathrm{e}^{-\beta\,\mathscr{E}}$$

is the classical Maxwellian.

We suppose that the expansion

$$w = w^{(0)} + \hbar^2 w^{(1)} + \mathcal{O}(\hbar^4)$$

holds. By proceedings in a formal way, as $\hbar \mapsto 0$ the Wigner equation gives the semiclassical Boltzmann equation in the parabolic band approximation

$$\frac{\partial w^{(0)}}{\partial t} + \mathbf{v} \cdot \nabla_x w^{(0)} + \frac{e}{m^*} \nabla_x \Phi \cdot \nabla_v w^{(0)} = \mathscr{C}^{(0)}[w^{(0)}]. \tag{2.192}$$

At first order in $\hbar^2$ we have

$$\frac{\partial w^{(1)}}{\partial t} + \mathbf{v} \cdot \nabla_x w^{(1)} + \frac{e}{m^*} \nabla_x \Phi \cdot \nabla_v w^{(1)} - \frac{e}{24 m^3} \frac{\partial^3 \Phi}{\partial x_i \, x_j \, x_k} \frac{\partial^3 w^{(0)}}{\partial v_i \, v_j \, v_k} = \mathscr{C}^{(1)}, \tag{2.193}$$

with $\mathscr{C}^{(1)}$ to be modeled.

Since $w^{(0)}$ must be positive, being a solution of the semiclassical Boltzmann equation, we make the following first assumption

$$\mathscr{C}[w] = \mathscr{C}^{(0)}[w^{(0)}] + \hbar^2 \mathscr{C}^{(1)}[w^{(1)}] = \mathscr{C}_C[w^{(0)}] - \hbar^2 \nu \left(w^{(1)} - w^{(1)}_{eq} \right) + \mathcal{O}(\hbar^4) \tag{2.194}$$

with $\mathscr{C}_C[w^{(0)}]$ semiclassical collision operator $(w^{(0)} > 0!)$

and $\nu > 0$ quantum collision frequency.

Remark 2.3 At variance with other approaches, only the $\hbar^2$ correction to the collision term has a relaxation form. This assures that as $\hbar \mapsto 0$ one gets the semiclassical scattering of electrons with phonons and impurities.

The value of the quantum collision frequency ν is a fitting parameter that can be determined comparing the results with the experimental data.

We require that $\mathscr{C}[w]$ conserves the electron density (second assumption)

$$\int_{\mathbb{R}^3} \mathscr{C}[w] \, \mathrm{d}^3 \mathbf{v} = 0.$$

Proposition 2.1 *The collision operator $\mathscr{C}[w]$ of the form (2.194) satisfies up to terms $\mathcal{O}(\hbar^4)$ the following properties:*

1. *Ker $(\mathscr{C}[w])$ is given by the quantum Maxwellian*

$$w_{(eq)} = w^{(0)}_{eq} + \hbar^2 w^{(1)}_{eq},$$

with $w^{(0)}_{eq}$ the classical Maxwellian.

2.

$$-k_B \int_{\mathbb{R}^3} \mathscr{C}^{(0)}[w^{(0)}] \ln \frac{w^{(0)}}{\exp(-\frac{\beta m^* v^2}{2})} \mathrm{d}^3 \boldsymbol{v} = -k_B \int_{\mathbb{R}^3} \left[\ln w^{(0)} + \frac{\beta m^* v^2}{2} \right] \mathscr{C}^{(0)} \mathrm{d}^3 \boldsymbol{v} \geq 0,$$

3.

$$-\frac{1}{2} \mathscr{C}^{(1)}[w^{(1)}] \left(w^{(1)} - w^{(1)}_{eq} \right) \geq 0.$$

Moreover the equality holds if and only if w is the quantum Maxwellian, defined above.

Properties 1 and 3 are straightforward. Property 2 is based on the proof in [45–47] valid in the classical case.

2.2.4.7 Quantum Corrections in the High Field Approximation

In the case of high electric fields, it is possible to get an approximation for $w^{(1)}$ by a suitable Chapman-Enskog expansion. Let us introduce the dimensionless variables $\tilde{\mathbf{x}} = \frac{\mathbf{x}}{l_0}$, $\tilde{t} = \frac{t}{t_0}$, $\tilde{\mathbf{v}} = \frac{\mathbf{v}}{v_0}$, with l_0, t_0 and $v_0 = l_0/t_0$ typical length, time and velocity. Let l_Φ be the characteristic length of the electrical potential and $1/t_C$ the characteristic collision frequency. After scaling the collision frequency according to $\tilde{\nu} = t_C \, \nu$, Eq. (2.193) can be rewritten as

$$\frac{1}{t_0} \frac{\partial w^{(1)}}{\partial t} + \frac{v_0}{l_0} \mathbf{v} \cdot \nabla_x w^{(1)} + \frac{v_0}{l_\Phi} \left[\frac{e}{m^*} \nabla_x \Phi \cdot \nabla_v w^{(1)} - \frac{e}{24 m^3} \frac{\partial^3 \Phi}{\partial x_i \, x_j \, x_k} \frac{\partial^3 w^{(0)}}{\partial v_i \, v_j \, v_k} \right] = -\frac{1}{t_C} \nu \left(w^{(1)} - w^{(1)}_{eq} \right).$$

We will continue to denoted the scaled variables as the unscaled ones for simplifying the notation. Note that the scaling of $w^{(1)}$ is unimportant.

Let us introduce the characteristic length associated with the quantum correction of the collision term (a kind of mean free path in a semiclassical context) $l_C = v_0 \, t_C$ We assume that the quantum effects occur in the high field and collision dominated regime, where drift and collision mechanisms have the same characteristic length. Therefore we set formally $\frac{l_C}{l_\Phi} = 1$ and observe that in the high frequency regime

the Knudsen number $\alpha = \dfrac{l_C}{l_0}$ is a small parameter. Substituting in the previous equation, we get

$$\alpha \frac{\partial w^{(1)}}{\partial t} + \alpha \mathbf{v} \cdot \nabla_x w^{(1)} + \frac{e}{m^*} \nabla_x \Phi \cdot \nabla_v w^{(1)} - \frac{e}{24 m^3} \frac{\partial^3 \Phi}{\partial x_i \, x_j \, x_k} \frac{\partial^3 w^{(0)}}{\partial v_i \, v_j \, v_k} = -\nu \left(w^{(1)} - w^{(1)}_{eq} \right).$$

The zero order in α gives

$$\frac{q}{m^*} \nabla_x \Phi \cdot \nabla_v w^{(1)} - \frac{e}{24 m^3} \frac{\partial^3 \Phi}{\partial x_i \, x_j \, x_k} \frac{\partial^3 w^{(0)}}{\partial v_i \, v_j \, v_k} = -\nu \left(w^{(1)} - w^{(1)}_{eq} \right)$$

and by Fourier transforming one has

$$w^{(1)}(\mathbf{x}, \mathbf{v}, t) = \mathscr{F}^{-1} \left\{ \frac{1}{\nu + \frac{ie}{m^*} \boldsymbol{\eta} \cdot \nabla_x \Phi} \left[-\frac{ie}{24 m^{*3}} \frac{\partial^3 \Phi}{\partial x_i \, x_j \, x_k} \eta_i \eta_j \eta_k \mathscr{F} w^{(0)}(\boldsymbol{\eta}) + \nu \mathscr{F} w^{(1)}_{eq}(\boldsymbol{\eta}) \right] \right\} (\mathbf{x}, \mathbf{v}, t).$$

Approximating $w^{(0)}$ with f_{ME}, we obtain

$$w(\mathbf{x}, \mathbf{v}, t) \approx f_{ME}(\mathbf{x}, \mathbf{v}, t) + \hbar^2 w^{(1)}(\mathbf{x}, \mathbf{v}, t), \tag{2.195}$$

which will be used in the next section for evaluating the unknown quantities in the moment system, associated with the Wigner equation.

In analogy with the semiclassical case, multiplying (2.190) by suitable weight functions ψ, depending in the physical relevant cases on the velocity $\mathbf{v}$, and integrating over the velocity, one has the balance equation for the macroscopic quantities of interest

$$\frac{\partial}{\partial t} \int_{\mathbb{R}^3} w(\mathbf{x}, \mathbf{v}, t) \ \psi(\mathbf{v}) \, \mathrm{d}^3 \mathbf{v} + \nabla_x \int_{\mathbb{R}^3} \psi(\mathbf{v}) \mathbf{v} \cdot w \, \mathrm{d}^3 \mathbf{v} + \frac{q}{m^*} \int_{\mathbb{R}^3} \psi(\mathbf{v}) \, \Theta[\Phi] w \, \mathrm{d}^3 \mathbf{v} = \int_{\mathbb{R}^3} \psi(\mathbf{v}) \, \mathscr{C}[w] \, \mathrm{d}^3 \mathbf{v}. \tag{2.196}$$

In the 8-moment model the basic variables are the moments relative to the weight functions $1, m^* \mathbf{v}, \dfrac{1}{2} m^* v^2, \dfrac{1}{2} m^* v^2 \mathbf{v}$.

By evaluating (2.196) for $\psi = 1$, under the assumption that the necessary moments of $w^{(1)}(\mathbf{x}, \mathbf{v}, t)$ and $\dfrac{\partial^3 w^{(0)}}{\partial v_i\, v_j\, v_k}$ with respect to v exist, one has

$$\frac{q}{m^*}\int_{\mathbb{R}^3} \Theta[\Phi] w \,\mathrm{d}^3\,\mathbf{v} = \frac{e}{m^*}\nabla_x \cdot \int_{\mathbb{R}^3} \nabla_v w^{(0)}\,\mathrm{d}^3\,\mathbf{v}$$
$$+\hbar^2\left[\frac{e}{m^*}\nabla_x \Phi \cdot \int_{\mathbb{R}^3} \nabla_v w^{(1)}\,\mathrm{d}^3\,\mathbf{v} - \frac{e}{24m^3}\frac{\partial^3 \Phi}{\partial x_i\, x_j\, x_k}\int_{\mathbb{R}^3}\frac{\partial^3 w^{(0)}}{\partial v_i\, v_j\, v_k}\,\mathrm{d}^3\,\mathbf{v}\right] = 0,$$

obtaining the continuity equation

$$\frac{\partial}{\partial t} n + \frac{\partial (n V_i)}{\partial x^i} = 0. \tag{2.197}$$

In order to get other moment equations we observe that from (2.195) it follows

$$\frac{e}{m^*}\nabla_x \Phi \cdot \int_{\mathbb{R}^3} \psi(\mathbf{v})\,\nabla_v w^{(1)}\,\mathrm{d}^3\,\mathbf{v} \; - \frac{e}{24m^3}\frac{\partial^3 \Phi}{\partial x_i\, x_j\, x_k}\int_{\mathbb{R}^3}\psi(\mathbf{v})\,\frac{\partial^3 w^{(0)}}{\partial v_i\, v_j\, v_k}\,\mathrm{d}^3\,\mathbf{v}$$
$$+\nu\int_{\mathbb{R}^3}\psi(\mathbf{v})\,\left(w^{(1)} - w^{(1)}_{eq}\right)\,\mathrm{d}^3\,\mathbf{v} = 0, \tag{2.198}$$

for each weight function $\psi(\mathbf{v})$ such that the integrals exist.

By taking into account (2.198), multiplying Eq. (2.190) by the weight functions $m^*\,\mathbf{v}$, $\frac{1}{2}\,m^*\,v^2$, $\frac{1}{2}\,m^*\,v^2\mathbf{v}$, after integration one finds the balance equations for momentum, energy and energy-flux

$$\frac{\partial}{\partial t}(nV_i) + \frac{\partial (nU_{ij})}{\partial x^j} + n\,e\,E_i = nC^i_p, \left(W^{(0)}, V^{(0)}_i S^{(0)}_i\right), \tag{2.199}$$

$$\frac{\partial}{\partial t}(nW) + \frac{\partial (nS_j)}{\partial x^j} + neV^{(0)}_k E^k = nC_W(W^{(0)}), \tag{2.200}$$

$$\frac{\partial}{\partial t}(nS_i) + \frac{\partial (nF_{ij})}{\partial x^j} + \frac{5}{3}n\frac{e}{m^*}E_i W^{(0)} = nnC^i_W, \left(W^{(0)}, V^{(0)}_i, S^{(0)}_i\right). \tag{2.201}$$

Here $V^{(0)}_i$, $W^{(0)}$ and $S^{(0)}_i$ are the zero order components of the average velocity, energy and energy-flux. Also for other quantities, the superscript (0) will mean zero order with respect to $\hbar^2$. The components of the flux of momentum and the flux of energy-flux are defined as

$$U_{ij} = \frac{1}{n(x,t)}\int_{\mathbb{R}^3} m^*\, v_i\, v_j\, w(x,v,t)\,\mathrm{d}^3\,\mathbf{v},$$
$$F_{ij} = \frac{1}{n(x,t)}\int_{\mathbb{R}^3} \frac{1}{2}\,m^* v_i\, v_j\, v^2\, w(x,v,t)\,\mathrm{d}^3\,\mathbf{v}.$$

The production terms are defined as

$$
\begin{aligned}
n\, C_p^i, &= \int_{\mathbb{R}^3} m^*\, v_i\, \mathscr{C}[w]\, \mathrm{d}^3\, \mathbf{v}, \\
n\, C_W &= \int_{\mathbb{R}^3} \frac{1}{2}\, m^* v^2\, \mathscr{C}[w]\, \mathrm{d}^3\, \mathbf{v}, \\
n\, n C_W^i, &= \int_{\mathbb{R}^3} \frac{1}{2}\, m^* v^2\, v_i\, \mathscr{C}[w]\, \mathrm{d}^3\, \mathbf{v}.
\end{aligned}
$$

Remark 2.4 The quantum corrections affect only the free streaming part, while the drift and production terms appear only at the zero order.

Therefore $C_W(W^{(0)})$, $C_p^i, \left(W^{(0)}, V_i^{(0)}, S_i^{(0)}\right)$ and $C_W^i, \left(W^{(0)}, V_i^{(0)}, S_i^{(0)}\right)$ are as in the semiclassical case.

The system (2.197), (2.199)–(2.201) is not closed because of the presence of the unknown quantities U_{ij}, F_{ij}, C_p^i, C_W and C_W^i,. We solve the closure problem with the approximation (2.195), assuming a collision dominated high field regime for the quantum effects. The results are given by the following proposition

Proposition 2.2 *In the high field approximation one has*

$$
\begin{aligned}
J_i &= n\, V_i = n\, V_i^{(0)} + \mathscr{O}(\hbar^4), \\
W &= W^{(0)} - \frac{\hbar^2 \beta\, e}{24 m^*}\, \Delta\, \Phi + \mathscr{O}(\hbar^4), \\
U_{ij} &= U_{ij}^{(0)} - \frac{\hbar^2 \beta\, e}{12 m^*}\, \frac{\partial^2 \Phi}{\partial x_i\, \partial x_j} + \mathscr{O}(\hbar^4), \\
S_i &= S_i^{(0)} - \frac{\hbar^2 \beta^2\, e^2}{24 m^{*2} \nu} \left(2 \frac{\partial^2 \Phi}{\partial x_i\, \partial x_r} \frac{\partial\, \Phi}{\partial\, x_r} + \frac{\partial\, \Phi}{\partial\, x_i} \Delta \Phi \right) \\
&\quad - \frac{\hbar^2\, e}{8 m^{*2} \nu} \frac{\partial}{\partial\, x_i}\, \Delta\, \Phi + \mathscr{O}(\hbar^4), \\
F_{ij} &= F_{ij}^{(0)} - \frac{\hbar^2 \beta\, e^3}{3 m^{*3} \nu^2}\, \frac{\partial\, \Phi}{\partial\, x_{(i}} \frac{\partial^2 \Phi}{\partial x_{j)} \partial x_r} \frac{\partial \Phi}{\partial x_r} - \frac{\hbar^2\, e^2}{4 m^{*3} \nu^2}\, \frac{\partial^3 \Phi}{\partial x_i\, \partial x_j\, \partial x_r} \frac{\partial \Phi}{\partial x_r} \\
&\quad - \frac{\hbar^2\, \beta\, e^3}{12 m^{*3} \nu^2} \left(\frac{\partial \Phi}{\partial\, x_i} \frac{\partial \Phi}{\partial\, x_j}\, \Delta\, \Phi + |\nabla\, \Phi|^2 \frac{\partial^2 \Phi}{\partial x_i\, \partial x_j} \right) \\
&\quad - \frac{\hbar^2\, e^2}{4 m^{*3} \nu^2}\, \frac{\partial \Delta \Phi}{\partial x_{(i}} \frac{\partial\, \Phi}{\partial x_{j)}} - \frac{\hbar^2\, e}{24 m^{*2}} \left(\Delta \Phi\, \delta_{ij} + 5 \frac{\partial^2 \Phi}{\partial x_i\, \partial x_j} \right) \\
&\quad - \frac{\hbar^2\, e}{4 m^{*2} \nu} \left(\frac{\partial \Delta \Phi}{\partial x_{(i}}\, V_{j)} + \frac{\partial^3 \Phi}{\partial x_{(i}\, x_j\, x_{k)}} V_k \right) + \mathscr{O}(\hbar^4).
\end{aligned}
$$

In the previous relationships round brackets indicate symmetrization, e.g.

$$A_{i\,(jk)} = \frac{1}{2}\left(A_{ijk} + A_{ikj}\right),$$
$$A_{(ijk)} = \frac{1}{3!}\left(A_{ijk} + A_{ikj} + A_{jik} + A_{jki} + A_{kij} + A_{kji}\right).$$

Remark 2.5 In the limit of high frequency $\nu \to \infty$ one has the simplified model

$$\begin{aligned}
J_i &= n\,V_i = n\,V_i^{(0)} + \mathscr{O}(\hbar^4),\\
W &= W^{(0)} - \frac{\hbar^2\beta\,e}{24m^*}\,\Delta\,\Phi + \mathscr{O}(\hbar^4),\\
U_{ij} &= U_{ij}^{(0)}\,\delta_{ij} - \frac{\hbar^2\beta\,e}{12m^*}\,\frac{\partial^2\Phi}{\partial x_i\,\partial x_j} + \mathscr{O}(\hbar^4),\\
S_i &= S_i^{(0)} + \mathscr{O}(\hbar^4),\\
F_{ij} &= F_{ij}^{(0)} - \frac{\hbar^2\,e}{24m^{*2}}\,\left(\Delta\Phi\,\delta_{ij} + 5\frac{\partial^2\Phi}{\partial x_i\,\partial x_j}\right).
\end{aligned}$$

From Eq. (2.195) one sees that in the limit $\nu \to \infty$, $w^{(1)}$ reduces to the quantum correction of the equilibrium Wigner function $w_{eq}^{(1)}$. The resulting quantum corrections to the tensor U_{ij} are the same as those obtained in [31] by using a shifted Wigner function, but with the semiclassical contribution which contains also a heat flux, not added *ad hoc*.

2.2.4.8 Quantum Corrected Energy-Transport and Crystal Heating Model

Assuming the same scaling of Sect. 2.2.4.4, one gets (formally) the energy-transport equations (3.72) and (3.74) with the closure relations

$$\begin{aligned}
V_i = \frac{1}{\Delta}\;&\left\{c_{22}^{(e)}\left[\frac{U_{ik}}{n}\frac{\partial n}{\partial x_k} + \frac{\partial U_{ik}}{\partial x_k} - e\frac{\partial\Phi}{\partial x_i}\right]\right.\\
&\left.-c_{12}^{(e)}\left[\frac{F_{ik}}{n}\frac{\partial n}{\partial x_k} + \frac{\partial F_{ik}}{\partial x_k} - \frac{5e}{3m^*}W^{(0)}\frac{\partial\Phi}{\partial x_i}\right]\right\},\\
S_i = \frac{1}{\Delta}\;&\left\{c_{11}^{(e)}\left[\frac{F_{ik}}{n}\frac{\partial n}{\partial x_k} + \frac{\partial F_{ik}}{\partial x_k} - \frac{5e}{3m^*}W^{(0)}\frac{\partial\Phi}{\partial x_i}\right]\right.\\
&\left.-c_{21}^{(e)}\left[\frac{U_{ik}}{n}\frac{\partial n}{\partial x_k} + \frac{\partial U_{ik}}{\partial x_k} - e\frac{\partial\Phi}{\partial x_i}\right]\right\},
\end{aligned}$$

where

$$\Delta(W^{(0)}) = c_{11}^{(e)} c_{22}^{(e)} - c_{12}^{(e)} c_{21}^{(e)}.$$

If also the effect of the crystal heating need to be included, the lattice temperature is no longer constant and one has to take into the account equation (3.75) as well.

The zero order terms are strictly valid in the parabolic band case ($\alpha = 0$), in particular the $c_{ij}^{(e)}$'s. A simple way to extend the results in the case of Kane dispersion relation is to consider for the semiclassical part of $\mathbf{V}$ and $\mathbf{S}$ the relations (2.187)–(2.188), but including the quantum corrections for U_{ik} and F_{ik} according to the proposition 2.2.

For example, in the case $\nu \to 0$ the complete model reads as

$$\begin{aligned}
\frac{\partial n}{\partial t} + \frac{\partial (nV^i)}{\partial x^i} &= 0, \\
\frac{\partial (nW)}{\partial t} + \frac{\partial (nS^j)}{\partial x^j} + neV_k E^k &= nC_W, \\
\rho c_V \frac{\partial T_L}{\partial t} - \operatorname{div}\left[k(T_L)\nabla T_L\right] &= H, \\
\mathbf{E} &= -\nabla_x \Phi, \\
\epsilon \Delta \Phi_S &= -e(N_D - N_A - n),
\end{aligned}$$

along with the constitutive relations

$$\begin{aligned}
V_i &= D_{11}(W^{(0)}, T_L) \frac{\partial \log n}{\partial x_i} + D_{12}(W^{(0)}, T_L) \frac{\partial W}{\partial x_i} + D_{13}(W^{(0)}, T_L) \frac{\partial \phi}{\partial x_i} \\
&+ \frac{1}{\Delta} \left[\left(-c_{22}^{(e)} \frac{\hbar^2 \beta e}{12 m^*} \frac{\partial^2 \Phi}{\partial x_i \partial x_k} + c_{12}^{(e)} \frac{\hbar^2 e}{24 m^{*2}} \left(\Delta\Phi \, \delta_{ik} + 5 \frac{\partial^2 \Phi}{\partial x_i \partial x_k} \right) \right) \frac{\partial \log n}{\partial x_k} \right. \\
&\left. - c_{22}^{(e)} \frac{\partial}{\partial x_k} \left(\frac{\hbar^2 \beta e}{12 m^*} \frac{\partial^2 \Phi}{\partial x_i \partial x_k} \right) + c_{12}^{(e)} \frac{\partial}{\partial x_k} \left(\frac{\hbar^2 e}{24 m^{*2}} \left(\Delta\Phi \, \delta_{ik} + 5 \frac{\partial^2 \Phi}{\partial x_i \partial x_k} \right) \right) \right],
\end{aligned}$$

$$\begin{aligned}
S_i &= D_{21}(W^{(0)}, T_L) \frac{\partial \log n}{\partial x_i} + D_{22}(W^{(0)}, T_L) \frac{\partial W}{\partial x_i} + D_{23}(W^{(0)}, T_L) \frac{\partial \phi}{\partial x_i} \\
&+ \frac{1}{\Delta} \left[\left(c_{21}^{(e)} \frac{\hbar^2 \beta e}{12 m^*} \frac{\partial^2 \Phi}{\partial x_i \partial x_k} - c_{11}^{(e)} \frac{\hbar^2 e}{24 m^{*2}} \left(\Delta\Phi \, \delta_{ik} + 5 \frac{\partial^2 \Phi}{\partial x_i \partial x_k} \right) \right) \frac{\partial \log n}{\partial x_k} \right. \\
&\left. + c_{21}^{(e)} \frac{\partial}{\partial x_k} \left(\frac{\hbar^2 \beta e}{12 m^*} \frac{\partial^2 \Phi}{\partial x_i \partial x_k} \right) - c_{11}^{(e)} \frac{\partial}{\partial x_k} \left(\frac{\hbar^2 e}{24 m^{*2}} \left(\Delta\Phi \, \delta_{ik} + 5 \frac{\partial^2 \Phi}{\partial x_i \partial x_k} \right) \right) \right].
\end{aligned}$$

If one introduces the equation of state

$$W^{(0)} = \frac{3}{2} k_B T, \tag{2.202}$$

the previous energy-transport model can be written using the electron density and temperature T, besides the electrical potential, as variables. However, it is crucial to remark that (2.202) is valid only in the parabolic band case (in analogy with the monatomic gas dynamics) and it is not justified in the non parabolic case, e.g. the Kane dispersion relation. In this latter case it is more appropriate to retain the energy W as fundamental variable.

References

1. Adler, M.: Accurate calculations of the forward drop and power dissipation in thyristors. IEEE Trans. Electron Dev. **ED-25**, 16–22 (1979)
2. Alì, G.: PDAE models of integrated circuits. Math. Comput. Mod. **51**, 915–926 (2010)
3. Alì, G., Bartel, A., Culpo, M., de Falco, C.: Analysis of a PDE thermal element model for electrothermal circuit simulation. In: Roos, J., Costa, L.R.J. (eds.) Proceedings of Scientific Computing in Electrical Engineering SCEE 2008, Espoo. Mathematics in Industry, vol. 14, pp. 273–280. Springer, Heidelberg (2010)
4. Alì, G., Bartel, A., Günther, M., Tischendorf, C.: Elliptic partial differential-algebraic multiphysics models in electrical network design. Math. Models Methods Appl. Sci. **13**(9), 1261–1278 (2003)
5. Alì, G., Bartel, A., Günther, M.: Parabolic differential-algebraic models in electric network design. SIAM J. MMS **4**(3), 813–838 (2005)
6. Alì, G., Mascali, G., Pulch, R.: Hyperbolic PDAEs for semiconductor devices coupled with circuits. In: Roos, J., Costa, L.R.J. (eds.) Proceedings of Scientific Computing in Electrical Engineering SCEE 2008, Espoo. Mathematics in Industry, vol. 14, pp. 305–312. Springer, Heidelberg (2010)
7. Anile, A., Mascali, G., Romano, V.: Recent developments in hydrodynamical modeling of semiconductors. In: Mathematical Problems in Semiconductor Physics. Lecture Notes in Mathematics, vol. 1832, pp. 1–56. Springer, Berlin/Heidelberg (2003)
8. Anile, A., Romano, V., Russo, G.: Extended hydrodynamical model of carrier transport in semiconductors. SIAM J. Appl. Math. **61**, 74–101 (2000)
9. Anile, A., Romano, V.: Non parabolic band transport in semiconductors: closure of the moment equations. Contin. Mech. Thermodyn. **11**, 307–325 (1999)
10. Barker, J., Ferry, D.: Self-scattering path-variable formulation of high-field, time-dependent, quantum kinetic equations for semiconductor transport in the finite-collision-duration regime. Phys. Rev. Lett. **42**, 1779–1781 (1979)
11. Bartel, A.: Partial differential-algebraic models in chip design – thermal and semiconductor problems. Ph.D. thesis, Bergische Universität Wuppertal (2003)
12. Bartel, A., Pulch, R.: A concept for classification of partial differential algebraic equations in nanoelectronics. In: Bonilla, L., Moscoso, M., Platero, G., Vega, J. (eds.) Progress in Industrial Mathematics at ECMI 2006. Mathematics in Industry, vol. 12, pp. 506–511. Springer, Berlin (2007)
13. Bedrosian, G.: A new method for coupling finite element field solutions with external circuits and kinematics. IEEE Trans. Magn. **29**(2), 1664–1668 (1993)

14. Bíró, O., Preis, K.: On the use of the magnetic vector potential in the finite-element analysis of three-dimensional eddy currents. IEEE Trans. Magn. **25**(4), 3145–3159 (1989)
15. Bossavit, A., Kettunen, L.: Yee-like schemes on staggered cellular grids: a synthesis between FIT and FEM approaches. IEEE Trans. Magn. **36**(4), 861–867 (2000)
16. Carrillo, J., Gamba, I., Majorana, A., Shu, C.W.: A Weno-solver for the transients of boltzmann-poisson system for semiconductor devices: performance and comparisons with Monte Carlo methods. J. Comput. Phys. **184**, 498–525 (2003)
17. Chryssafis, A., Love, W.: A computer-aided analysis of one dimensional thermal transient in n-p-n power transistors. Solid-State Electron. **22**, 249–256 (1978)
18. Clemens, M., Weiland, T.: Regularization of eddy-current formulations using discrete grad-div operators. IEEE Trans. Magn. **38**(2), 569–572 (2002)
19. Clemens, M.: Large systems of equations in a discrete electromagnetism: formulations and numerical algorithms. IEE Proc. Sci. Meas. Technol. **152**(2), 50–72 (2005)
20. Culpo, M.: Numerical algorithms for system level electro-thermal simulation. Ph.D. thesis, Bergische Universität Wuppertal (2009)
21. Culpo, M., de Falco, C.: Dynamical iteration schemes for coupled simulation in nanoelectronics. Proc. Appl. Math. Mech. **8**, 10,065–10,068 (2008)
22. Dreyer, W.: Maximisation of the entropy in non-equilibrium. J. Phys. A: Math. Gen. **20**, 6505–6517 (1987)
23. Dreyer, W., Struchtrup, H.: Heat pulse experiment revisited. Contin. Mech. Thermodyn. **5**, 3–50 (1993)
24. Estévez Schwarz, D., Tischendorf, C.: Structural analysis of electric circuits and consequences for MNA. Int. J. Circuit Theory Appl. **28**(2), 131–162 (2000)
25. de Falco, C., Culpo, M.: Dynamical iteration schemes for multiscale simulation in nanoelectronics. Proc. Appl. Math. Mech. **8**, 10,061–10,064 (2008)
26. Feldmann, U., Günther, M.: CAD-based electric-circuit modeling in industry I: mathematical structure and index of network equations. Surv. Math. Ind. **8**(2), 97–129 (1999)
27. Franz, A.F., Franz, G.A., Selberherr, S., Ringhofer, C., Markowich, P.: Finite boxes—a generalization of the finite-difference method suitable for semiconductor device simulation. IEEE Trans. Electron Devices **ED-30**, 1070–1082 (1983)
28. Fromlet, F., Markowich, P., Ringhofer, C.: A wignerfunction approach to phonon scattering. VLSI Des. **9**, 339–350 (1999)
29. Fukahori, K.: Computer simulation of monolithic circuit performance in the presence of electro-thermal interactions. Ph.D. thesis, University of California, Berkeley (1977)
30. Galler, M., Schürrer, F.: A deterministic solution method for the coupled system of transport equations for the electrons and phonons in polar semiconductors. J. Phys. A: Math. Gen. **37**, 1479–1497 (2004)
31. Gardner, C.: The quantum hydrodynamic model for semiconductors devices. SIAM J. Appl. Math. **54**, 409–427 (1994)
32. Gaur, S., Navon, D.: Two-dimensional carrier flow in a transistor structure under nonisothermal conditions. IEEE Trans. Electron Devices **ED-23**, 50–57 (1976)
33. De Gersem, H., Munteanu, I., Weiland, T.: Construction of differential material matrices for the orthogonal finite-integration technique with nonlinear materials. IEEE Trans. Magn. **44**(6), 710–713 (2008)
34. Glowinski, R., He, J., Lozinski, A., Rappaz, J., Wagner, J.: Finite element approximation of multi-scale elliptic problems using patches of elements. Numer. Math. **101**(4), 663–687 (2005)
35. Griepentrog, E., März, R.: Differential-Algebraic Equations and Their Numerical Treatment. Teubner, Leipzig (1986)
36. Günther, M.: A joint DAE/PDE model for interconnected electrical networks. Math. Comput. Model. Dyn. Syst. **6**, 114–128 (2000)
37. Günther, M., Wagner, Y.: Index concepts for linear mixed systems of differential-algebraic and hyperbolic-type equations. SIAM J. Sci. Comput. **22**(5), 1610–1629 (2000)
38. Haas, H., Schmellebeck, F.: Approximation of nonlinear anisotropic magnetization characteristics. IEEE Trans. Magn. **28**(2), 1255–1258 (1992)

39. Haus, H.A., Melcher, J.R.: Electromagnetic Fields and Energy. Prentice Hall, Englewood Cliffs (1989)
40. Ho, C.W., Ruehli, A.E., Brennan, P.A.: The modified nodal approach to network analysis. IEEE Trans. Circuits Syst. CAS **22**, 505–509 (1975)
41. Janes, E.: Information theory and statistical mechanics. Phys. Rev. **106**, 620–630 (1957)
42. Kosaku, Y.: Functional Analysis. Springer, Berlin/New York (1980)
43. Lions, J.L., Magenes, E.: Problèmes aux limites non Homogènes et Applications, vol. 1. Dunod, Paris (1968)
44. Lucht, W., Strehmel, K., Eichler-Liebenow, C.: Indexes and special discretization methods for linear partial differential algebraic equations. BIT **39**(3), 484–512 (1999)
45. Majorana, A.: Space homogeneous solutions of the Boltzmann equation describing electron-phonon interactions in semiconductors. Transp. Theory Stat. Phys. **20**, 261–279 (1991)
46. Majorana, A.: Conservation laws from the Boltzmann equation describing electron-phonon interactions in semiconductors. Transp. Theory Stat. Phys. **22**, 849–859 (1993)
47. Majorana, A.: Equilibrium solutions of the non-linear Boltzmann equation for an electron gas in a semiconductors. Il Nuovo Cimento **108B**, 871–877 (1993)
48. Marrocco, A., Anile, A., Romano, V., Sellier, J.: 2d numerical simulation of the mep energy-transport model with a mixed finite elements scheme. J. Comput. Electron. **4**, 231–259 (2005)
49. Mascali, G., Romano, V.: Hydrodynamical model of charge transport in GAAs based on the maximum entropy principle. Contin. Mech. Thermodyn. **14**, 405–423 (2002)
50. McCalla, W.J.: Fundamentals of computer aided circuit simulation. Kluwer Academic, Boston (1988)
51. Pulch, R., Günther, M., Knorr, S.: Multirate partial differential algebraic equations for simulating radio frequency signals. Eur. J. Appl. Math. **18**, 709–743 (2007)
52. Quarteroni, A., Valli, A.: Numerical Approximation of Partial Differential Equations. Computational Mathematics. Springer, Berlin/New York (1997)
53. Romano, V.: Non parabolic band transport in semiconductors: closure of the production terms in the moment equations. Contin. Mech. Thermodyn. **12**, 31–51 (2000)
54. Romano, V.: Non parabolic band hydrodynamical model of silicon semiconductors and simulation of electron devices. Math. Methods Appl. Sci. **24**, 439–471 (2001)
55. Romano, V.: 2d numerical simulation of the mep energy-transport model with a finite difference scheme. J. Comput. Phys. **221**, 439–468 (2007)
56. Romano, V., Zwierz, M.: Electron-phonon hydrodynamical model for semiconductors. ZAMP **61**, 1111–1131 (2010)
57. Romano, V.: Quantum corrections to the semiclassical hydrodynamical model of semiconductors based on the maximum entropy principle. J. Math. Phys. **48**, 123504 (2007)
58. Romano, V., Scordia, C.: Simulations of an electron-phonon hydrodynamical model based on the maximum entropy principle. In: Roos, J., Costa, L.R.J. (eds.) Proceedings of Scientific Computing in Electrical Engineering SCEE 2008, Espoo. Mathematics in Industry, vol. 14, pp. 289–296. Springer, Heidelberg (2010)
59. Schöps, S., Bartel, A., de Gersem, H., Günther, M.: DAE-index and convergence analysis of lumped electric circuits refined by 3-D magnetoquasistatic conductor models. In: Roos, J., Costa, L.R.J. (eds.) Proceedings of Scientific Computing in Electrical Engineering SCEE 2008, Espoo. Mathematics in Industry, vol. 14, pp. 341–348. Springer, Heidelberg (2010)
60. Selberherr, S.: Analysis and Simulation of Semiconductor Devices. Springer, Wien/New York (1984)
61. Shannon, C.: A mathematical theory of communication. Bell Syst. Tech. J. **27**, 379–423, 623–656 (1948)
62. Wachutka, G.: Rigorous thermodynamic treatment of heat generation and conduction in semiconductor device modeling. IEEE Trans. Comput. Aided Des. **9**, 1141–1149 (1990)
63. Weiland, T.: A discretization model for the solution of Maxwell's equations for six-component fields. Int. J. Electron. Commun. **31**, 116–120 (1977)

64. Wigner, E.: On the quantum correction for thermodynamic equilibrium. Phys. Rev. **40**, 749–759 (1932)
65. Wu, N.: The Maximum Entropy Method. Springer, New York (1997)
66. Yee, K.S.: Numerical solution of initial boundary value problems involving Maxwell's equations in isotropic media. IEEE Trans. Antennas Propag. **14**(3), 302–307 (1966)